UNIVERSIDADE DE BRASÍLIA

INSTITUTO DE GEOCIÊNCIAS

PROGRAMA DE PÓS-GRADUAÇÃO EM GEOLOGIA

METANOGÊNESE E VARIAÇÕES ISOTÓPICAS DO CARBONO EM AMBIENTE DE DEPOSIÇÃO DE RESÍDUOS SÓLIDOS: O ATERRO CONTROLADO DO JOCKEY CLUB DE BRASÍLIA - DF

GIOVANNA ORLETTI DEL REY

ORIENTADOR: PROF. ROBERTO VENTURA SANTOS

COORIENTADOR: PROF. LUCIANO SOARES DA CUNHA

DISSERTAÇÃO DE MESTRADO EM GEOQUÍMICA

PUBLICAÇÃO N° 451

BRASÍLIA - DF

2020

UNIVERSIDADE DE BRASÍLIA

INSTITUTO DE GEOCIÊNCIAS

PROGRAMA DE PÓS-GRADUAÇÃO EM GEOLOGIA

METANOGÊNESE E VARIAÇÕES ISOTÓPICAS DO CARBONO EM AMBIENTE DE DEPOSIÇÃO DE RESÍDUOS SÓLIDOS: O ATERRO CONTROLADO DO JOCKEY CLUB DE BRASÍLIA - DF

GIOVANNA ORLETTI DEL REY

DISSERTAÇÃO DE MESTRADO SUBMETIDA AO INSTITUTO DE GEOCIÊNCIAS DA UNIVERSIDADE DE BRASÍLIA COMO PARTE DOS REQUISÍTOS NECESSÁRIOS PARA A OBTENÇÃO DO GRAU DE MESTRE.

APROVADA POR:

_____

PROF. ROBERTO VENTURA SANTOS (UnB)
(ORIENTADOR)

_____

PROF. GERALDO RESENDE BOAVENTURA (UnB)
(EXAMINADOR INTERNO)

_____

PROFA. ANELIZE BAHNIUK RUMBELSPERGER (UFPR)
(EXAMINADOR EXTERNO)

AGRADECIMENTOS

Primeiramente, gostaria de agradecer a Deus e meus espíritos guardiões pela proteção e amparo que nunca faltaram. Agradeço imensamente por minha família, meus pais Mary e Antônio, meus irmãos Lorena e Ângelo, e minha tia Clelinha por sempre acreditarem em mim e me apoiarem incondicionalmente (mesmo de longe). Ao meu companheiro de vida Hichemm por todo carinho, amor e compreensão que serei sempre grata.

Agradeço à Universidade de Brasília, especialmente os Laboratórios de Geoquímica e Geocronologia pelo apoio logístico e por fornecer os materiais de amostragem e análises, à CAPES pelo apoio financeiro, aos meus prezados orientadores Roberto e Luciano por todo incentivo e por acreditarem no meu trabalho. Também agradeço a toda a equipe de alunos e professores do projeto RAEESA que me ajudaram de alguma forma.

Agradeço muito todo o auxílio recebido durante as campanhas de campo da minha querida Gabi, prof Luciano, Galego e Vagner. Aos técnicos Myller, Fernando, André, Mancini e o doutorando Christian pela prestatividade e ajuda com as análises.

No mais, agradeço a todos meus amigos que me apoiaram, de perto ou de longe, e tornaram possível a realização desse mestrado.

RESUMO

Os principais produtos gerados pela decomposição de resíduos sólidos descartados em lixões, aterros controlados ou aterros sanitários são o lixiviado, e gases como metano (CH_4) e dióxido de carbono (CO_2). O lixiviado pode ser definido como como um líquido escuro, de mau cheiro e com composição complexa, a qual é dependente dos estágios de decomposição da matéria orgânica, da natureza dos resíduos lançados, das condições ambientais e da idade e modo de operação do aterro. As etapas de degradação da matéria orgânica envolvem processos aeróbicos e anaeróbicos que definem os estágios de estabilização biológica de um aterro. A metanogênese ocorre ao final do processo de degradação anaeróbica e tem o início marcado pela produção de CH_4. Neste sentido, este trabalho se propõe a avaliar o estágio de estabilização biológica do Aterro Controlado do Jockey Club de Brasília – DF (ACJC) e seus efeitos na região de entorno a partir de uma abordagem geoquímica e isotópica. Variações sazonais, principalmente no que se diz respeito ao regime de chuvas, alteram parâmetros geoquímicos e acabam influenciando na estabilidade biológica do ACJC. Isso se deve ao fato de que água da chuva atua como o principal mecanismo de entrada de oxigênio no sistema, favorecendo a oxidação aeróbica da matéria orgânica. O processo de metanogênese por fermentação do ácido acético (CH_3COOH) é o principal processo atuante na produção de gases no ACJC, evidenciado pela concentrações dos gases CO_2 e CH_4 medidos nos queimadores presentes no ACJC e pela comparação de parâmetros físicos, químicos (oxigênio dissolvido, pH, NO_3^-, NH_4^+, SO_4^{2-}, Fe) e isotópicos ($\delta^{13}C$ do carbono inorgânico dissolvido). A percolação de lixiviado é um fator ambiental agravante nas adjacências do ACJC, visto que a disposição de resíduos neste local não dispõe de barreiras impermeabilizantes. Os dados químicos e isotópicos presentes nesse trabalho trazem evidências de que a qualidade dos aquíferos da região adjacente ao ACJC, especialmente em profundidades mais rasas, vem sendo afetada pela percolação de lixiviado. Além disso, a interação lixiviado (reduzido) com o aquífero (oxidado) leva a formação de zonas de oxirredução, identificadas pela presença de espécies reduzidas como NH_4^+ e Fe^{2+} no aquífero mais raso. A interação do lixiviado com o latossolo também altera a geoquímica da água subterrânea, indicada pela alta concentração de Fe^{2+} observada no poço raso monitorado.

ABSTRACT

Primary contaminants generated in dumpsites and landfills are leachate and gases, such as methane (CH_4) and carbon dioxide (CO_2). Leachate is a dark liquid with a very complex composition, which will be dependent on the stages of organic matter degradation, the nature of the waste discarded, the environmental conditions and, the age and operation of the landfill. The stages of organic matter degradation involve aerobic and anaerobic processes, which will define the biological stability of a landfill. Methanogenesis occurs at the end of the anaerobic degradation process and begins with the production of CH_4. This dissertation proposes to evaluate the biological stabilization stage of the Jockey Club of Brasília Landfill (JCBL) and its effects on the surrounding environment through geochemical and isotopic data. Seasonal variations, especially regarding the rainfall regime, change geochemical parameters, which also end up influencing the JCBL's biological stability. Rainwater acts as an oxygen carrier into the system, favoring the process of organic matter aerobic oxidation. Methanogenesis by fermentation of acetic acid (CH_3COOH) is the main process of gas production within the landfill, indicated by concentrations of CO_2 and CH_4 in the gas wells spread through the JCBL area and by comparing parameters such as dissolved oxygen, pH, NO_3^-, NH_4^+, SO_4^{2-}, Fe and isotopic ratio of dissolved inorganic carbon (δ^{13}C-DIC). Since the disposal of waste in JCBL lack engineered liner, leachate seepage is potential source of groundwater contamination. The chemical and isotopic data provided in this dissertation provide evidence that the quality of aquifers in close to the JCBL, especially at shallower depths, has been affected by leachate. In addition, the interaction between a reduced leachate with an oxidized aquifer leads to the formation of redox zones, identified by reduced species such as NH_4^+ and Fe^{2+} in the shallower aquifer. The interaction of the leachate with the oxisol also alters the groundwater geochemistry, indicated by the high concentration of Fe^{2+} observed in the shallow well monitored.

SUMÁRIO

LISTA DE FIGURAS

LISTA DE TABELAS

LISTA DE SÍBOLOS E ABREVIATURAS

ACJC / JCBL	Aterro Controlado do Jockey Club / Jockey Club of Brasília Landfill
ADASA	Agência Reguladora de Águas, Energia e Saneamento do Distrito Federal
AGEFIS	Agência de Fiscalização do Distrito Federal
CAESB	Companhia de Saneamento Ambiental do Distrito Federal
CODEPLAN	Companhia de Planejamento do Distrito Federal
DF	Distrito Federal
DIC	*Dissolved Inorganic Carbon* ou Carbono Inorgânico Dissolvido
DOC	*Dissolved Organic Carbon* ou Carbono Orgânico Dissolvido
Eh	Potencial redox em relação ao eletrodo de hidrogênio
EMBRAPA	Empresa Brasileira de Pesquisa Agropecuária
IBAMA	Instituto Brasileiro do Meio Ambiente e dos Recursos Naturais Renováveis
INMET	Instituto Nacional de Meteorologia
ORP	Potencial de oxidação-redução
PDAD	Pesquisa Distrital por Amostra de Domicílios
PNB	Parque Nacional de Brasília
PNRS	Plano Nacional de Resíduos Sólidos
pH	Potencial Hidrogeniônico
SLU	Serviço de Limpeza Urbana do Distrito Federal
UnB	Universidade de Brasília
URE	Unidade de Recebimento de Entulhos
ZEE	Zoneamento Ecológico-Econômico do Distrito Federal

1. INTRODUÇÃO

A prática inapropriada de descarte de resíduos sólidos representa uma fonte preocupante de contaminação dos recursos hídricos que, não raramente, são utilizados pela população de centros urbanos. O lixiviado e gases como metano (CH_4) e dióxido de carbono (CO_2) são os principais contaminantes gerados pela degradação da matéria orgânica presente nos aterros (Adeolu et al., 2011; Carneiro, 2002; Engelmann et al., 2018; van Breukelen et al., 2003). O lixiviado pode ser definido como um líquido escuro, de mau cheiro e com composição complexa, contendo uma fração orgânica e outra inorgânica (ex. cálcio, magnésio, amônia, sódio, potássio, ferro, sulfatos, cloretos), incluindo metais pesados (ex. chumbo, zinco, níquel, cobre, cromo, cádmio) (Adeolu et al., 2011; Lee e Ko, 2006). A composição química e microbiológica do lixiviado, assim como a geração de gases no aterro, varia com os estágios de decomposição da matéria orgânica, com a natureza dos resíduos lançados, idade, condições ambientais e com o modo de operação do aterro (Engelmann et al., 2018; Kjeldsen et al., 2002).

As etapas de degradação da matéria orgânica envolvem processos aeróbicos e anaeróbicos que definem os estágios de estabilização biológica de um aterro (Kjeldsen et al., 2002). Um aterro encontra-se em estágio aeróbico quando o oxigênio livre é utilizado para o consumo da matéria orgânica, resultando em um aumento da temperatura e na produção de CO_2 (Engelmann et al., 2018; Kjeldsen et al., 2002). Uma vez que a disponibilidade de oxigênio diminui, inicia-se o processo de degradação anaeróbica. O estágio de metanogênese ocorre ao final deste processo e tem o início marcado pela produção de CH_4 (Christensen et al., 2001; Kjeldsen et al., 2002; Porowska, 2015; Wimmer et al., 2013). O estágio de decomposição da matéria orgânica é definido a partir da correlação de parâmetros como pH, Demanda Bioquímica de Oxigênio (DBO), Demanda Química de Oxigênio (DQO), concentração de metais pesados e composição do gás gerado (Kjeldsen et al., 2002; Porowska, 2016). A definição do estágio de estabilização é fundamental tanto para se avaliar o potencial de emissão de gases e lixiviados a longo prazo quanto para encerrar as atividades do aterro (He et al., 2011; Wimmer et al., 2013).

A percolação do lixiviado é um dos principais processos de emissão de poluentes nas proximidades de aterros não planejados. A degradação (microbial ou não) de substâncias orgânicas, adsorção e troca iônica são mecanismos naturais de proteção dos aquíferos que atenuam a difusão e dispersão do lixiviado no meio ambiente subterrâneo. Esses processos, no entanto, são frequentemente insuficientes em evitar a formação de plumas de contaminação

(Christensen et al., 2001; van Breukelen et al., 2003). Os efeitos nocivos destas plumas são reduzidos por interações físicas e químicas dos contaminantes com solos e rochas e também pelo processo de diluição (MacFarlane et al., 1983; Christensen et al., 2001).

A utilização de parâmetros convencionais de monitoramento são por vezes pouco eficientes para se identificar fontes de poluição, principalmente em situações em que há possibilidade de fontes múltiplas (Castañeda et al., 2012; Engelmann et al., 2018; North et al., 2006). Nestes casos, a combinação de dados sobre metais pesados, íons inorgânicos dissolvidos, pH, oxigênio dissolvido (OD) complementados por traçadores isotópicos, particularmente isótopos estáveis, tem se mostrado uma ferramenta robusta (Castañeda et al., 2012; Engelmann et al., 2018; North et al., 2006; Porowska, 2015; Wimmer et al., 2013). A utilização conjunta desses parâmetros permite a identificação mais precisa de fontes de contaminação e, também, do estágio de estabilidade biológica de aterros. As razões isotópicas do carbono são particularmente interessantes devido à relação direta deste parâmetro com as etapas de degradação da matéria orgânica. Por exemplo, em condições avançadas de decomposição da matéria orgânica e com o estabelecimento da fase de metanogênese, a razão isotópica do carbono inorgânico dissolvido (δ^{13}C-DIC) é um traçador robusto uma vez que pode atingir valores próximos a + 20‰ (Engelmann et al., 2018; Grossman et al., 2002; Hackley et al., 1996; North et al., 2006; Porowska, 2015; van Breukelen et al., 2003; Wimmer et al., 2013).

O Aterro Controlado do Jockey Club de Brasília (ACJC) situa-se numa área de grande relevância ambiental e econômica. Localizado a aproximadamente 20 km da capital federal, as atividades de lançamento de resíduos se iniciaram de forma irregular juntamente com a construção de Brasília. Além de estar localizado em um divisor de águas de duas unidades hidrográficas, as adjacências do aterro são ocupadas por residências, chácaras de produção agrícola e uma importante área de preservação ambiental: o Parque Nacional de Brasília. Considerando o potencial de risco ao meio ambiente, mesmo após o encerramento de suas operações, é fundamental se conhecer o estágio de evolução do aterro e seu potencial de emissão de poluentes. A partir dessas informações é possível se estabelecer estratégias que atenuem efeitos nocivos ao meio ambiente. Diante dessa problemática, esta dissertação se propõe a avaliar o estágio de estabilização do ACJC e seus efeitos na região de entorno a partir de uma abordagem geoquímica e isotópica.

1.1. OBJETIVOS

O objetivo principal deste projeto é definir o estágio de estabilização do ACJC com base em parâmetros geoquímicos.

Os objetivos específicos são:

▪ Estudar as variações sazonais dos parâmetros geoquímicos e isotópicos e as implicações para a estabilidade biológica do ACJC;

▪ Definir parâmetros químicos e isotópicos que identifiquem a pluma de contaminação e suas interações com os níveis freáticos.

Como resultado das conclusões dos dois artigos desta dissertação, sugere-se procedimentos para monitoramento geoquímico que possibilite um melhor gerenciamento e utilização de produtos decorrentes da decomposição dos resíduos do ACJC.

1.2. ESTRUTURA DA DISSERTAÇÃO

Esta dissertação está subdividida em capítulos introdutórios, dois artigos científicos, conclusões e sugestões, e anexos. Em resumo, cada item desta dissertação apresentará os seguintes conteúdos:

O Capítulo 1 apresenta a introdução dos principais processos que serão abordados na dissertação e detalha os objetivos principais e específicos do projeto.

O Capítulo 2 apresenta o embasamento teórico e bibliográfico acerca dos diferentes processos geoquímicos que foram abordados neste projeto.

O Capítulo 3 apresenta as principais características do ACJC, como localização, aspectos fisiográficos e operação do aterro.

O Capítulo 4 discorre detalhadamente sobre os materiais e métodos utilizados no trabalho.

O Capítulo 5 apresenta os resultados e discussões em forma de dois artigos científicos: o primeiro artigo fala discorre sobre implicações das variações sazonais dos parâmetros geoquímicos para o processo de estabilização do ACJC; e o segundo apresenta os parâmetros

químicos e isotópicos utilizados no estudo da pluma de contaminação do próxima ao ACJC e as consequências das interações com os níveis freáticos.

Por fim, o Capítulo 6 explicita as conclusões dos dois artigos produtos desta dissertação. São apresentadas sugestões de trabalhos futuros, e uma metodologia de monitoramento químico para auxiliar programas de remediação ambiental que possibilite melhor utilização e gerenciamento de produtos decorrentes da decomposição dos resíduos.

2. FUNDAMENTAÇÃO TEÓRICA

GEOCHEMICAL PROCESSES IN A LANDFILL ENVIRONMENT

2.1. INTRODUCTION

Waste disposal may be classified based on its structure, impermeabilization, and operation mode. Landfills are a common kind of waste disposal in which organic matter are decomposed by complex biogeochemical reactions. If not properly monitored, these landfills may be a dangerous source of contaminants to the atmosphere and groundwater. The risk of groundwater pollution is particularly critical because most landfills have initiated their activities as dumpsites without engineered liners. In this context, assessing the biological stability of the landfill as well as the chemical interactions between contamination plume and subsurface are essential to better manage their hazardous impact.

The following sections review the main geochemical processes occurring in a landfill environment as well as the main impacts of their products in the surrounding environment.

2.2. LANDFILLS

Landfills are a common procedure of waste disposal that usually offer risks to human health and environment, especially because most of this sites started irregularly and lack engineered liners (Kjeldsen et al., 2002; van Turnhout et al., 2018). They usually receive a mixture of different types of waste, such as municipal, industrial, commercial and sometimes chemical refuse (Barlaz and Ham, 1993; Kjeldsen et al., 2002). The main contaminants produced in landfills are leachate and gases, such as methane (CH_4) and carbon dioxide (CO_2) (Barlaz and Ham, 1993; Christensen et al., 2001; Engelmann et al., 2018; Mohammadzadeh and Clark, 2011).

Leachate is induced by rainfall that percolates through the refuse layers, promoting leaching and biodegradation reactions that result in a very complex solution (Adeolu et al., 2011; Kjeldsen et al., 2002; Lee and Ko, 2006). Leachate is usually composed by (1) dissolved organic matter, usually organic acids; (2) inorganic components, such as calcium (Ca), magnesium (Mg), sodium (Na), potassium (K), ammonium (NH_4^+), iron (Fe), manganese (Mn), chloride (Cl^-), sulfate (SO_4^{2-}), and bicarbonate (HCO_3^-); (3) heavy metals, as cadmium (Cd), chromium

(Cr), copper (Cu), lead (Pb), nickel (Ni) and zinc (Zn); and (4) xenobiotic organic compounds, which includes aromatic hydrocarbons, chlorinated aliphatics, phenols, pesticides and plasticizers (Christensen et al., 2001; Kjeldsen et al., 2002). The chemical and microbiological composition of leachates will dependent of the nature of the residues, landfill age, operational mode and mechanisms of organic matter degradation (Engelmann et al., 2018; Gurijala and Suflita, 1993; Kjeldsen et al., 2002; Kulikowska and Klimiuk, 2008). Additionally, leachate composition can be affected by environmental conditions such as rainfall regime and temperature (Aghdam et al., 2018; Barella et al., 2013; Porowska, 2015; Shalini et al., 2010).

TYPES OF LANDFILLS

Solid refuse has been historically discarded without any sanitary precautions. In order to avoid malodor and ward off insects and rodents, covering the waste with a soil layer became a common procedure in many landfills. This procedure, however, does not avoid leachate percolation at the base of the landfill, unless the refuse in placed on a proper impermeable liner (Lee and Jones-Lee, 2004; Nisiyama, 2019).

According to the Brazilian National Plan of Solid Waste (PNRS, 2011), there are three main ways of disposing solid waste: sanitary landfills, dumpsites and controlled landfills. In sanitary landfills, the refuse is managed in a proper way to avoid risks to human health and environmental impacts: solid waste is disposed in impermeable liner and leachate generated is collected and treated. This type of landfill also requires a proper monitoring network of groundwater and gas emissions (PNRS, 2011). Dumpsites have no sanitary precautions and offer great risks to the environment and human health (PNRS, 2011). Controlled landfills are also an improper way of discarding refuse since the only sanitary precaution is covering of the residue with a soil layer (PNRS, 2011).

Depending on local soil conditions, Tchobanoglous and O'Leary (2002) proposed different geotechnical methods of landfilling: a) Canyon/Depression: should be applied on areas with natural or anthropogenic (quarries, mines) slopes; b) Area: this method is indicated for areas with low phreatic level and soils that are difficult to excavate; c) Trench: should be applied in areas with deep phreatic level and soils that excavate easier (Nisiyama, 2019). Other type of landfilling is the bioreactors landfills that differ from the traditional types of landfilling because they allow fluid insertion in order to accelerate biodegradation reaction and, at the same time, enhance CH_4 production. This technique involves humidity control by the insertion of liquids

in order to increase humidity and ensure an optimum condition of microbiological activity (Shalini et al., 2010; Warith, 2003; Reinhart et al., 2002; Nisiyama, 2019).

Landfill can be operated either by anaerobic or aerobic processes, depending on the air inflow in the buried waste (Matsufuji et al., 1993; Wang et al., 2006). Semi-aerobic landfills have minor influence of air inflow accompanied by a collection system for runoff water and leachate (Matsufuji et al., 1993). Leachate recirculation is also a common procedure in semi-aerobic landfills and consists in pumping the produced leachate back to the waste layers (Matsufuji et al., 1993; Wang et al., 2006).

The rates of organic matter decomposition depend on landfill operation mode, as shown by studies that monitor the landfill loss of weight that a landfilled waste had during a defined period (Matsufuji et al., 1993). As demonstrated by Matsufuji et al. (1993), the decomposition rate in an aerobic landfill will rapidly reach 70% in approximately 3 to 4 years. In contrast, in an anaerobic landfill the same rate will be reached in approximately 7 to 8 years. For semi-aerobic and recirculatory semi-aerobic type of landfill, Matsufuji et al. (1993) obtained a short term evaluation of the decomposition rate. It was found that the recirculatory type had a rate about 10% higher than the semi-aerobic type after 18 months. This result also supports the fact that an introduction of oxygen is indeed helpful in accelerating organic matter degradation (Wang et al., 2006). These different operation mode will also have impact in the gas production within the landfill (Matsufuji et al., 1993; Nag et al., 2018, 2016; van Turnhout et al., 2018; Wang et al., 2006).

2.3. ORGANIC MATTER DEGRADATION PROCESS AND BIOLOGICAL STABILITY OF LANDFILLS

The degradation process of carbon-based components buried in landfills involves a series of chemical reactions that characterize chemically and isotopically the leachate composition. The initial process of organic matter degradation is aerobic and involves the consumption of oxygen available in the buried refuse, resulting in CO_2 production (Kjeldsen et al., 2002). Oxygen will supply energy to aerobic bacteria and may be fully consumed under excess of organic carbon (Rivett et al., 2008). Once the waste becomes anaerobic, the cellulosic and hemicellulosic materials will be hydrolyzed and fermented to alcohols and carboxylic acids (Barlaz and Ham, 1993; Kjeldsen et al., 2002; Mohammadzadeh and Clark, 2011). Then, acetogenic reactions will convert these products to acetate, hydrogen and CO_2 (Barlaz and Ham, 1993; Kjeldsen et

al., 2002). The activity of hydrolytic, fermentative and acetogenic bacteria will lead to a decrease in pH of the solution, which increases the solubility of some compounds (Kjeldsen et al., 2002).

Primary redox reactions also participate in the degradation process. In the absence of oxygen, other microorganisms will use different electron acceptors to oxidize organic matter. The sequential utilization of these acceptors ensures the most efficient utilization of energy utilization by bacteria, which will preferentially use NO_3^-, then MnO_2, $Fe(OH)_3$ and, lastly, SO_4^{2-} (Rivett et al., 2008). The following equations describe the oxidation of acetic acid (CH_3COOH) as the environment becomes increasingly reduced:

2.1) $CH_3COOH + 2O_2 \rightarrow 2CO_2 + 2H_2O$

2.2) $3CH_3COOH + 4NO_3^- \rightarrow 2N_2 + 6CO_2 + 6H_2O$

2.3) $CH_3COOH + 4MnO_2 + 2HCO_3^- + 2H^+ \rightarrow 4MnCO_3 + 4H_2O$

2.4) $CH_3COOH + 5Fe(OH)_3 + 3HCO_3^- \rightarrow 5FeCO_3 + 11H_2O$

2.5) $CH_3COOH + SO_4^{2-} \rightarrow HS^- + HCO_3^- + CO_2 + H_2O$

Equation 2.1 represents aerobic oxidation, in which organic matter is consumed in order to produce two moles of CO_2 and two moles of H_2O in a very oxidized environment (Eh ~ +334 mV; Rivett et al., 2008). Once oxygen becomes depleted, denitrification will then occur in a solution Eh of approximately +231 mV (Equation 2.2; Rivett et al., 2008). Manganese (Equation 2.3), iron (Equation 2.4), and sulphate reduction (Equation 2.5) will then become energetically viable. The use of these electron acceptors is accompanied by a decrease in the solution Eh reaches until this parameter gets as low as -699 mV (Rivett et al., 2008). The continuous depletion of these ions will finally end up in methane production therefore initiating a methanogenic phase.

In the methanogenic phase, methane concentration reaches measurable values since it begins to be produced together with CO_2 (Equation 2.6; Kjeldsen et al., 2002). During the fermentation of acetic acid, CH_3COOH molecule is consumed by methanogenic bacteria in order to produce one mole of CO_2 and one mole of CH_4 (Equation 2.6) (Baedecker and Back, 1979; Barlaz and Ham, 1993; Engelmann et al., 2018; Mohammadzadeh and Clark, 2008). CH_4 can also be produced by CO_2 reduction under very anoxic conditions, as demonstrated by Equation 2.7 (Baedecker and Back, 1979).

2.6) $CH_3COOH \rightarrow CO_2 + CH_4$

2.7) $CO_2 + 4H_2 \rightarrow CH_4 + 2H_2O$

The understanding of the different phases of organic matter decomposition are useful to determine the landfill biological stability and evaluate long-term potential emission of gases and leachates (He et al., 2011). It is also essential to determine whether the landfill has reached the required conditions for its closure (He et al., 2011; Wimmer et al., 2013). The different stabilization stages are characterized by specific physicochemical and microbiological parameters such as pH, biochemical oxygen demand (BOD), chemical oxygen demand (COD), dissolved organic carbon (DOC), and biogas composition (Kjeldsen et al., 2002; Porowska, 2016; Wimmer et al., 2013; Zmora-nahum et al., 2005).Therefore, these stages can be classified as:

1 – Aerobic/acid phase: characterized by aerobic and anaerobic oxidation, which will consume the organic molecules resulting in the production of CO_2 (Equations 2.1 to 2.5), and in an accumulation of organic acids resulting in a pH decrease (Barlaz and Ham, 1993; Kjeldsen et al., 2002; Matsufuji et al., 1993). The pH on this phase ranges from 4.5 to 7.5 and BOD/COD ratio has been reported to be between 0.4 and 0.7 (Christensen et al., 2001; Kjeldsen et al., 2002).

2 – Initial methanogenic: This phase begins when CH_4 production reaches measurable values and is accompanied by an increase on pH (Barlaz and Ham, 1993; Kjeldsen et al., 2002). Methanogenic bacteria will then consume the accumulated acids in order to produce CH_4 and CO_2 (Equation 2.6). BOD/COD ratio will also decrease as the organic acids are being consumed (Christensen et al., 2001; Kjeldsen et al., 2002).

3 – Stable methanogenic: In this phase, methane production will reach its maximum rate and will decrease as the organic acids are consumed by methanogenic bacteria (Kjeldsen et al., 2002). The pH continues to increase and the environment becomes alkaline with values between 7.5 and 9. In this phase, BOD/COD ratio usually present value below 0.1, with an average value of 0.06 (Christensen et al., 2001; Kjeldsen et al., 2002).

4 – Air intrusion: The main characteristic of this phase is the re-oxygenation of the buried waste, which can lead to a decrease in CH_4 due to oxidation. Oppositely, CO_2 concentrations are expected to increase and may be accompanied by a slight pH decrease (Kjeldsen et al., 2002). The air intrusion in the landfill will be mainly dependent on density differences between landfill and atmosphere, diffusion, barometric pumping and wind-induced exchange (Kjeldsen et al., 2002; Bozkut el at., 1999)

5 – CO_2 phase/aerobic: DOC concentration still high and the increase in oxygen will again support aerobic oxidation, leading to CO_2 production and an increase in nitrogen gas (Kjeldsen et al., 2002; Wimmer et al., 2013).
6 – Background: This phase represents the end of landfill activities, when gas and leachate emissions ceased and there is no major influence of landfill leachate in the environment (Kjeldsen et al., 2002; Wimmer et al., 2013).

CARBON ISOTOPIC VARIATIONS IN THE METHANOGENIC PROCESS

Variations on carbon isotopes and its relationship to the methanogenesis have been described in a few studies (Conrad, 2005; Hackley et al., 1996; Wimmer et al., 2013). Since the high carbon isotope fractionation values between CO_2 and CH_4 at low temperatures (e.g. +68.2‰ at 25°C; Bottinga, 1969), mass balance indicates that CO_2 produced by methanogenesis will be isotopically very heavy (Grossman et al., 2002; Hackley et al., 1996; North et al., 2006; Porowska, 2015; van Breukelen et al., 2003; Wimmer et al., 2013).

Wimmer et al. (2013) have described the isotopic variations of the dissolved inorganic carbon (DIC) in respect to the biological stability of the organic waste mater (Figure 2.1). In an initial aerobic phase, δ^{13}C-DIC is mainly dependent on the organic carbon signature from the refuse, resulting in values between -20 and -25‰ (Wimmer et al., 2013). As the organic matter degradation reaches more advanced stages, δ^{13}C-DIC values become positive (around +15‰), characterizing a methanogenic phase (Grossman et al., 2002; Hackley et al., 1996; North et al., 2006; Porowska, 2015; van Breukelen et al., 2003; Wimmer et al., 2013). Natural air intrusion or in situ aeration changes the isotopic signature again to negative values (Porowska, 2016; Wimmer et al., 2013).

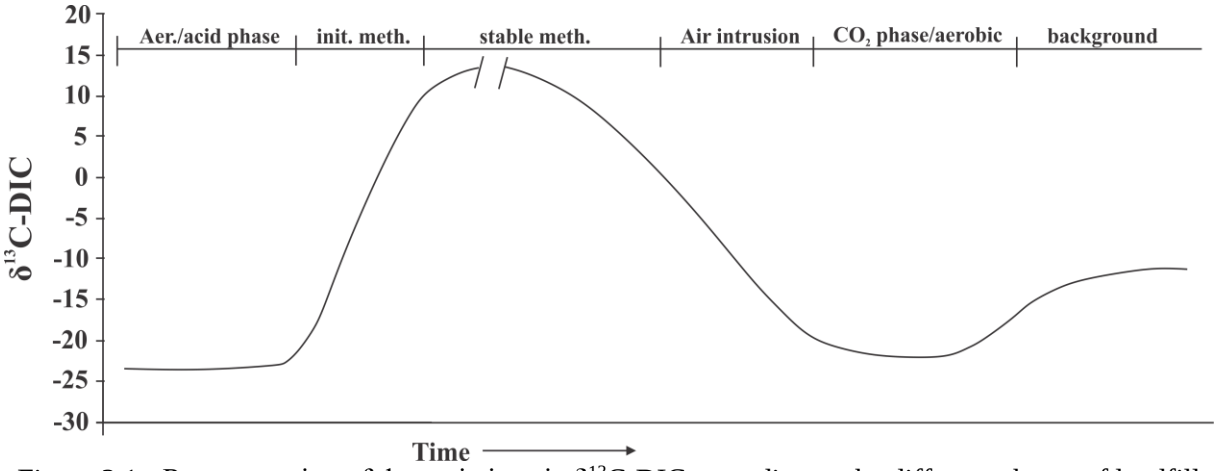

Figure 2.1 - Representation of the variations in δ^{13}C-DIC according to the different phases of landfill stability in an estimated chronological sequence. Adapted from Wimmer et al. (2013).

These distinct isotopic values occur due to the methanogenic process (Equation 2.6 and 2.7). In the fermentation of acetic acid (Equation 2.6), a depletion of ^{13}C in CH_4 is indicated by a decrease in $\delta^{13}C$-CH_4 to approximately -50‰. On the other hand, $\delta^{13}C$-CO_2 produced during this reaction is enriched in ^{13}C, presenting values between -10 and +20‰ (Conrad, 2005; Wimmer et al., 2013). In the CO_2 reduction (Equation 2.7), the CH_4 produced present $\delta^{13}C$ values between -60 and -110‰ (Botz et al., 1996; Wimmer et al., 2013).

GAS PRODUCTION IN LANDFILLS

The assessment of gas production in landfills is a useful tool to understand the biological stability, landfill age and operation mode (Kjeldsen et al., 2002; Matsufuji et al., 1993; Nag et al., 2018; Porowska, 2016). During the different stabilization stages, there will be general trends of gas production, which are demonstrated in Figure 2.2. The start of methane production will be dependent on the O_2 and H_2 depletion, characterizing the end of the aerobic/acid phase and the beginning of the methanogenic phase (Figure 2.2) (Kjeldsen et al., 2002). The CO_2 production is distributed throughout all the stabilization phases, and it will reach its maximum at the end of the aerobic/acid phase, when it will then be produced together with CH_4 (Figure 2.2) (Kjeldsen et al., 2002).

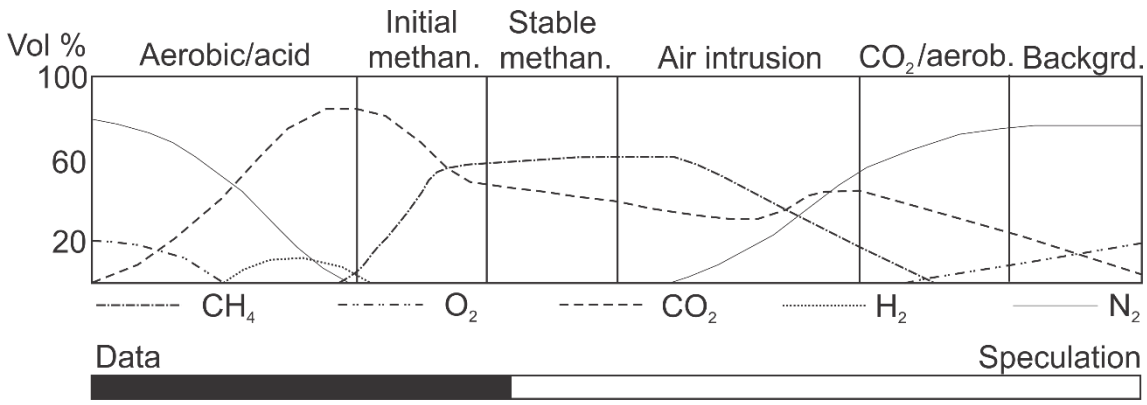

Figure 2.2 - General trends of gas production in a landfill during its different phases stabilization. Data and speculation period are demonstrated based on Kjeldsen et al. (2002). Adapted from Kjeldsen et al. (2002).

The landfill age can be assessed by the concentrations of hydrogen sulfide (H_2S). Kim (2006) and Porowska (2016) found that concentrations over 1 ppm of H_2S were observed in new landfills, while in old landfills this gas was observed in concentrations lower than 0.01 ppm.

The production of CO_2 and CH_4 will also vary depending on to the different operation mode (Matsufuji et al., 1993; Nag et al., 2018, 2016; van Turnhout et al., 2018; Wang et al., 2006). Figure 2.3 shows the amount of these gases generated in a period of 10 years considering the different landfill operation mode. In terms of CO_2 production (Figure 2.3-A), the aerobic operation mode presented the highest concentrations. The air inflow into the buried waste accelerates organic matter degradation, supporting aerobic oxidation and producing CO_2 (Matsufuji et al., 1993; Wang et al., 2006). In fact, in order to improve the leachate quality and avoid the CH_4 production, the aerobic operation mode is more indicated (Nag el al., 2016). This operation mode is also more effective in decreasing the biodegradable carbon in leachate (van Turnhout et al., 2018).

An anaerobic type of landfill will be mainly driven by the methanogenic process, which will produce same proportions of CO_2 and CH_4, as illustrated by the Equation 2.6. This type of landfill will also be responsible for the largest amount of CH_4 production, reaching about $1.6x10^9$ L of this gas after a 5-year period (Figure 2.3-B) (Matsufuji et al., 1993). The effectiveness of the methanogenic process can be assessed by monitoring moisture content and pH (Barlaz and Ham, 1993). Additionally, Cossu et al. (2016) found that one way to enhance methane production is to reduce volatile fatty acids by aerating the system in order to increase pH until the environment becomes optimum for the metabolism of methanogenic bacteria.

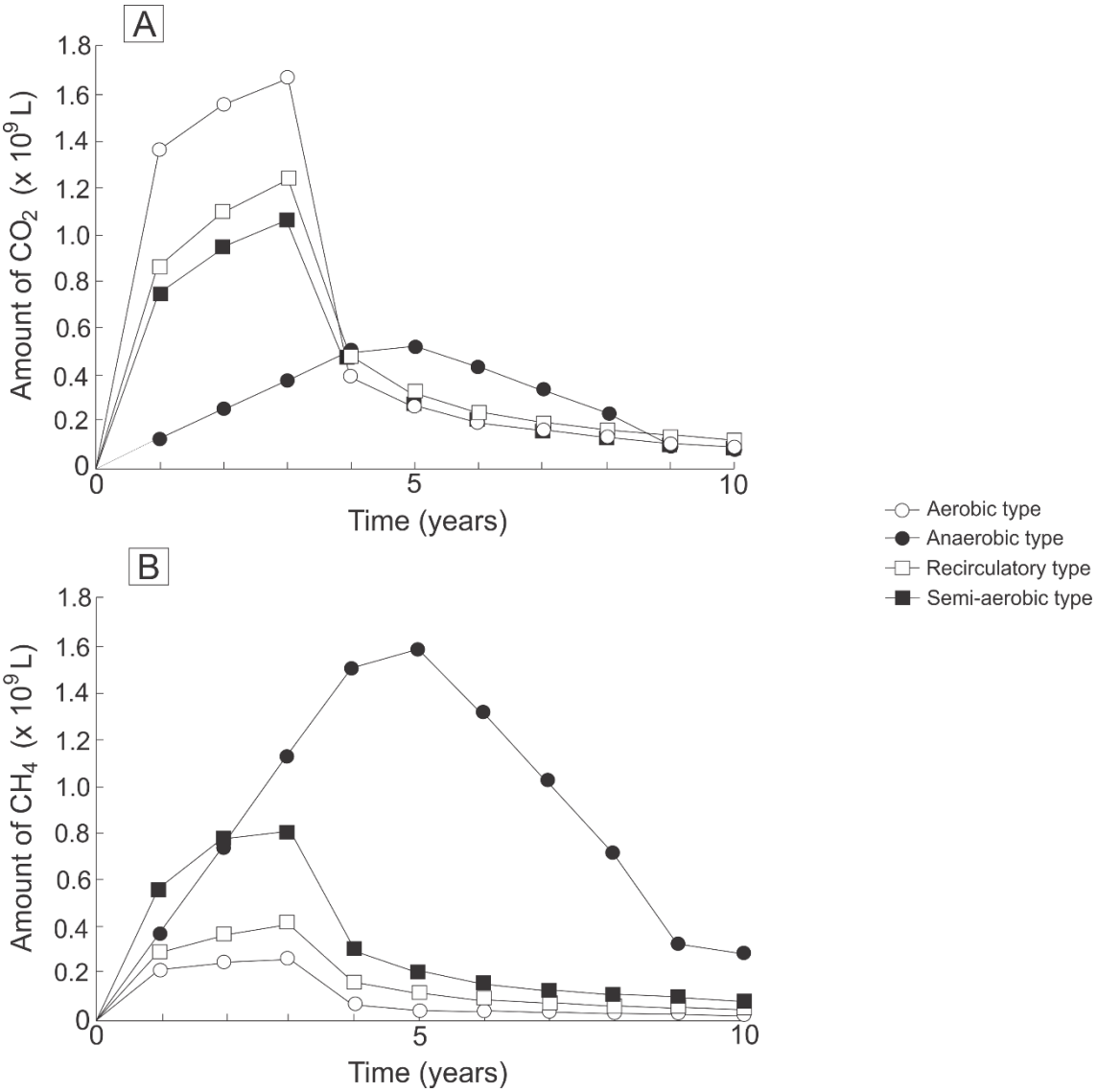

Figure 2.3 - Change in the amount of A) CO_2, and B) CH_4 produced by different operation modes in landfills. Adapted from Matsufuji et al. (1993).

2.1. GEOCHEMISTRY OF LANDFILL LEACHATE PLUMES

Aquifers have natural ways on attenuating the propagation of contaminants such as adsorption, dilution, precipitations, volatilization, and ion exchange reactions (Christensen et al., 2001). When natural processes are usually not sufficient to avoid the propagation of pollutants through aquifers, a contamination plume is formed (Adeolu et al., 2011; Engelmann et al., 2018; Loizidou and Kapetanios, 1993; van Breukelen et al., 2003). Percolation of landfill leachate has been highly reported in literature particularly concerning source of groundwater contamination (Adeolu et al., 2011; Engelmann et al., 2018; Hackley et al., 1996; Han et al., 2014; MacFarlane

et al., 1983; Mohammadzadeh and Clark, 2011; Porowska, 2015; van Breukelen et al., 2003; Wimmer et al., 2013).

There are two main interesting geochemical processes that will be addressed in this section: 1) the assimilation on methanogenic CO_2 in the dissolved inorganic carbon (DIC) aquifer pool; and 2) the redox gradient that is formed by the percolation of highly reduced leachate in an often-oxidized environment.

Generally, non-contaminated groundwater will present values of δ^{13}C-DIC from -4 to -30‰, depending on the aquifer's source of carbon (O'Leary, 1988). In leachate-contaminated groundwater, the inorganic carbon may be sourced by the organic matter biodegradation from the landfill, leading to positive values of δ^{13}C-DIC in groundwater samples (Atekwana and Krishnamurthy, 2004; Engelmann et al., 2018; Haarstad and Mæhlum, 2013; Porowska, 2015). Thus, the distinct isotope signature of the inorganic carbon from landfill leachate and groundwater can provide valued information about carbon transfer between these two environments (Engelmann et al., 2018; Grossman et al., 2002; North et al., 2004; Porowska, 2015; van Breukelen et al., 2003; Wimmer et al., 2013). The assessment of the δ^{13}C-DIC in leachate-contaminated groundwater can also inform about the carbon cycle, biogeochemical processes, and contaminants flow through water resources (Engelmann et al., 2018; Grossman et al., 2002; Mohammadzadeh and Clark, 2011; van Breukelen et al., 2003; Zhou et al., 2015).

The percolation of a highly reduced leachate in an often-oxidized environment frequently lead to a redox gradient. This redox zonation in groundwater have already been reported in the literature (Albrechtsen et al., 1999; Baedecker and Back, 1979; Christensen et al., 2001). The schematic distribution of the redox zones through the streamline is demonstrated on Figure 2.4. These processes may be affected by hydrogeological and geochemical factors and should be carefully evaluated (Albrechtsen et al., 1999; Christensen et al., 2001). The chemical changes in the aquifer will be dependent on its capacity to accept electrons. The process of organic matter oxidation inside the plume will also follow the primary redox sequence demonstrated by the Equations 2.1 to 2.5 (Christensen et al., 2001).

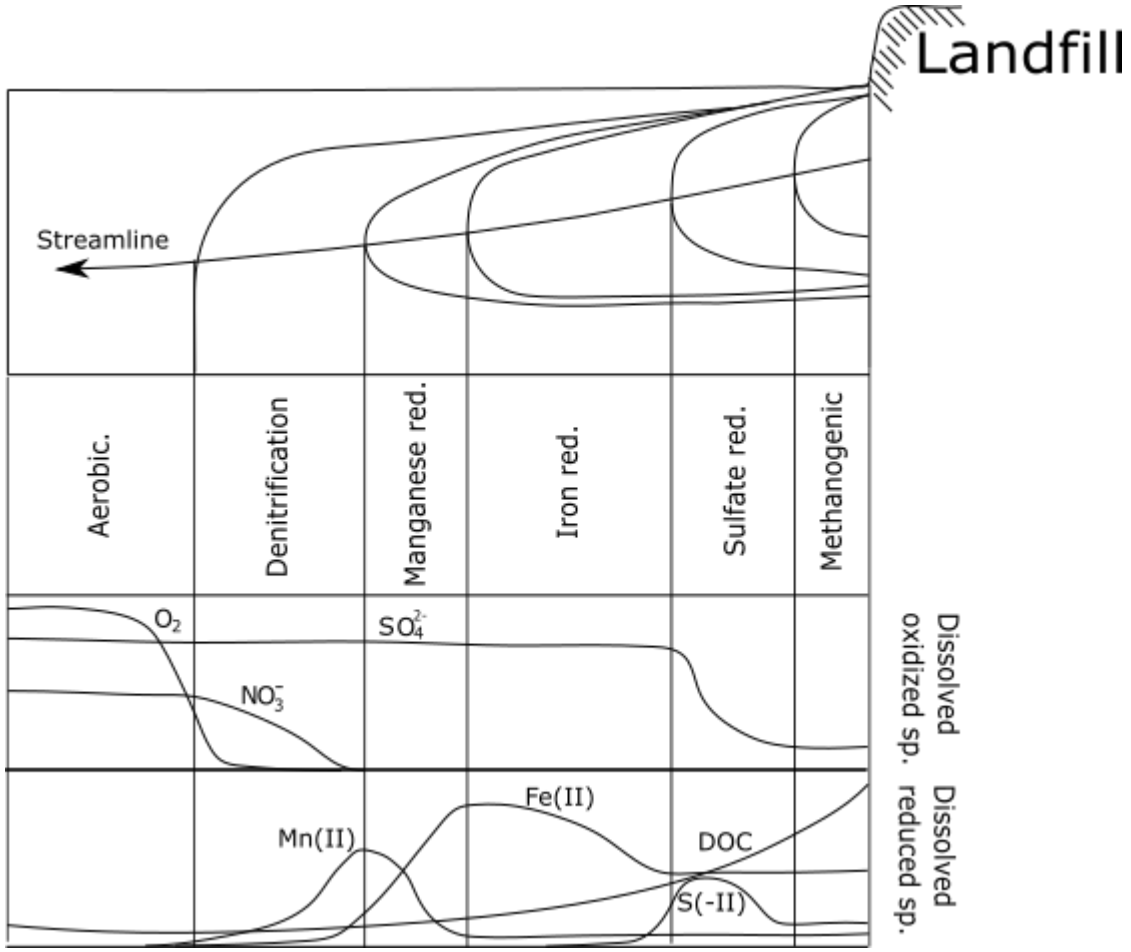

Figure 2.4 - Schematic redox zonation in a groundwater environment and the distribution of the dissolved oxidized and reduced species on each zone. Adapted from Christensen et al. (2001).

3. CARACTERIZAÇÃO DA ÁREA DE ESTUDO

3.1. LOCALIZAÇÃO

O antigo Aterro Controlado do Jockey Club de Brasília (ACJC), no qual opera a Unidade de Recebimento de Entulhos (URE), está situado no centro-oeste do Distrito Federal a aproximadamente 20km de Brasília, a uma elevação de 1120m (Figura 3.1). O aterro é limitado a oeste pela nascente do Córrego Cabeceira do Valo, a oeste e sul pela Vila Estrutural, onde residem aproximadamente 40.000 moradores (PDAD, 2015), e, a nordeste pelo Parque Nacional de Brasília (PNB).

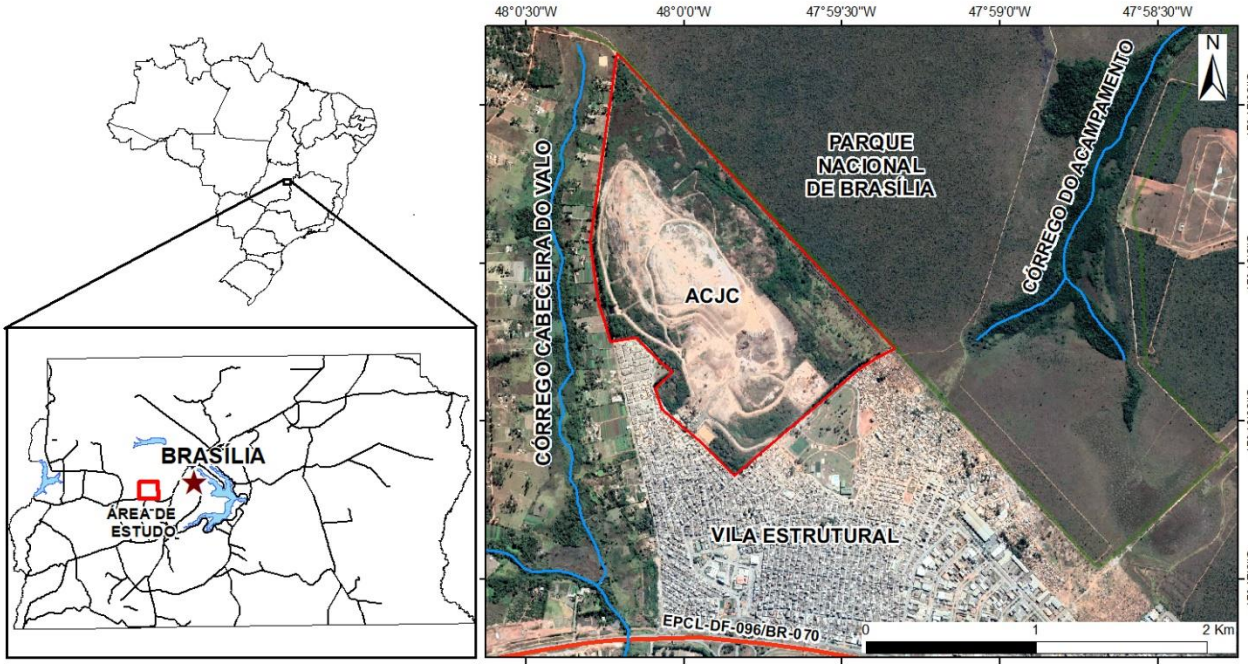

Figura 3.1 - Localização do ACJC.

3.2. HISTÓRICO E ATUAL OPERAÇÃO DO ACJC

As atividades de lançamento de resíduos sólidos no aterro tiveram início na década de 70, sendo estas oficialmente encerradas em 20 de Janeiro de 2018 (Carneiro, 2002; Cavalcanti, 2013; SLU, 2018). Durante os anos de funcionamento, o ACJC foi considerado um dos maiores da América Latina, com aproximadamente 200 ha de área e 50 metros de altura de resíduos sólidos depositados (Campos, 2018; Barbosa et al., 2015).

Os primeiros indícios de deposição de lixo na região onde hoje se situa o ACJC foram observados no limite sul da sua atual área, que ocorreu até meados de 1978 (Pereira et al., 1997; Nisiyama, 2019). Nesta época, os resíduos eram colocados em trincheiras de 2 a 4 metros de profundidade. O lixo depositado era compactado e recoberto com uma camada de solo de aproximadamente 50 cm de espessura. O solo utilizado para cobertura era retirado do próprio local durante a abertura de uma nova célula (Cavalcanti, 2013; Santos, 1996).

O progressivo aumento populacional do DF a partir de 1978 levou à crescente demanda por áreas de disposição final para os resíduos sólidos, dando início as atividades dentro dos atuais limites do ACJC. A partir de 1985 o ACJC se tornou a única área disponível para o lançamento de resíduos do DF, estando completamente coberta no final de 1996 (Carneiro, 2002; Greentec, 2012). A disposição de lixo era realizada em trincheiras de 80 a 100 metros de comprimento, 20 a 30 metro de largura e aproximadamente 4 metros de profundidade (Araújo, 1996; Santos, 1996). A Figura 3.2 ilustra de maneira cronológica como se deu a disposição de resíduos na região entre os anos de 1964 e 1997.

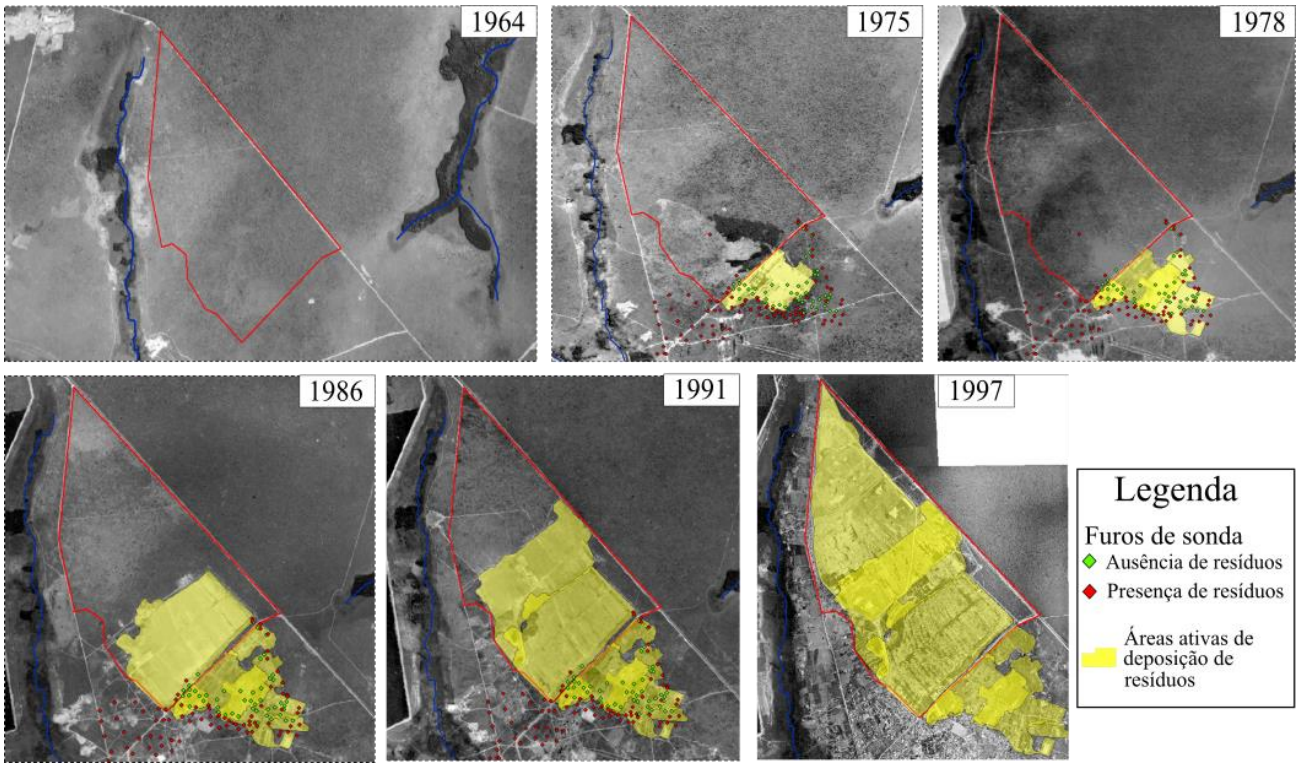

Figura 3.2 - Histórico da deposição de resíduos sólidos na área do ACJC entre os anos de 1964 e 1997. Fonte: Nisiyama (2019).

A disposição de resíduos em trincheiras já encerradas ocorreu até 2011 entre as porções sul e central da área do ACJC. Em 2012 iniciou-se a deposição de resíduos na porção norte da área,

próximo ao limite do aterro com a nascente do córrego Cabeceira do Valo. A partir de 2015, uma faixa de aproximadamente 300 metros de largura no limite do ACJC com o PNB tornou-se uma área embargada polo IBAMA. Neste mesmo período, mudanças administrativas e de operação do aterro permitiram a classificação deste como um aterro controlado (SLU, 2016; Nisiyama, 2019).

Quanto a composição dos resíduos lançados durante décadas no ACJC, estudos gravimétricos realizados por Junqueira (1995), Amorim e Aguiar (1978) e Distrito Federal (2018) indicam que os resíduos orgânicos compõem a maior porcentagem, seguido de papéis, plásticos, metais, vidros (Figura 3.3).

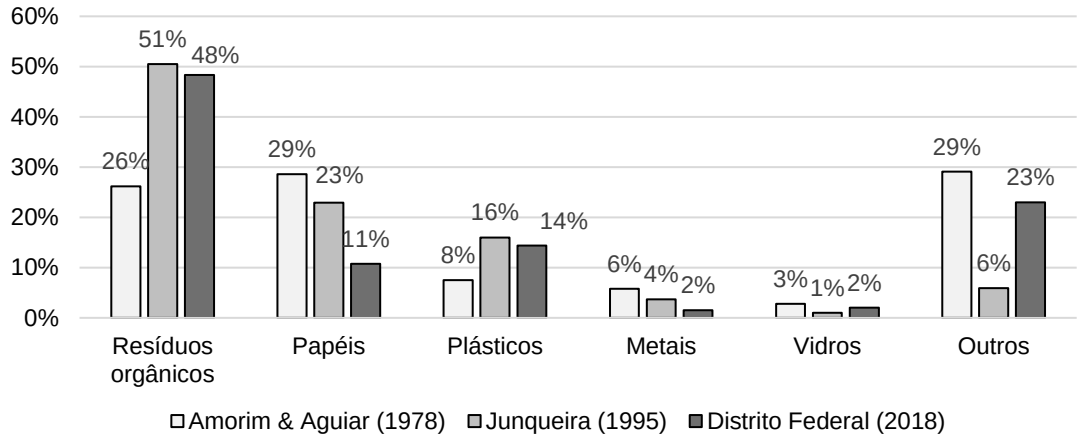

Figura 3.3 - Composição gravimétrica dos resíduos do DF. Fonte: Nisiyama (2019).

Com o encerramento das atividades de lançamento de resíduos sólidos domiciliares no ACJC e com a conformação do terreno, foi inaugurada no local, no fim de janeiro de 2018, a Unidade de Recebimento de Entulho (URE) com objetivo de receber resíduos de construção civil, podas e galhas. Para que essa atividade de recebimento fosse iniciada, o Sistema de Limpeza Urbana do Distrito Federal (SLU) implementou o Sistema de Gestão de Resíduos da Construção Civil. Esse sistema orienta os transportadores particulares, públicos e prestadores de serviços da SLU como realizar um cadastramento para fazer uso da URE. Esse cadastro permite que a AGEFIS faça a fiscalização dos veículos cadastrados para evitar a ocorrência de disposição de resíduos em vias e locais públicos (SLU, 2018).

Entre janeiro e setembro de 2019 aproximadamente 1.100.000 toneladas de resíduos foram recepcionados pela URE (SLU, 2019). Essa unidade conta com 149 drenos de captação e queima de gás, além de drenos de captação de percolados que direcionam os fluídos para uma

lagoa impermeabilizada. Segundo o SLU (2018), esses fluídos percolados retidos são posteriormente recirculados em áreas cujas atividades se encerraram dentro da Unidade. Este procedimento é realizado com o intuito de auxiliar na compactação dos resíduos e reduzir o volume dos líquidos pela evaporação.

3.3. ASPECTOS FISIOGRÁFICOS

O clima do Distrito Federal pode ser definido como tropical de savana e temperado chuvoso de inverno seco segundo a classificação de Köppen. Neste tipo climático, destacam-se duas estações com características distintas: inverno seco e com temperaturas amenas de aproximadamente 19°C; e verão quente e chuvoso, com temperaturas de aproximadamente 22°C (Cavalcanti, 2013). Como observado no gráfico da Figura 3.4, a média mensal de volume pluviométrico medida na estação do Jockey Club tem seus maiores valores entre os meses de outubro a abril, caracterizando o período de chuvas. Em contrapartida, a média pluviométrica entre os meses de maio a setembro não chegam a ultrapassar 50 mm, caracterizando o período de estiagem.

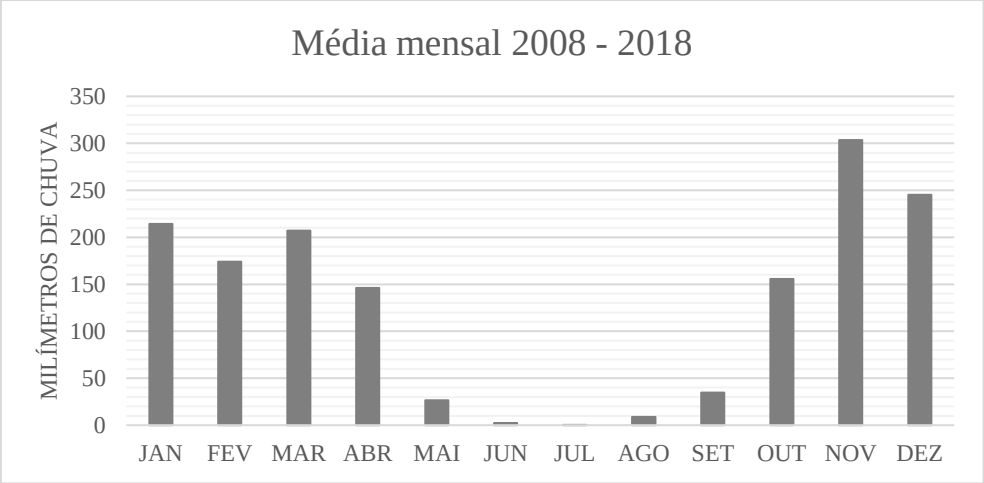

Figura 3.4 - Média mensal pluviométrica observada na estação do Jockey Club entre 2008 e 2018. Fontes dos dados: CAESB (2018).

A vegetação presente na região do ACJC era originalmente característica do bioma Cerrado, semelhante à encontrada no PNB. Este bioma possui árvores baixas, tortuosas e com ramificações irregulares (Cavalcanti, 2013). A intensa modificação do solo na região ocorreu principalmente entre os anos de 1991 e 1997, com a distribuição de lotes nas adjacências do aterro, corroborando também para a expansão da deposição de lixo no ACJC (Figura 3.2).

Segundo a CODEPLAN (2017), a área do ACJC é classificada geomorfologicamente como Plano Intermediário, com altitudes variando de 950 a 1200 metros (Figura 3.5). A região é caracterizada por chapadas, relevo suave ondulado com declividade menor que 10%, com restrita amplitude topográfica e presença de rampas longas. Na área ocorre o predomínio do processo de pedogênese sobre o transporte e deposição (Novaes-Pinto, 1994).

Quanto a hidrografia, cabe ressaltar que o ACJC está localizado em uma região caracterizada como um divisor hidrográfico. A área delimita a sub-bacia do córrego Cabeceira do Valo, localizado a oeste do aterro, o qual drena suas águas para sul até encontrar o córrego Vicente Pires e, posteriormente o córrego Riacho Fundo (Figura 3.5). O córrego do Cabeceira do Valo é utilizado pelos moradores para irrigação de hortaliças, piscicultura e dessedentação de animais. A área do aterro também delimita a sub-bacia do Córrego do Acampamento, localizado dentro dos limites do PNB. Já a norte, delimita a sub-bacia do Ribeirão Bananal. Todos os cursos d'água citados são pertencentes a bacia do Paranoá e estão divididos entre as unidades hidrográficas do Córrego Bananal e Riacho Fundo (Figura 3.5).

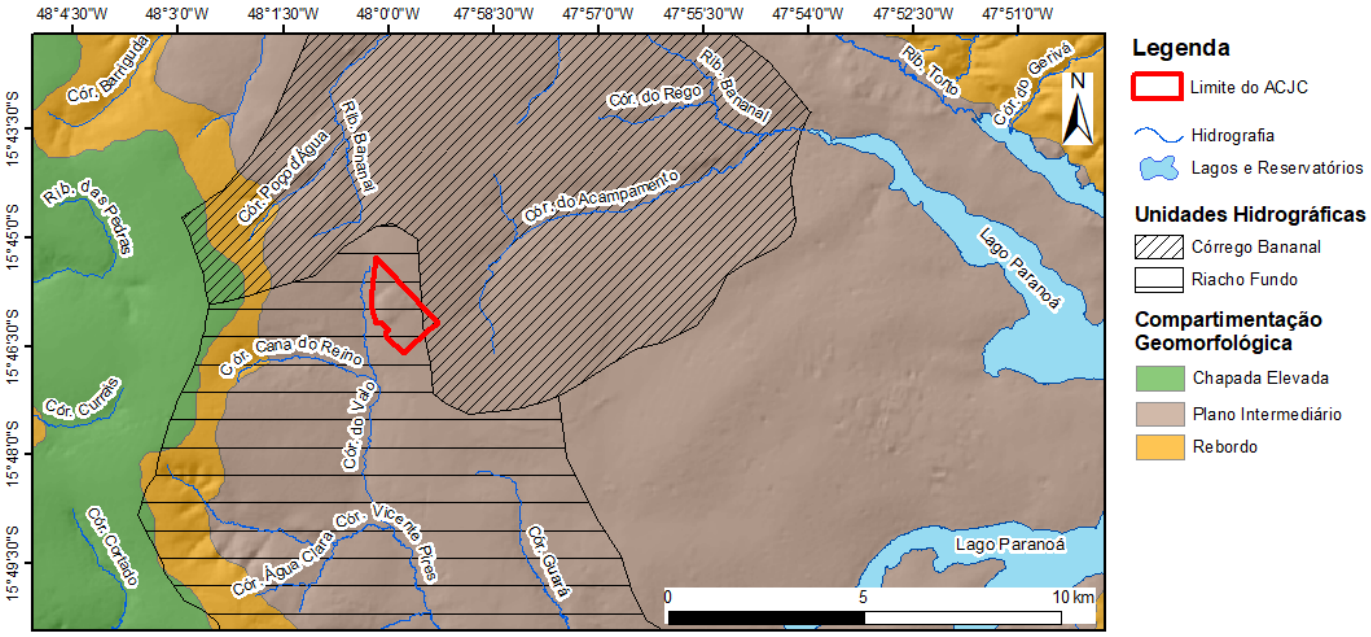

Figura 3.5 - Mapa Geomorfológico e Hidrográfico da região do ACJC. Fonte dos dados: ZEE (2011).

A distribuição dos solos no DF está diretamente relacionada à compartimentação geomorfológica da região. As três principais classes descritas são os Latossolos Vermelhos (LV), Latossolo Vermelho-Amarelo (LVA) e Cambissolo (C). Estes solos ocupam cerca de 85,5% da área total do DF. Na região do ACJC estão presentes as classes LV, LVA e, próximo

às drenagens, solos hidromórficos, classificados como Gleissolo Háplico (Figura 3.6). A classe de latossolos é caracterizada por intensa lixiviação de bases trocáveis. São solos de textura argilosa, não hidromórficos, com alta concentração de oxi-hidróxidos de ferro (goetita e hematita) e alumínio (gibbsita). São solos porosos, permeáveis e fortemente drenados (EMBRAPA, 1978). Os LV e LVA diferenciam-se apenas pela cor do horizonte B, sendo este uma variação do vermelho ao amarelo nos LVA. Quanto aos Gleissolos Háplicos, estes apresentam textura muito argilosa, plásticos, com estrutura granular no horizonte superficial. Horizontes húmicos e associação com Organossolo também são comuns neste tipo de solo (ZEE, 2011).

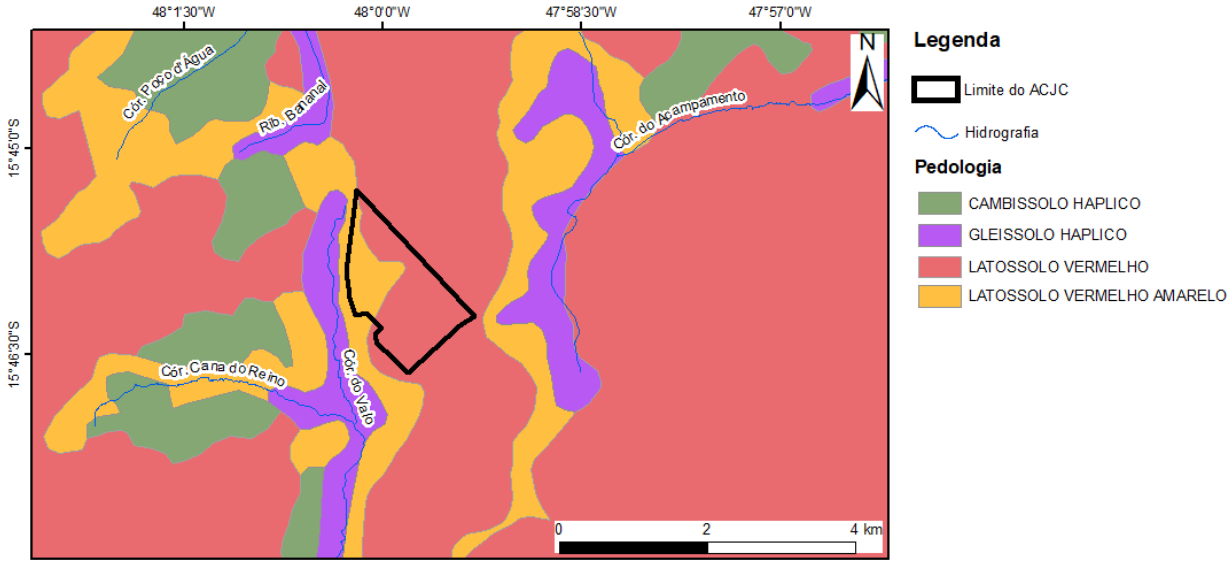

Figura 3.6 - Mapa Pedológico da região do ACJC. Fonte dos dados: ZEE (2011).

A hidrogeologia da região do ACJC é segmentada em aquíferos de domínio intergranular (ou poroso), e fraturado (Figura 3.7) (Campos e Gonçalves, 2015). Devido a predominância de latossolos na região, o principal sistema aquífero do domínio intergranular é o P1 (Figura 3.7-A). Este sistema é caracterizado pela alta condutividade hidráulica vertical (> 10^{-6} m/s), vazões médias de aproximadamente 0,8 m³/h e espessura acima de 20 metros (Campos, 2004). Os gleissolos háplicos fazem referência ao sistema P3 (Figura 3.7-A). Este sistema apresenta solos com espessura entre 5 e 10 metros e com baixa condutividade hidráulica (<10^{-6} m/s).

Os aquíferos que compõem o sistema fraturado estão diretamente relacionados à geologia local. Neste caso, a área do ACJC está situada sobre a Formação Ribeirão do Torto, do Grupo Paranoá. Esta formação é caracterizada por ardósias e a presença de lentes quartizíticas (Campos et al.,

2013). Quanto a classificação hidrogeológica, o domínio fraturado da região do ACJC pertence ao Sistema Paranoá e Subsistema A (Campos, 2004) (Figura 3.7-B). A nível local, a presença de lentes quartizíticas onde o ACJC está situado leva ao desenvolvimento de zonas de maior permeabilidade, o que afeta diretamente a propagação de contaminantes nos solos e sistemas aquíferos (Carneiro, 2002; Barbosa et al., 2015).

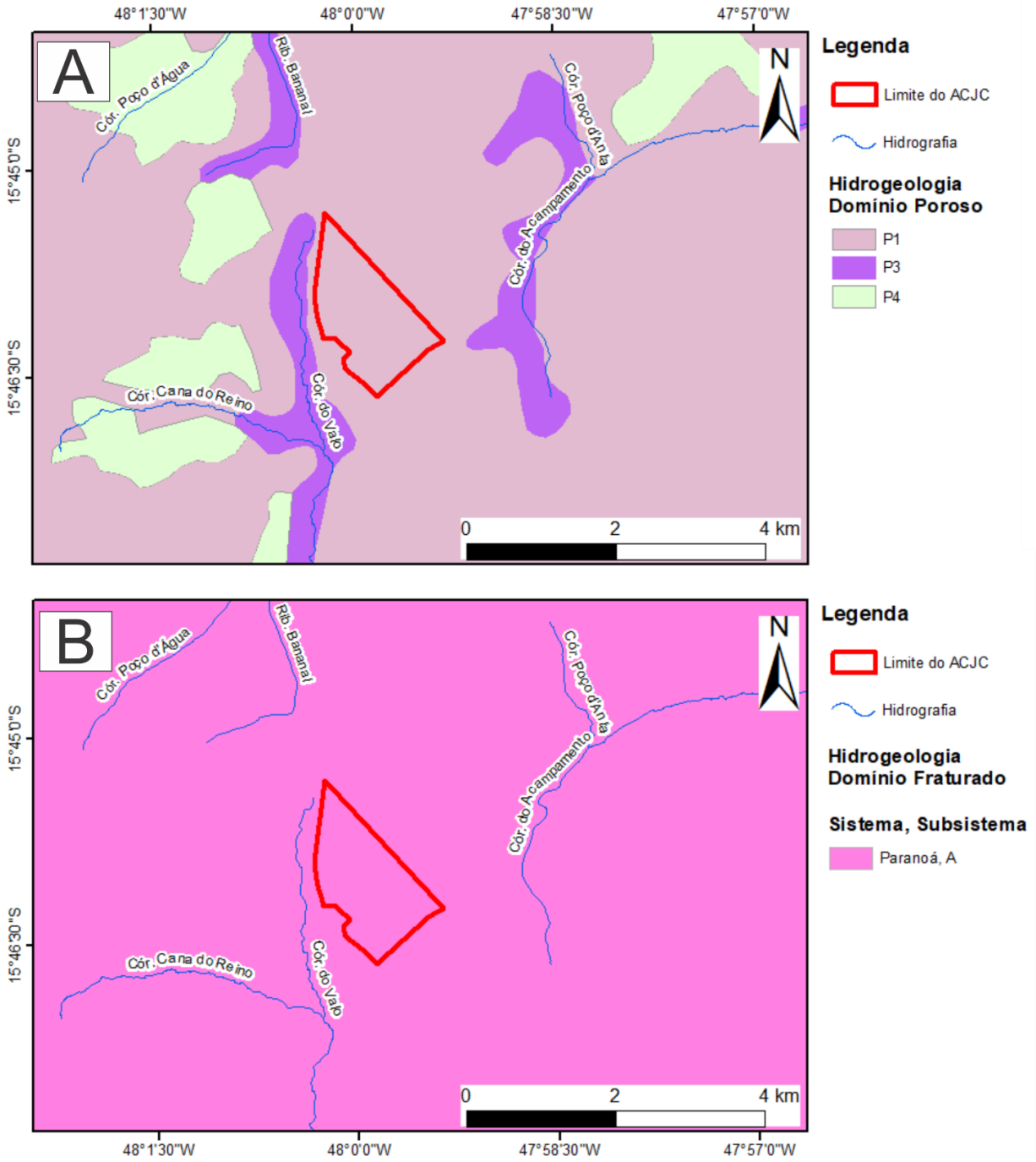

Figura 3.7 - Mapas Hidrogeológicos da região do ACJC sendo, A) Domínio Intergranular (ou Poroso) e B) Domínio Fraturado. Fonte dos dados: ZEE (2011).

4. MATERIAIS E MÉTODOS

4.1. AMOSTRAGEM E PRESERVAÇÃO

Neste estudo foram coletadas amostras de lixiviado e águas subterrânea e superficial, com distribuição de pontos conforme a Figura 4.1. As campanhas de amostragem foram realizadas a cada dois meses e tiveram por objetivo cobrir um ciclo hidrológico, caracterizados por períodos de chuva e seca. Os dados pluviométricos utilizados nesta pesquisa foram coletados na estação do Jockey Club, localizada dentro dos limites atuais do ACJC e foram fornecidos pela CAESB. No Anexo 1 são apresentados detalhes sobre a coleta das amostras, incluindo datas de realização das campanhas, tipos de amostras coletadas (lixiviado, água superficial e/ou água subterrânea) e período sazonal que a amostra representa (chuva ou seca).

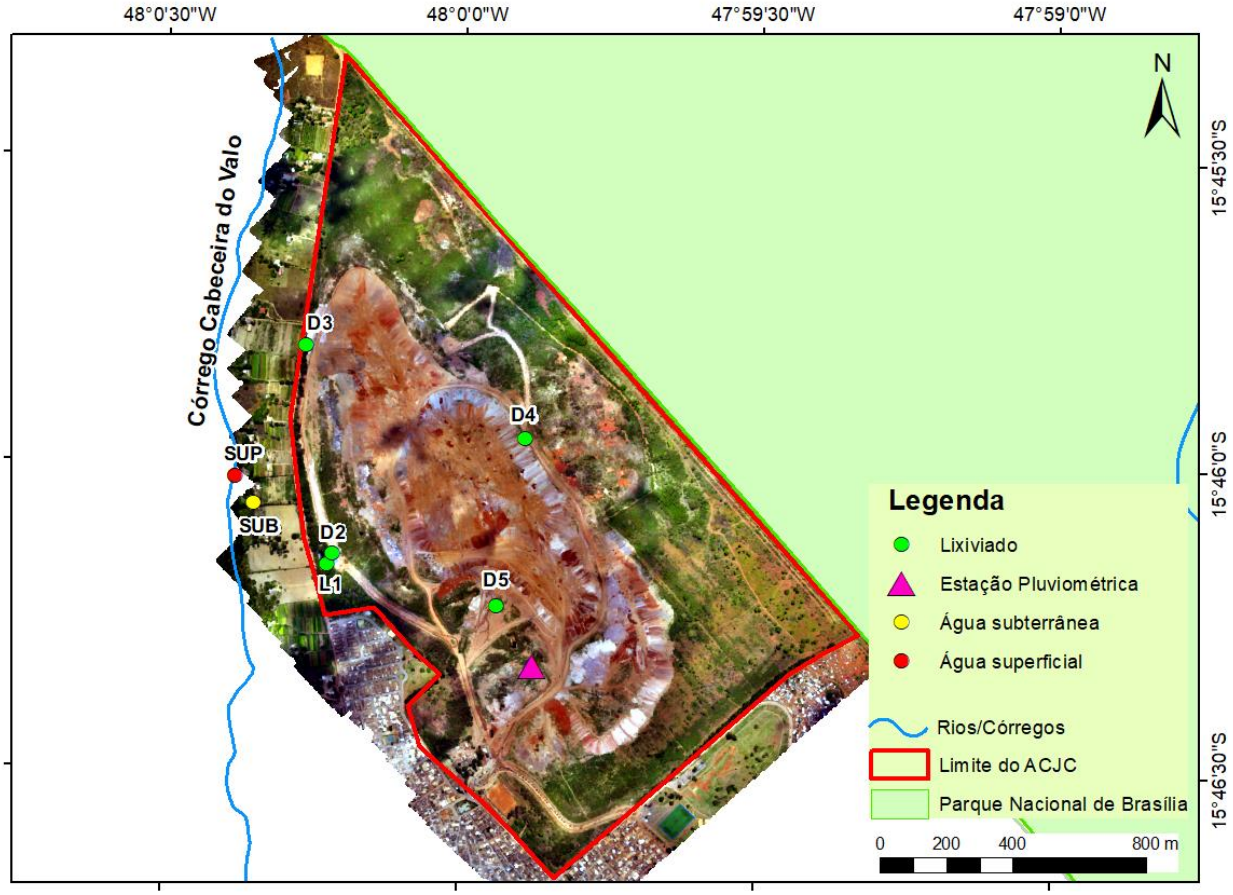

Figura 4.1 - Localização dos pontos de amostragem e da estação pluviométrica

As amostras de lixiviado foram coletadas em cinco pontos conforme mostra a Figura 4.1. Os pontos foram escolhidos de forma a cobrir os principais fluxos de saída de lixiviado dentro do ACJC. O ponto L1 representa a lagoa de contenção e o ponto D2 é o dreno de chegada de

lixiviado na lagoa, como demonstrado na Figura 4.2-A e B. Os pontos D3, D4 e D5 são drenos que se diferenciam pela profundidade e pela propensão a serem afetados por processos de superfície, como, por exemplo, a chuva. Os pontos D3 e D5 são pouco afetados pela chuva e representam variações de longo prazo no aterro, sendo D3 mais raso e D5 mais profundo (Figura 4.2-C e E, respectivamente). O ponto D4 é um dreno superficial e aflorante que pôde ser amostrado apenas durante o período chuvoso Figura 4.2-D.

Figura 4.2 - Fotos representativas dos cinco pontos de amostragem de lixiviado no ACJC. A) Ponto L1; B) Ponto D2; C) Ponto D3; D) Ponto D4 e E) Ponto D5, localizados espacialmente conforme o mapa da Figura 4.1.

As amostras de água subterrânea foram coletadas em um par de poços multiníveis pertencentes a Rede de Monitoramento das Águas Subterrâneas da ADASA, que se localizam a oeste do aterro (Figura 4.3-B). Um dos poços possui 30 metros de profundidade e é alimentado pelo aquífero de domínio intergranular. O outro possui cerca de 130 metros de profundidade e capta

água do domínio fraturado. O par de poços está localizado a aproximadamente 130 metros de distância do ACJC, como demonstrado na Figura 4.3.

A amostragem de água superficial foi realizada no Córrego Cabeira do Valo, localizado a oeste do aterro. O ponto fica próximo aos poços multiníveis e a aproximadamente 210 metros do ACJC (Figura 4.3-A). Neste ponto, o dono da chácara realiza o bombeamento temporário de água para fins de irrigação. O córrego apresenta pouca correnteza e é coberto por vegetação (Figura 4.3-A).

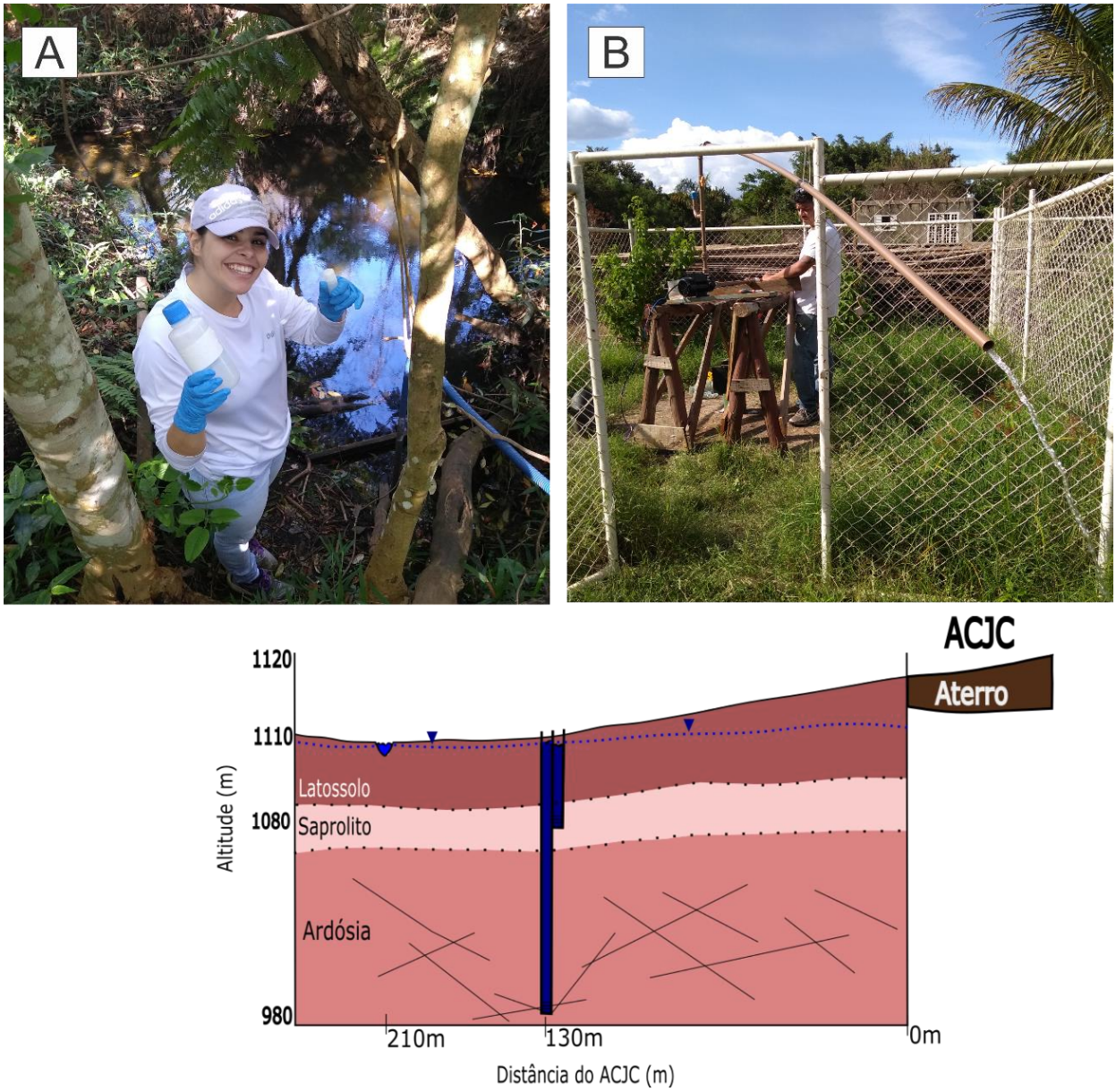

Figura 4.3 - Fotos representativas dos pontos de coleta água superficial (A) e subterrânea (B) assim como a distância destes até o ACJC

Os frascos de polietileno de 500 ml e 20 ml utilizados na amostragem de água e lixiviado foram primeiramente lavados com água destilada e, em seguida, com HNO_3 5% (v/v) e aquecidos a 50°C por 48 horas. Após este período, foram lavados continuamente com água destilada e deixados em repouso até a secagem.

As amostras para análises dos componentes orgânicos (DOC total e δ^{13}C-DOC) foram armazenadas em frascos de vidro âmbar de 60 mL. Antes da coleta, esses frascos foram embalados em papel alumínio e aquecidos em mufla à 450°C por 1 hora de forma a eliminar quaisquer eventuais contaminações.

Antes da coleta, os frascos foram ambientados três vezes com a água ou lixiviado do ponto amostrado. Em seguida, preencheu-se os frascos evitando-se o aprisionamento de gases atmosféricos. Para as águas subterrâneas, os poços foram previamente purgados, retirando aproximadamente três vezes o volume da água do poço. Este procedimento teve por objetivo assegurar que a amostra de água que está sendo coletada seja representativa da característica real do aquífero. Após a amostragem, todas amostras foram mantidas em isopor com gelo à uma temperatura de aproximadamente 4°C até que as análises fossem realizadas.

4.2. PROCEDIMENTOS ANALÍTICOS

O roteiro esquemático das alíquotas coletadas e técnicas analíticas utilizadas é apresentado na Figura 4.4. A descrição detalhada de cada procedimento será apresentada nos tópicos desta seção.

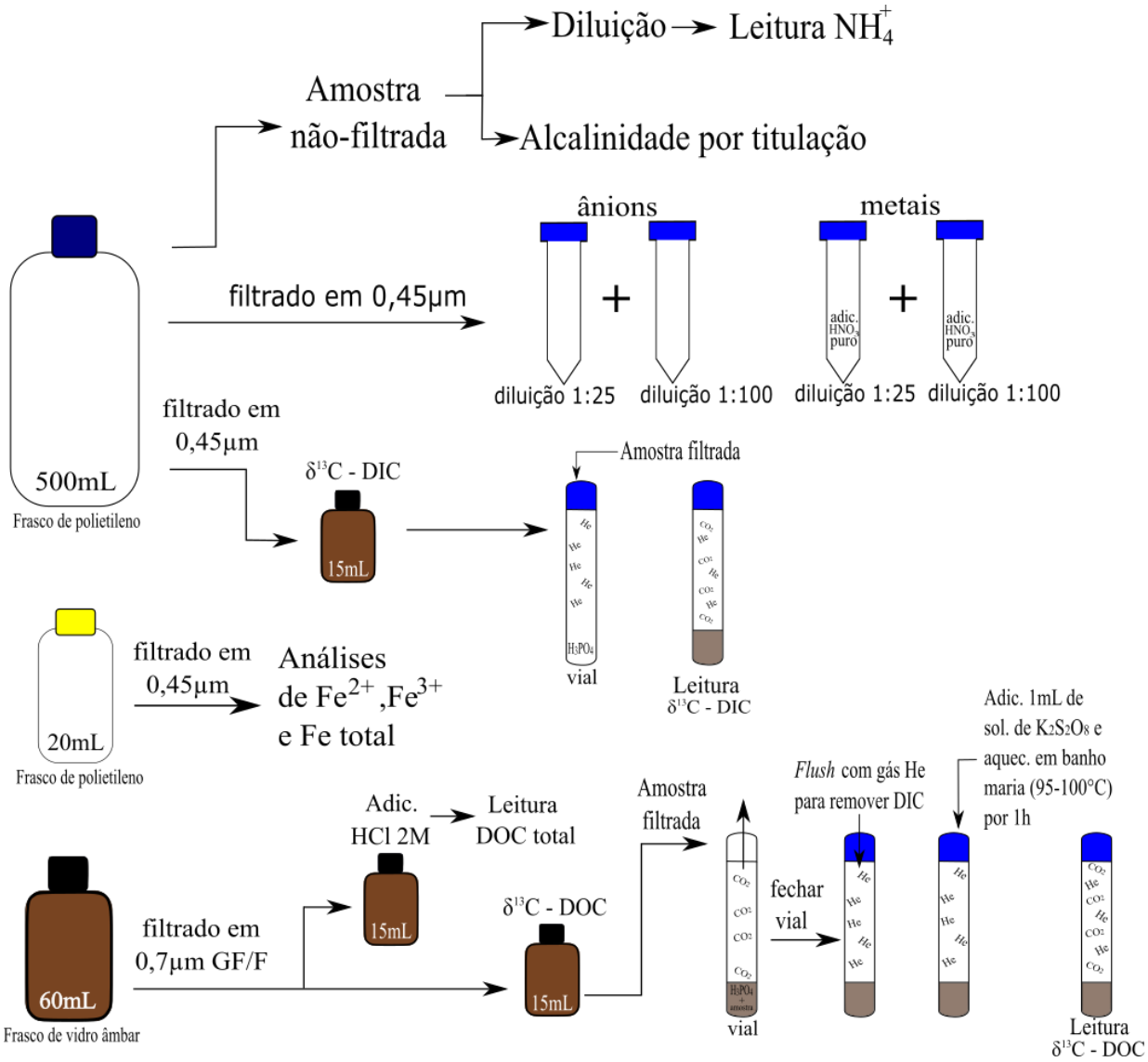

Figura 4.4 - Fluxograma da divisão das alíquotas coletas em campo e resumo das técnicas analíticas aplicadas.

PARÂMETROS DETERMINADOS IN-SITU

Os seguintes parâmetros foram determinados in-situ: pH, condutividade elétrica (CE), potencial de oxidação-redução (ORP) e oxigênio dissolvido (OD). Os dados de pH foram obtidos com sonda multi-parâmetro WTW acoplado ao leitor pH/Cond 340i (precisão de 0,01); e os dados de ORP foram obtidos com eletrodo de vidro com anel de platina (precisão de 0,01 mV). A CE foi medida com a sonda EUTECH Cond 6+ acoplada ao eletrodo EC-CONSEN91B (resolução de 1 µS/cm). O OD foi determinado com o auxílio da sonda FiveGo da marca Mettler Toledo

(precisão de 0,01 mg/L). Todas as sondas foram calibradas antes de cada campanha de amostragem.

ALCALINIDADE E ÍON AMÔNIO (NH_4^+)

As determinações de alcalinidade e concentração do íon NH_4^+ foram realizadas com as amostras não-filtradas, logo após o retorno das campanhas de amostragem. A alcalinidade foi determinada pelo método titulométrico utilizando o titulador automático da marca Schott, modelo Titroline easy do Laboratório de Geoquímica da UnB. Para tal, uma solução de ácido sulfúrico (H_2SO_4) foi lentamente adicionada à 25 mL de amostra até que o pH atingisse o valor de 4,2 (concentração do ácido: 1,0 M para lixiviado e 0,4 M para amostras de água). A alcalinidade da amostra foi calculada conforme a Equação 4.1, onde $[H_2SO_4]$ é a concentração da solução de ácido sulfúrico em mol/L; MM (HCO_3^-) é a massa molar do íon bicarbonato em g/mol; $V(H_2SO_4)$ é o volume em ml de solução de ácido sulfúrico para que o pH da amostra atingisse 4,2; e $V_{amostra}$ o volume em ml da amostra.

4.1) $$Alcalinidade\left(em\ \frac{mg}{L}HCO_3^-\right) = \frac{[H_2SO_4]*MM\ (HCO_3^-)*1000\left(\frac{mg}{g}\right)*V(H_2SO_4)}{V_{amostra}}$$

Para a determinação do íon NH_4^+ foi necessário realizar a diluição das amostras de lixiviado e de água do aquífero intergranular, visto que a concentração deste íon ultrapassava o limite de detecção do procedimento analítico (entre 0 e 2.50 mg/L). As diluições de 1:250 e 1:2500 para as amostras de lixiviado e de 1:25 para água do aquífero intergranular foram realizadas com água ultrapura (Milli-Q). Após esse procedimento, adicionou-se o kit de reação do amônio que consiste em: estabilizador mineral, álcool polivinílico e reagente Nessler. A solução foi homogeneizada e a leitura foi realizada pelo método colorimétrico em 425 nm no equipamento de marca HACH modelo DR 2000 do Laboratório de Geoquímica da UnB.

ÂNIONS E METAIS

As alíquotas para análise das concentrações de ânions e metais foram previamente filtradas utilizando-se um filtro de seringa PES com poros de 0,45 µm da marca Analítica. As amostras foram então diluídas em 1:100 e 1:25 sendo que as frações utilizadas para a determinação de metais foram acidificadas com de ácido nítrico (HNO_3) (pH da amostra ≈ 2). A concentração dos ânions fluoreto (F^-), cloreto (Cl^-), nitrato (NO_3^-), fosfato (PO_4^{3-}) e sulfato (SO_4^{2-}) foram determinados por cromatografia iônica (IC) da marca Dionex modelo ICS90 no Laboratório de

Geoquímica da UnB. As características do sistema utilizado foram: fluxo isocrático de eluente Na_2CO_3:$NaHCO_3$ 3,5:1 mM a 1,2 ml/min e pressão aproximada de 1500 psi; volume de injeção de 25 µL definido por alça de amostragem; detector de condutividade suprimida modelo CS5; coluna e pré-coluna do tipo troca iônica com superfície funcionalizada de alquil amônio quaternário, modelos AS14A e AG14A, respectivamente; supressor de condutividade modelo AMMS-300 regenerado com H_2SO_4 50 mM.

Um total de 24 metais foram determinados para cada amostra por Espectrometria de Emissão Atômica por Plasma Acoplado Indutivamente (ICP-OES, Agilent 5100) sendo estes: Ca, Mg, Na, K, Al, As, Ba, Cd, Co, Cr, Cu, Fe, Li, Mn, Mo, Ni, P, Pb, Si, Sr, Ti, V, Zn e Zr. O plasma foi mantido pelo gás argônio a um fluxo principal de 11,98 L/min, pressão de argônio 527,9 kPa, fluxo de gás auxiliar de 1,00 L/min, fluxo do nebulizador 0,7 L/min, *back pressure nebulizer* 307,9 kPa e potência RF de 1199,6 W. Vale ressaltar que, como não houve digestão da amostra antes da realização das análises, as concentrações dos metais apresentados referem-se às espécies dissolvidas.

Os resultados das análises foram avaliados segundo o balanço iônico dos íons presentes em maior concentração: Ca^{2+}, Mg^{2+}, Na^{+}, K^{+} e NH_4^{+} para cátions e, para ânions, Cl^{-}. NO_3^{-}, SO_4^{2-} e HCO_3^{-} (referente a alcalinidade). O erro prático (EP) foi calculado conforme a Equação 4.2 e a diluição que apresentou menor erro foi a utilizada na análise de dados. No cálculo do balanço iônico e EP as concentrações foram expressas em meq/L.

4.2) $$EP\ (\%) = \frac{(\sum cátions - \sum ânions)}{\sum (cátions + ânions)} * 100$$

DETERMINAÇÃO DE FERRO FERROSO (Fe^{2+}), FÉRRICO (Fe^{3+}) E FERRO TOTAL

A determinação das concentrações de Fe^{2+}, Fe^{3+} e Fe total foi realizada utilizando metodologia adaptada de Viollier et al. (2000) em Espectrofotômetro T-60 UV-VIS PG INSTRUMENTS do Laboratório de Geoquímica da UnB. Para isso, as seguintes soluções foram utilizadas:

A) Ferrozina 10^{-2} M em CH_3COONH_4 10^{-1} M (complexante com Fe^{2+})

B) Hidroxilamina (H_2NOH HCl) 1,4 M em HCl 2 M (redutor)

C) Acetato de amônio (CH_3COONH_4) 10 M e pH 9,5 ajustado com NH_4OH (tampão)

A curva de calibração com concentrações de 0; 0,5; 1,0; 3,0 e 5,0 de Fe^{2+} foram preparadas com $FeCl_2$.

As amostras foram previamente filtradas em membranas de 0,45 µm de poro antes das análises. Posteriormente foi adicionado 0,2 mL de ferrozina (solução A) em 2,0 mL de amostra ambientadas e, em sequência, a absorbância foi medida em 562 nm para a determinação de Fe^{2+}. Neste 2,2 mL de solução, foi a adicionado de 0,2 mL de hidroxilamina (solução B) e, depois, deixado em repouso por 10 minutos, garantindo a completa redução do Fe. Em seguida, 0,1 mL da solução tampão (solução C) foi adicionada, ajustando-se o pH. Assim, a concentração de Fe total foi determinada em 562 nm. A concentração de Fe^{3+} foi calculada através da diferença entre Fe total e Fe^{2+}. Os resultados de absorbância foram plotados em uma curva titulométrica e as concentrações foram calculadas a partir de uma curva de calibração, multiplicando-as sempre pelos devidos fatores de diluição.

ANÁLISES ISOTÓPICAS (δ^{13}C-DIC, δ^{13}C-DOC) E CARBONO ORGÂNICO DISSOLVIDO (DOC) TOTAL

As amostras para a determinação da razão isotópica do carbono inorgânico dissolvido (δ^{13}C-DIC) foram filtradas em filtros de seringa PES (Analítica) com poros de 0,45 µm. Após filtradas, as amostras foram devidamente seladas e preservadas em ambiente frio (0 – 4°C) para que, no dia seguinte, fossem preparadas para leitura. Os frascos de borossilicato utilizados para a análise da δ^{13}C-DIC foram previamente preparados com três gotas de ácido fosfórico (H_3PO_4) e submetidos ao procedimento de *flush* de com gás hélio (He), expulsando assim os gases atmosféricos (Figura 4.4). Posteriormente, as amostras foram inseridas nos frascos com seringa (0,1 ml para o lixiviado e 1,0 ml para as amostras de água). A reação da amostra com o H_3PO_4 no interior do vial leva a liberação de CO_2, cuja razão isotópica foi determinada utilizando o Gas Bench II conectado ao espectrômetro de massa Delta V Plus (IRMS) da marca Thermo Fisher Scientific. Esta razão é expressa pela notação delta (δ) em "*per mille*" (‰), na qual se

compara a razão isotópica da amostra a um padrão previamente definido que, neste caso, é o Vienna Pee Dee Belemnite (VPDB).

Para a determinação da razão isotópica do carbono orgânico dissolvido (δ^{13}C-DOC) e da concentração total do DOC, as amostras foram filtradas em filtros de vidro (Whatman GF/F) com poros de 0,7 µm. Os filtros foram previamente queimados em mufla a 450°C por 1 hora, assim como os recipientes de amostragem e de preservação da amostra. Assim como na análise de δ^{13}C-DIC, as amostras filtradas foram armazenadas em ambiente frio (0 – 4°C) até data de análise. Para a determinação do δ^{13}C-DOC a amostra foi inserida em frascos de borossilicato já contendo aproximadamente três gotas de H_3PO_4 (Figura 4.4). Os frascos abertos foram deixados de repouso para que houvesse a liberação do DIC. Em seguida os frascos foram fechados e submetido ao procedimento de *flush* de com gás hélio (He) (Figura 4.4). Em sequência, foi inserida 1 ml de solução de persulfato de potássio ($K_2S_2O_8$) e aquecido em banho maria a 95–100 °C por 1 hora, oxidando a matéria orgânica e liberando o CO_2 para a parte gasosa do frasco (Figura 4.4). O equipamento utilizado e os valores do padrão de comparação das leituras de δ^{13}C-DOC foram os mesmos utilizados para na determinação do δ^{13}C-DIC. Em ambos métodos, as amostras foram analisadas em duplicatas.

As alíquotas separadas para determinação do DOC total contaram com uma etapa de acidificação com HCl 2 M (pH ≈ 2) com o intuito de preservação e liberar o DIC presente na amostra. As concentrações de DOC total foram determinadas por oxidação catalítica a alta temperatura (HTCO) com detecção infravermelha de CO_2 no equipamento Total Carbon Analyzer (Shimadzu TOC-L CPH/CPN) do Laboratório de Inorgânica e Materiais (LIMA) do Instituto de Química da UnB. O método aplicado foi o NPOC, utilizando ar sintético como *carrier gas*. As amostras foram analisadas em duplicatas e o coeficiente de variação entre elas foi de aproximadamente 1%.

5. RESULTADOS E DISCUSSÃO

5.1. ARTIGO 1: SEASONAL VARIATIONS OF GEOCHEMICAL PARAMETERS FOR A TROPICAL LANDFILL: IMPLICATIONS FOR LANDFILL STABILIZATION

Authors:

1 - Giovanna Orletti Del Rey* [a] (*corresponding author: giovannaodelrey@gmail.com)

2 - Roberto Ventura Santos [a]

3 - Luciano Soares da Cunha [a]

4 - Gabriela Silva Ferreira [a]

[a] University of Brasília – UnB, Asa Norte, 70910-900, Brasília - DF, Brazil

Abstract:

Landfills stabilization stages and organic matter decomposition depend on parameters such as the age of the landfill, the composition of the deposits, and the level of confinement. In the absence of free oxygen, redox agents (e.g., SO_4^{2-}, NO_3^-) and methanogenesis reactions control the decomposition of organic matter. The landfill biological stability is usually assessed by parameters such as pH, biochemical oxygen demand, chemical oxygen demand, dissolved organic carbon, concentration of heavy metals, and biogas composition. This study evaluates the stabilization stage of a 50 years old tropical landfill located in Central Brazil, by application of physicochemical analyses, dissolved carbon isotope data ($\delta^{13}C$), redox reactions, and concentration of released CO_2 and CH_4 gases. Seasonal variations of these parameters are modified by rainwater inflow, which carries oxygen into the landfill. An increase in oxygen leads to a decrease in carbon isotopic composition of dissolved CO_2 and an increase in redox-dependent species such as Fe^{3+}, SO_4^{2-}, and NO_3^-. Our data show that most of the landfill is at the stable methanogenic stage and that periodic oxygen input by rainwater affects methane production. Therefore, in order to improve methane production, landfills should avoid rainwater inflow into the landfill and set a closed recirculation procedure.

Keywords

Landfill

Stabilization process

Organic matter

Stable isotope

Redox

1. Introduction:

Municipal solid waste (MSW) landfills are a low-cost way of dispose refuse that may involve risks to human health and environment, mainly because most landfills started as dumpsites without engineered liners (Kjeldsen et al., 2002; van Turnhout et al., 2018). Primary contaminants generated in landfills are leachate and gases, such as methane (CH_4) and carbon dioxide (CO_2). Leachate produced in MSW is induced by rainfall that percolates through the refuse layers. It is accompanied by leaching and biodegradation reactions that result in a very complex effluent composed of organic and inorganic compounds (Adeolu et al., 2011; Kjeldsen et al., 2002; Lee and Ko, 2006).

Microbiological and chemical compositions of leachates depends on different aspects, including the nature of the deposits, landfill age, operational mode and mechanisms of organic matter degradation (Engelmann et al., 2018; Kjeldsen et al., 2002). Environmental conditions such as seasonal rainfall and temperature variations can also affect leachate composition (Barella et al., 2013; Porowska, 2015). Generally, leachate is composed of (1) dissolved organic matter, usually organic acids; (2) inorganic macrocomponents, such as calcium (Ca), magnesium (Mg), sodium (Na), potassium (K), ammonium (NH_4^+), iron (Fe), manganese (Mn), chloride (Cl^-), sulfate (SO_4^{2-}), and bicarbonate (HCO_3^-); (3) heavy metals, such as cadmium (Cd), chromium (Cr), copper (Cu), lead (Pb), nickel (Ni) and zinc (Zn); and (4) xenobiotic organic compounds, which includes aromatic hydrocarbons, chlorinated aliphatics, phenols, pesticides and plasticizers (Christensen et al., 2001; Kjeldsen et al., 2002).

Landfills are complex biological systems that may be biologically stable after decomposition of biodegradable organic matter (He et al., 2011; Shalini et al., 2010). The assessment of the long-term emission potential of gases and leachates, and hence the environmental impact of MSW, is mainly related to the biological stability of solid waste (He et al., 2011). The level of organic matter degradation is essential to assess the status of landfill leachate and to determine whether it has reached the required conditions for landfill closure (He et al., 2011; Wimmer et al., 2013). The stored waste in landfills undergoes complex stages of biological and chemical reactions, during which the refuse decomposition can vary in different parts of the landfill (Kjeldsen et al., 2002).

Landfills biological stability is usually assessed based on parameters such as pH, Biochemical Oxygen Demand (BOD), Chemical Oxygen Demand (COD), the concentration of heavy metals and biogas composition (Kjeldsen et al., 2002; Porowska, 2016). Dissolved Organic Carbon

(DOC) concentration is also an important parameter to assess the landfill stabilization process because this concentration decreases consistently during maturation, reaching the lowest values at advanced stages (He et al., 2011; Zmora-nahum et al., 2005).

This study is aimed at evaluation of the stabilization stage of a tropical landfill located in Central Brazil. The chosen site is considered the largest MSW landfill in Latin America, with about 20 million tons of buried solid waste. We have used the carbon isotope composition ($\delta^{13}C$) of Dissolved Inorganic Carbon (DIC) ($\delta^{13}C$-DIC) and other geochemical parameters in order to constrain the degradation level of the organic matter. We have also addressed the seasonal variations of these parameters, especially the relationship between the isotopic data and the availability of electron acceptors in the system. Various studies have reported changes of $\delta^{13}C$-DIC in landfills during different stages of their evolution (Mohammadzadeh and Clark, 2008; Porowska, 2016, 2015; Wimmer et al., 2013); however, there are only a few investigations focused on large landfills in tropical areas. Most studies focused on the carbon isotope variations without considering water influx and its role as oxygen carrier into the system. Besides affecting the carbon isotopes, oxygen-rich waters also change redox dependent species such as Fe^{2+}, Fe^{3+}, SO_4^{2-}, NH_4^+, and NO_3^-. Under tropical conditions, temperatures tend to strengthen biological activities all year long, promoting faster decomposition of the organic matter. The Jockey Club of Brasília Landfill has been in operation for more than 50 years and is a unique area to address and better understand organic matter degradation in these environments.

1.1. Study area

The Jockey Club of Brasília Landfill (JCBL) is located in Brazil Federal District, about 20 km from Brasília downtown. The landfill was placed on a watershed at an elevation of 1120 meters. The Cabeceira do Valo stream borders the western side of the area, while the Brasília National Park and the spring of the Acampamento stream border its eastern side (Figure 5.1). A district that currently has about 40,000 people ("Vila Estrutural") was built around the JCBL since its early days.

The local climate is characterized by strong seasonality with a well-defined dry (May to September) and rainy (October to April) periods. About 90% of rainfall occurs between October and April, being the average precipitation close to 350 mm per month (INMET, 2018). Shallow and deep aquifers underlie the landfill site: the shallow aquifer is about 30 meters deep and comprises an Fe-rich oxisol, with a high hydrological conductivity (Campos, 2004); the deep

aquifer is hosted by fractured slates of the Paranoá Group locally interbedded with lenses of quartzite (Barbosa et al., 2015; Campos et al., 2013).

The deposition of waste in the landfill lasted until January 2018, when the area began to receive only construction waste (RCC) and tree pruning. During its operations, the JCBL was the largest MSW landfill of Latin America, covering an area of 200 ha and accumulating approximately 50 meters of residue (Barbosa et al., 2015; Koide and Bernardes, 1998). The estimated gravimetric composition grounded in the JCBL is about 40 to 50% composed by organic refuse, 20 to 25% by paper, 10 to 15% by plastic, 3 to 5% by metals, 1 to 3% by glass, and 10 to 20% by other materials. The JCBL operation mode involves leachate recirculation by pumping drained leachate from a treatment lagoon back to the trash dump.

2. Materials and methods

Landfill stability and organic matter degradation level were evaluated based on leachate geochemical parameters and concentration of released CO_2 and CH_4. Leachate sampling was performed every two months between September 2018 and September 2019 at five different sites (Figure 5.1), while gas was sampled once (April 2019) in the gas wells distributed through the landfill area (Figure 5.1).

The five sampling point of leachate are representative of the main outflow borders of the landfill: L1 is a leachate lagoon; D2 in a leachate drain that delivers liquids directly into the leachate lagoon; D3 is a leachate drain with low drainage; D4 is an outcropping drain that has fluids only during the rainy season, and D5 is also a leachate drain with better drainage then D3.

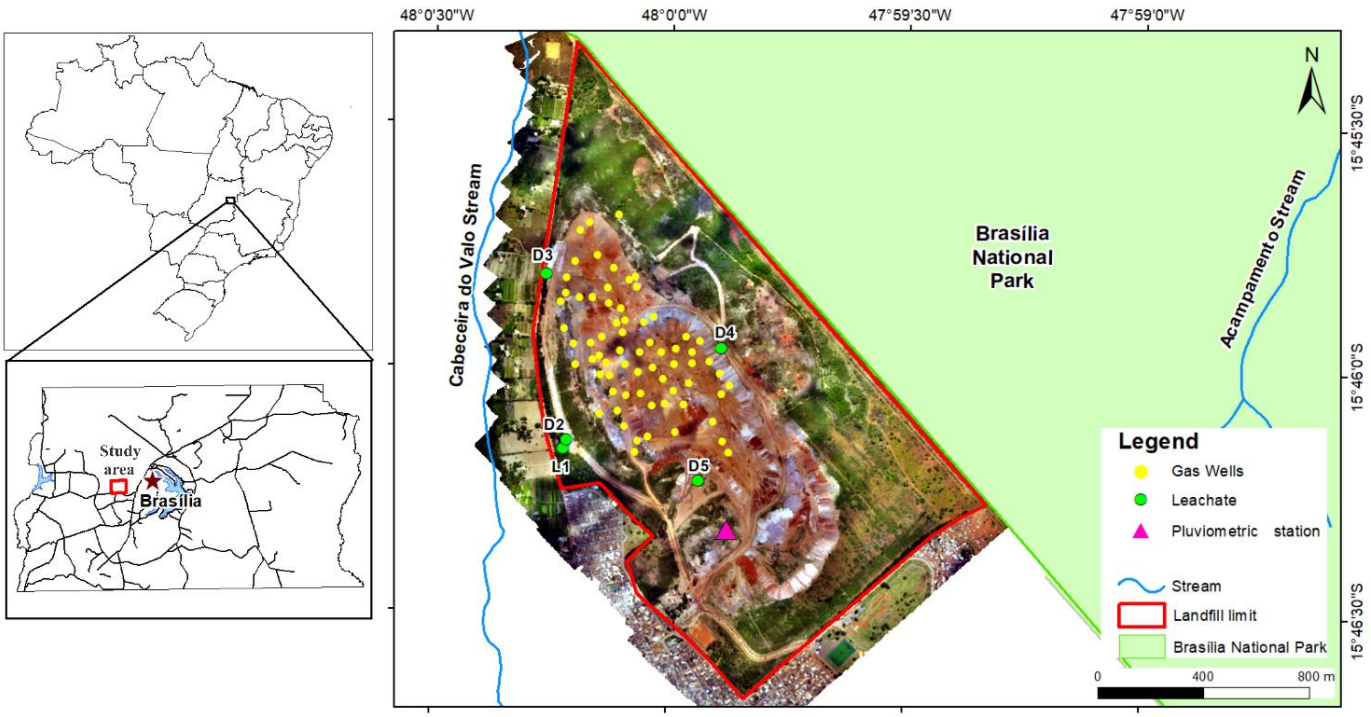

Figure 5.1 - Location of the Jockey Club of Brasília Landfill (JCBL), pluviometric station and sampling sites of leachate and gas.

2.1. Leachate

Leachate samples from each site was placed directly into three different containers: a 500mL polyethylene bottles (PE), a 60mL pre-combusted amber glasses for organic carbon analyses, and a 20mL PE container for metal analyses. After sampling, all containers were stored in cool environment (4°C) and rapidly transported to the Laboratory of Geochemistry of the University of Brasília. All bottles were previously washed with a solution of 5% (v/v) HNO_3 for approximately 72 hours and then rinsed with distilled water.

The following parameters were measured in situ: pH, electrical conductivity (EC), oxidation–reduction potential (ORP), and dissolved oxygen (DO). pH and ORP were measured with a WTW Multi-parameter instrument logged with pH/Cond 340i and ORP probe (precision of 0.01). EC was measured with a EUTECH Cond 6+ logged with electrode EC-CONSEN91B (resolution of 1 µS/cm). DO was measured with a Mettler Toledo FiveGo logged with DO probe (precision of 0.01 mg/L). All probes were calibrated before each fieldwork.

Once in the lab, samples for anions and metals determinations were filtered using 0.45µm filter and stored in two different vials. For anions, the filtered sample was diluted with ultra-pure water (1/100 and 1/25) and stored at 4°C until analysis. The anions F^-, Cl^-, NO_3^-, PO_4^{3-} and SO_4^{2-} were determined by ion chromatography (IC) using a (Dionex ICS90). For metals, the

filtered samples were preserved with 3 drops of concentrated HNO_3 (pH<2) and determined by Inductively Coupled Plasma Optical Emission Spectrophotometer (ICP-OES). Standard solutions of 1000 ppm from Vetec were used to prepare the IC and ICP calibration curves for each element analyzed. The analytic control of the results was validated by international standard samples Canada NWRI (National Water Research Institute) ION-915 and MIRAMICHI-02, batch 0310 and 1109, respectively. There was no previous digestion of the leachate samples, therefore, the concentrations of metals determined for this study represent the dissolved species.

2.1.1. Iron species, ammonium and bicarbonate alkalinity

Analysis for iron species (Fe^{2+} and Fe^{3+}), ammonium (NH_4^+) and alkalinity were performed in less than 3 hours after sampling. The determination for iron species were performed inside a glove box following the procedure described by Viollier et al. (2000). Samples were filtered in 0.45 µm and a solution of ferrozine 10^{-2} N in ammonium acetate (CH_3COONH_4) 10^{-1} N was added to act as a Fe^{2+} complexing agent. The Fe^{+2} concentration was determined by absorbance using a T60 UV/VIS (PG Instrument) spectrophotometer set at 562 nm. For total Fe, 0.2 mL of hydroxylamine (H_2NOH HCl) 1.4 M in HCl 2 M was added to the sample solution, which was left to rest for 10 minutes in order to reduce all the iron. Afterward, 0.1 mL of buffer solution (CH_3COONH_4) 10 M adjusted to pH 9.5 was added sample solution and the total iron determined using the spectrophotometer at 562 nm. The NH_4^+ measurement was performed with diluted samples (dilution with ultra-pure water) and measured by colorimetry using the ammonium reaction kit of HACH – DR 2000 set at 425 nm (mineral stabilizer, Nessler reagent and polyvinyl alcohol). The bicarbonate alkalinity was determined by titration method by adding H_2SO_4 to the solution and using a Schott titulator (Titroline easy model) until pH turned to 4.2.

2.1.2. Stable isotope analysis for DIC and DOC

The samples for δ^{13}C-DIC determination were filtered in 0.45 µm filters, while the aliquot for δ^{13}C-DOC analysis was filtered in pre-combusted 0.70 µm glass filters (Whatman GF/F). Samples were then preserved in sealed and cold conditions (0 – 4°C). Prior to isotopic analysis, borosilicate-glass vials used for δ^{13}C-DIC determinations were filled with three drops of H_3PO_4 and flushed with helium flow in order to remove atmospheric gases and other interferences. Afterward, 0.1 ml of sample was introduced with syringe into the vials and let the DIC to be transferred to the gas phase as CO_2. For δ^{13}C-DOC determination, a borosilicate-glass vials

were initially filled with 0.1 ml sample aliquot and drops of H_3PO_4 in order to eliminate the DIC. The vials were then closed and flushed with helium flow. In sequence, 1 mL of potassium persulfate solution was added to the sample solution, which was then heated in water bath at 95–100 °C for 1 hour in order to oxidize the organic matter and release CO_2 to the vial head space (Engelmann et al., 2018; Zhou et al., 2015). The isotopic composition of DIC and DOC CO_2 was determined using a Gas Bench II device connected to a Delta V Plus mass spectrometer (IRMS - Thermo Fisher Scientific). Results are reported in the conventional delta (δ) expressed in per mil units (‰) relative to the Vienna Pee Dee Belemnite (VPDB). δ^{13}C-DIC and δ^{13}C-DOC determinations were performed in duplicates.

2.1.3. DOC determinations

Samples for DOC determinations were collected in 60 mL pre-combusted amber glasses and filtered in pre-combusted 0.70 µm glass filters (Whatman GF/F). The aliquots were diluted, acidified with HCl 2 M (pH ≈ 2) to remove DIC and stored in pre-combusted 15 mL amber glasses in a cold environment until analysis (0 – 4°C). The DOC concentrations were determined in duplicates by NPOC method, using high temperature catalytic oxidation (HTCO) with infrared detection of CO_2 in a Total Carbon Analyzer (Shimadzu TOC-L CPH/CPN). The coefficient of variation for duplicate measurements was generally 1%.

2.2. Gas measurements

The 150 gas wells in the JCBL are verticals semi-flamers that were built in 2000. These semi-flamers consist of concrete rings with 70 cm in diameter and 50 cm height filled with rock fragments with grain size from 125 to 450 mm. The wells were constructed as the refuse was grounded and there is no horizontal connection between them. The concentrations of CH_4 and CO_2 were determined in 70 of the 150 gas wells during April 2019. Before initiating the measurements, flames were putted out in each site and waited for 5 hours. Then, a lid was placed at the top of the gas well with an exit to determine the of gas concentration by a GEM 5000 (LandTec) instrument.

3. Results

3.1. Leachate geochemistry and availability of electron acceptors

Generally, the JCBL leachate can be characterized by high DOC content varying from 506.50 to 22.11 mg/L, average 229.25 mg/L; and high concentrations of inorganic components such as Cl^- (1,455.77 mg/L), SO_4^{2-} (229.91 mg/L), NH_4^+ (607.35 mg/L), Ca (112,11 mg/L), Na (776.19 mg/L), K (762.53 mg/L) and HCO_3^- (2,745.12 mg/L), which numbers in parenthesis represent

their average values. The concentrations of heavy metals (Cr, Cu, Ni and Zn) dissolved in the system are commonly below the analytical detection limit (0.007 mg/L). The exception is Zn that has a concentration of about 3 mg/L during the rainy season in all sampling sites. Regarding the physicochemical parameters, the average values for pH is 7.66, for conductivity is 9226 µS/cm, for temperature (T °C) is 26.68 °C and for dissolved oxygen (DO) is 1.08 mg/L.

Leachate geochemical parameters varies with sampling site and season (rainy and dry). Table 5.1 presents the average values for geochemical parameters during monitored time interval: rainy season refers to samples collected on December 2018, February 2019 and April 2019, while dry season refers to samples collected on September 2018, October 2018, June 2019 and September 2019.

The oxidation–reduction potential (ORP) values were determined during two periods: one on October, representing the dry season; and another on April, representing the rainy season. Positive ORP values were observed during the rainy season at the leachate lagoon (L1) (+67.5 mV) and the outcropping drain (D4) (+123 mV), representing an oxidizing environment (Table 5.1). Sites D2, D3, D5 and L1 presented negative ORP during the dry season, representing anoxic conditions (Table 5.1). The leachate drain D5 can be classified as the most reducing site, with ORP values varying from -323, during the rainy season, to -301 mV during the dry season (Table 5.1). The Eh values presented in Table 5.1 were estimated by applying a correction factor to the measured ORP as proposed by Nordstrom and Wilde (2005).

Table 5.1 - Average values for geochemical parameters during the rainy and dry seasons for each leachate sampling site. n.s. means not sampled and n.m. is not measured. 1) Eh calculated by adding a correction factor of 209 mV to ORP values (Nordstrom and Wilde, 2005)

		L1	**D2**	**D3**	**D4**	**D5**
pH	Rainy	8.20	7.66	7.29	7.70	7.36
	Dry	8.32	7.69	7.41	n.s.	7.35
Conductivity (µS/cm)	Rainy	7113	6653	9023	3330	11400
	Dry	11157	10167	10102	n.s.	12153
T (°C)	Rainy	25.23	26.57	28.57	27.33	31.25
	Dry	21.05	23.85	26.30	n.s.	28.35
DO (mg/L)	Rainy	3.88	0.88	0.17	1.97	0.13
	Dry	0.21	0.66	0.16	n.s.	0.16
ORP (mV)	Rainy	67.5	-41.5	-299.5	123.0	-323.0
	Dry	-32.8	-275.1	n.m.	n.s.	-301.0
Eh calculated[1] (mV)	Rainy	276.5	167.5	-90.5	332.0	-114.0
	Dry	176.2	-66.1	n.m.	n.s.	-92.0
Alkalinity (mg/L HCO_3^-)	Rainy	1888.49	2259.03	1916.02	705.56	2702.04
	Dry	2809.42	4345.16	3904.29	n.s.	3578.29
DOC (mg/L)	Rainy	152.38	267.34	189.01	57.17	293.14
	Dry	289.19	330.29	272.68	n.s.	307.70
Cl^- (mg/L)	Rainy	1211.16	1450.39	1464.55	296.18	2164.03
	Dry	1865.32	1929.79	1727.64	n.s.	2082.40
SO_4^{2-} (mg/L)	Rainy	212.65	314.28	477.61	558.79	128.86
	Dry	36.42	12.21	163.62	n.s.	11.43
NO_3^- (mg/L)	Rainy	10.62	13.01	<0.1	78.31	12.14
	Dry	3.35	6.51	<0.1	n.s.	<0.1
NH_4^+ (mg/L)	Rainy	304.05	602.19	602.35	150.88	666.62
	Dry	631.87	984.02	657.99	n.s.	656.21
Fe total (mg/L)	Rainy	1.33	1.43	0.90	0.31	0.62
	Dry	2.04	2.03	1.88	n.s.	1.95
Fe^{2+} (mg/L)	Rainy	0.27	0.27	0.32	0.01	0.21
	Dry	0.49	0.76	0.77	n.s.	0.88
Fe^{3+} (mg/L)	Rainy	1.06	1.16	0.58	0.30	0.41
	Dry	1.55	1.27	1.11	n.s.	1.07
Ca (mg/L)	Rainy	114.49	154.57	161.14	201.71	91.48
	Dry	53.16	53.08	111.65	n.s.	67.04
Mg (mg/L)	Rainy	69.16	74.91	477.61	75.34	128.01
	Dry	83.87	82.01	117.48	n.s.	124.75
Na (mg/L)	Rainy	629.85	647.14	621.03	228.95	882.13
	Dry	1025.09	1010.17	831.30	n.s.	941.05
K (mg/L)	Rainy	616.90	625.95	653.08	228.95	889.49
	Dry	993.75	997.21	887.89	n.s.	968.56

In order to better illustrate the magnitude of the seasonal variations among the sampling sites, the average values of pH, conductivity, alkalinity and DO are displayed in Figure 5.2. It shows that the sampling sites react differently upon rainfall regime, often with significant differences between seasons. For instance, sites L1 and D2 display large seasonal variations whereas sites D3 and D5 display a narrower variation on these parameters. The physicochemical parameters pH and DO show smaller variations between the seasons, except for sampling site L1 (Figure 5.2). On the other hand, parameters such as conductivity and alkalinity present very distinct values in both periods, even for sampling site D5. That means that the concentrations of ions in the system are susceptible to seasonal changes even in confined sites.

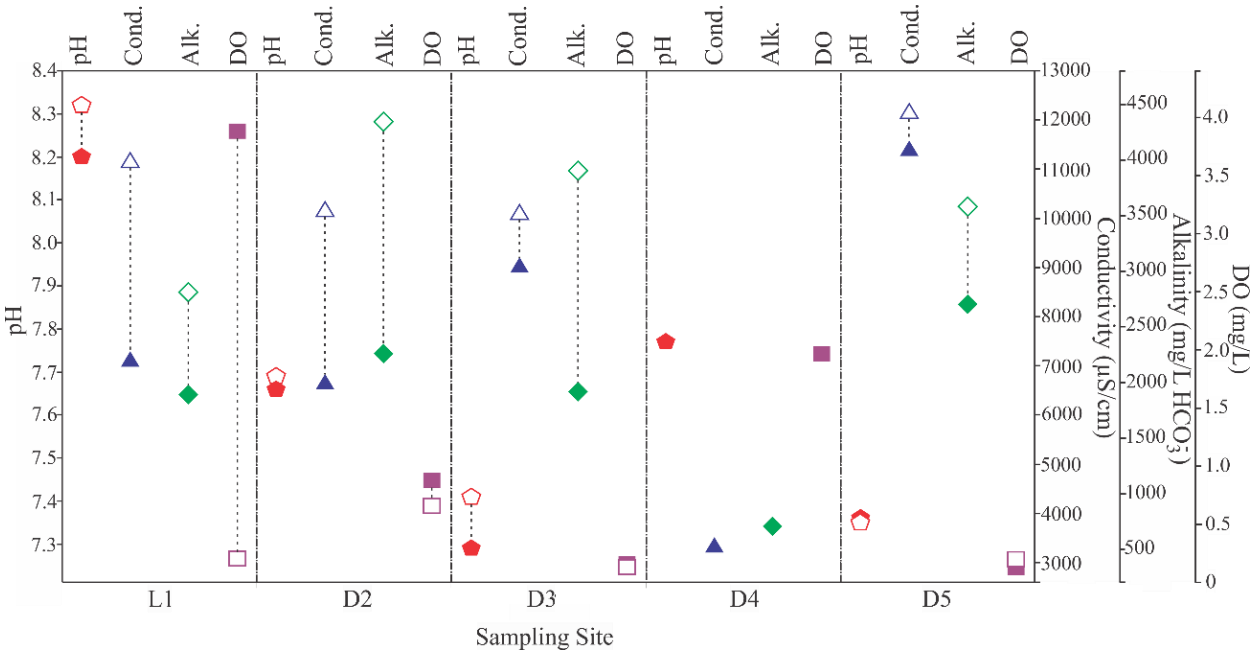

Figure 5.2 - Variation of chemical parameters at different sampling sites of the landfill. Empty symbols represent the dry season, while filled symbols represent rainy season. Each parameter has different scales/units, which are presented its respective y axis.

The availability of ions such as SO_4^{2-}, NO_3^- and Fe^{3+} (as $Fe(OH)_3$) can directly affect landfill stabilization process as they will act as organic matter oxidant agents. As observed in Figure 5.3, SO_4^{2-} has the largest variation range, varying from 558.79 mg/L on sampling site D4 to 11.43 mg/L on sampling site D5 (Figure 5.3). NO_3^- concentrations are also different between seasons, varying from 10.62 to 78.31 mg/L during the rainy season and <0.1 to 6.51 mg/L during the dry season (Figure 5.3, Table 5.1). Compared to NO_3^- concentrations, ammonium shows a larger variation range and higher values during the dry season (Figure 5.3).

Regarding the iron species, the highest concentrations of Fe^{3+} were observed during the dry season (Figure 5.3). However, when analyzing Table 5.1, Fe^{3+} is most likely to be present

during rainy season than Fe^{2+}. For example, on sampling site L1 the concentration of total Fe is 1.33 mg/L during the rainy season. In the sample, Fe^{2+} corresponds to 20.3% (0.27 mg/L), while Fe^{3+} corresponds to 79.7% (1.06 mg/L) of the total Fe (Table 5.1).

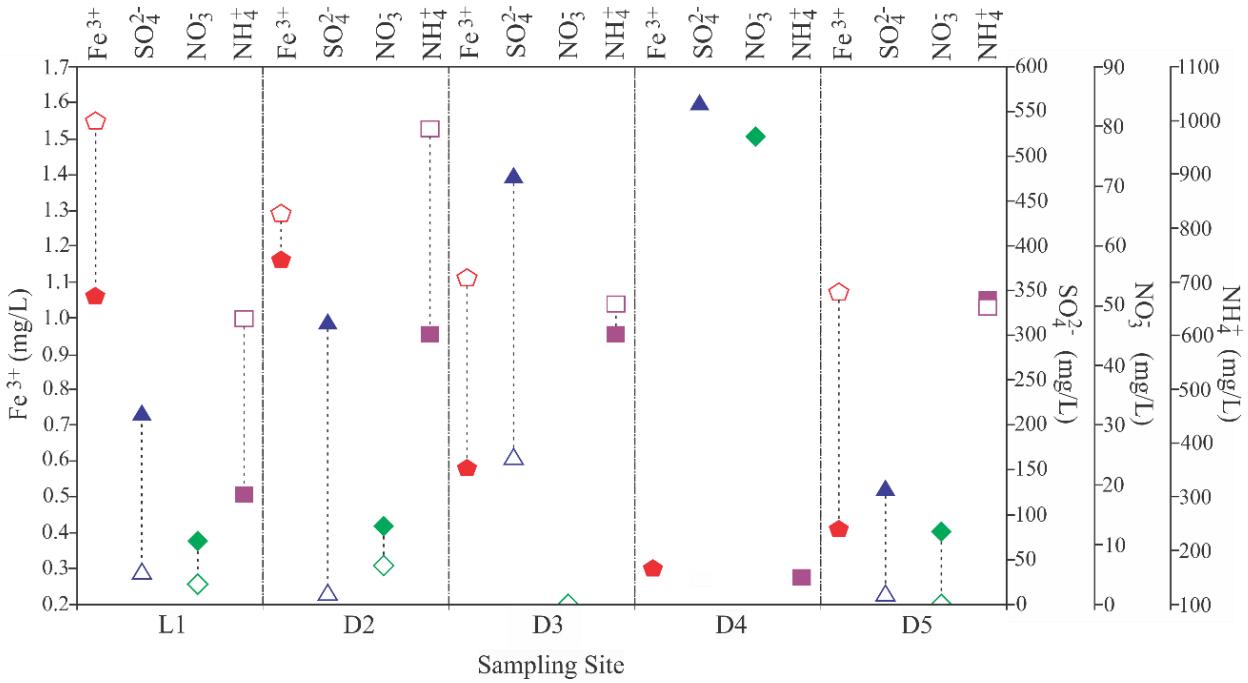

Figure 5.3 - Variation of ions at different sampling sites of the landfill. Empty symbols represent the dry season, while filled symbols represent the rainy season. Each parameter has different scales/units, which are presented its respective y axis.

3.2. Leachate carbon isotopic composition: δ^{13}C-DIC and δ^{13}C-DOC

The isotopic composition of inorganic and organic carbon of the studied sites are shown in Figure 5.4. There is a positive correlation between δ^{13}C-DIC and alkalinity, while δ^{13}C-DOC values do not present any correlation (Figure 5.4). The positive correlation between δ^{13}C-DIC and alkalinity is better observed on sampling sites L1, D2 and D4, indicating that these parameters are susceptible to surface events. These three sites also display the largest variation in δ^{13}C-DIC (from -2.3 to 19.5 ‰).

Despite the broad variation on alkalinity (green and orange ellipses on Figure 5.4), samples from sampling sites D3 and D5 display a narrow variation range of δ^{13}C values (from +11.6 to +16.8 ‰). Regarding the δ^{13}C-DOC, its narrow variation range indicates that the organic matter source is essentially the same, regardless of the sampling site.

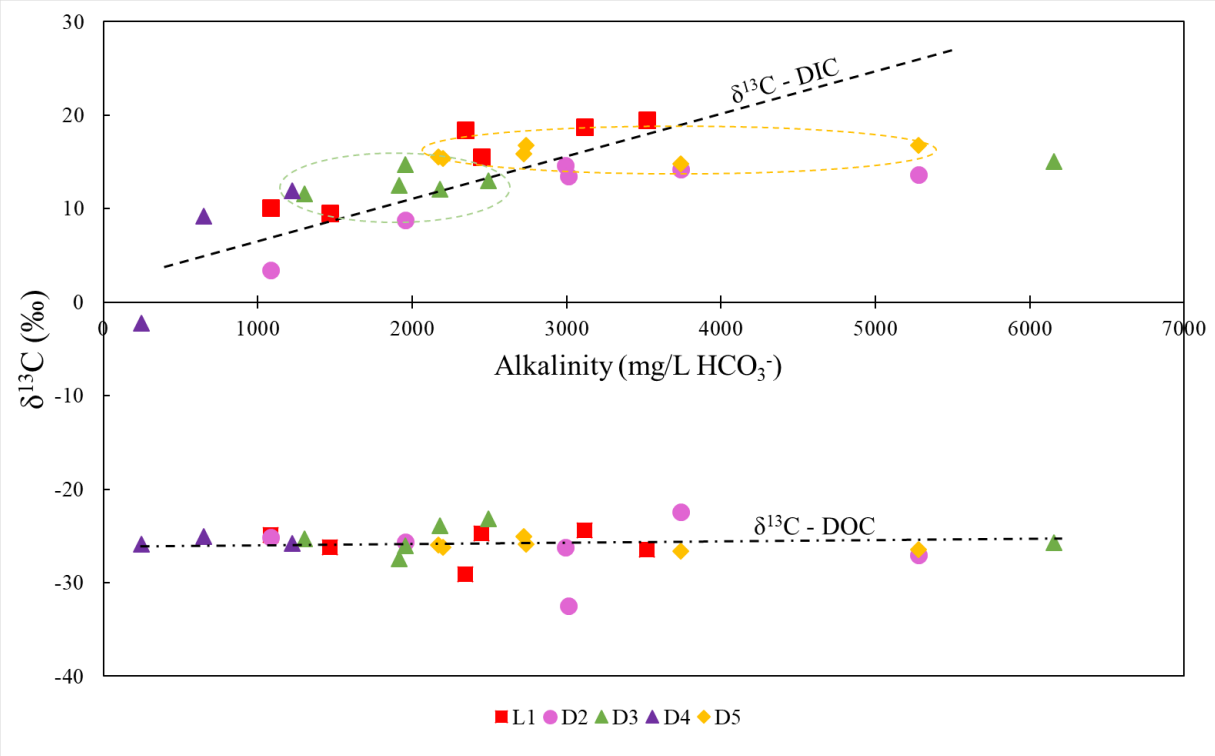

Figure 5.4 - Correlation between δ^{13}C-DIC and alkalinity for the five sampling sites.

3.3. CO_2 and CH_4 concentrations in JCBL.

The concentrations of CH_4 and CO_2 were used to characterize the spatial heterogeneity of gas production in the landfill, highlighting different stabilization stages in the JCBL. Table 5.2 presents the minimum and maximum concentrations, average values and standard deviation values for CO_2 and CH_4 in the 70 wells analyzed. In spite of the similar concentration range, there is a large standard deviation on the values, which indicate a heterogeneous nature of the landfill structure.

Table 5.2 - Maximum, minimum, average values and standard deviation of the 70 gas wells studied in the JCBL.

	CH_4 (% vol)	**CO_2 (% vol)**
Maximum measured concentration	57.9	58.4
Minimum measured concentration	1.9	0.6
Average concentration	38.9	33.4
Standard deviation	15.5	16.3

4. Discussion

4.1. Gas composition and the spatial heterogeneity of the JCB landfill

Gas concentrations and species released by landfills are important gauges of biochemical reactions related to organic matter degradation. At the initial stages of the landfill, aerobic biochemical reactions consume most available oxygen to produce essentially CO_2. After being covered by an impermeable layer, oxygen is entirely consumed and methanogenesis begins to take place. At this stage, methane concentration reaches measurable values since it begins to be produced together with CO_2 (Equation 5.1; Kjeldsen et al., 2002). The main chemical reactions responsible for methane formation are the fermentation of acetic acid (CH_3COOH) (Equation 5.1) and the reduction of CO_2 (Equation 5.2). In the first reaction, CH_3COOH molecule is consumed to produce one mole of CO_2 and one mole of CH_4 (Equation 5.1). In the second, CH_4 is produced by CO_2 reduction under very anoxic conditions (Equation 5.2).

5.1) $CH_3COOH \rightarrow CO_2 + CH_4$

5.2) $CO_2 + 4H_2 \rightarrow CH_4 + 2H_2O$

Measurements of CO_2 and CH_4 concentrations in the 70 wells of the JCBL indicate that most of the landfill area has already reached a methanogenic stage (Figure 5.5). The linear correlation between CO_2 and CH_4, as well as the proportion near to 1:1 for these gas species, point to fermentation of CH_3COOH as the main methanogenic process in the landfill (Equation 5.1). The deviation toward a slightly CH_4 enrichment along the correlation line may be explained by the lower solubility of this gas in water relative to CO_2 (Diamond and Akinfiev, 2003; Yamamoto et al., 1976). Figure 5.5 further suggests that other reactions are changing CH_4/CO_2 ratio of gas phase, as indicated by data points that plot in the upper right of Figure 5.5. Since fractionation of a CO_2+CH_4 mixture seems unrealistic to explain variations in this ratio, we argue that either CO_2 or CH_4 are been produced or consumed in the system. Data points with $CH_4/CO_2 < 1$, indicated in Figure 5.5 as depletion of CH_4, suggest that this gas is either been converted to CO_2 by oxidation reactions or is not been produced. Both scenarios can be explained by an increase in oxygen in the system. In contrast, data points with $CH_4/CO_2 > 1$ suggest that either CO_2 is been converted to CH_4 by reduction or that other biochemical reactions are taking place. This latter scenario is probably related to areas with a high level of confinement within the landfill.

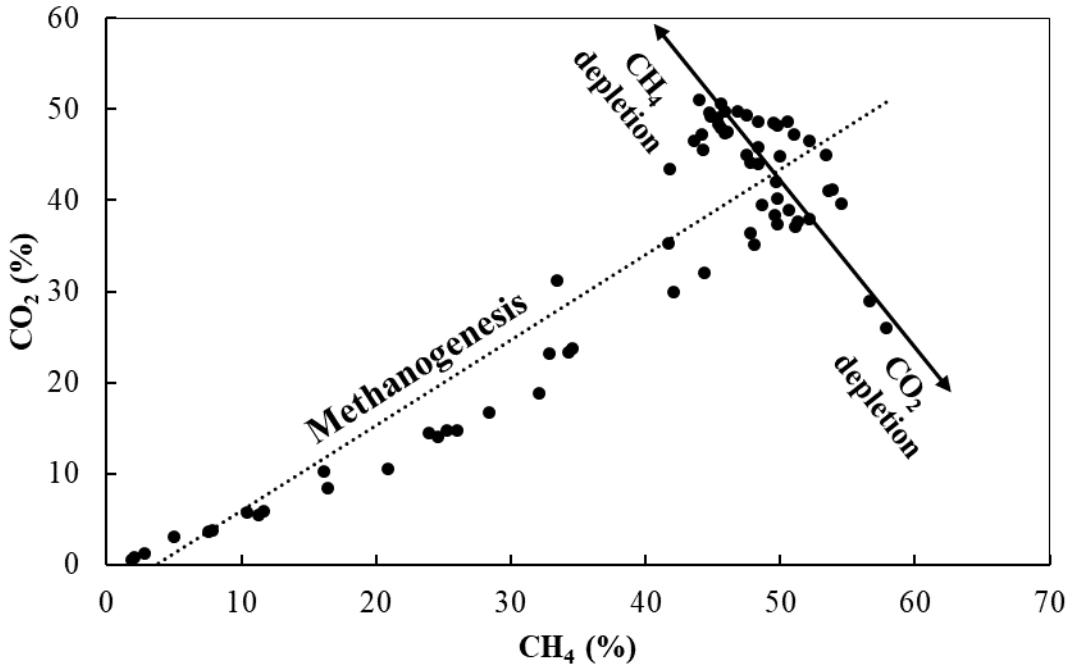

Figure 5.5 - Correlation between CO_2 and CH_4 concentrations on the 70 studied gas wells in the JCBL. Concentrations are in % vol. Arrows and dotted line indicate processes that may be occurring.

The geochemical data presented bellow will detail the mechanisms and reactions taking place within the landfill. Although the sampling sites may not match exactly the source of gas for the 70 wells shown in Figure 5.5, they will provide information about chemical processes occurring within the landfill that may explain features observed in the wells. These reactions are also important for a proper management of the system.

4.2. Redox reactions and organic matter availability

Redox reactions may occur in the presence of oxygen, known as aerobic oxidation, or in presence of redox agents (e.g., nitrate, manganese, iron, and sulfate), known as anaerobic oxidation. Organic matter will be oxidized by aerobic oxidation while oxygen is still available. Once this component becomes depleted and the redox potential decreases, anaerobic microorganisms initiate organic matter decomposition in presence of redox agents. At lower Eh conditions, and once these redox agents are depleted, methanogenesis of organic matter initiates (Rivett et al., 2008). In the case of the JCBL, the data discussed here indicates that the landfill organic matter is being decomposed both by aerobic oxidation, redox agents, and methanogenesis. The nature of the main process involved in the organic decomposition depends on seasonal variability and level of confinement of the sampling sites.

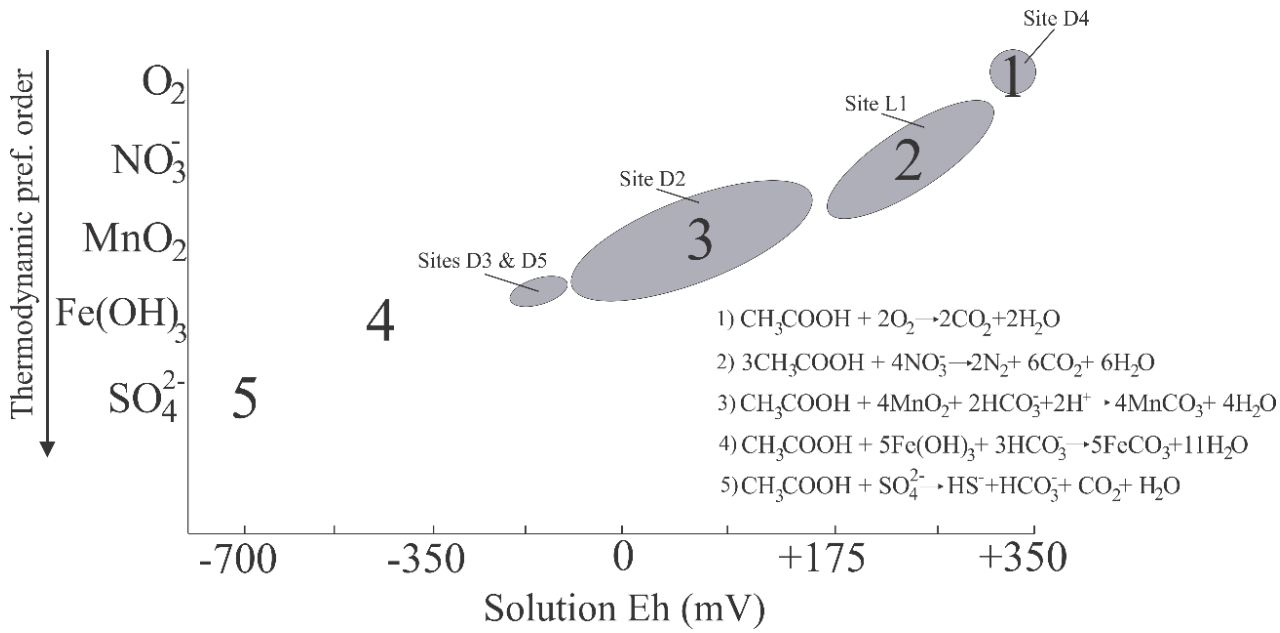

Figure 5.6 - Sequence of different electron acceptors of redox reactions that will participate in the oxidation of organic matter following the thermodynamic preferential order. Numbers indicate the ideal solution Eh, for which the respective reaction named on the figure will be favored. Dark ellipses indicate the Eh range for each sampling site and their approximate location in the redox sequence.

Figure 5.6 displays the relationship between Eh and redox reactions involving O_2, NO_3^-, MnO_2, $Fe(OH)_3$, and SO_4^{2-}. The sampling site from the JCBL plot at different Eh ranges, implying that each site is dominated by specific redox processes. For instance, site D4 and in part L1 display evidence of aerobic oxidation and a strong connection with surface processes. The oxidation reactions from site D4 results in the production of CO_2 accompanied by a decrease in pH and DOC (Figure 5.7), which is commonly reported in such conditions (Kjeldsen et al., 2002). Site L1 also presents evidence of aerobic oxidation during the rainy season, when transport of oxygen into the landfill by rainwater is more efficient. This interpretation is supported by the positive correlation between DOC, pH, and DO depicted in Figure 8. The amount of available oxygen will not only support aerobic respiration but will also oxidize reduced species. During the dry season, the depletion of electron acceptors in site L1 leads to degradation of organic

matter by methanogenesis, as indicated by the high δ^{13}C-DIC and pH values to be discussed below.

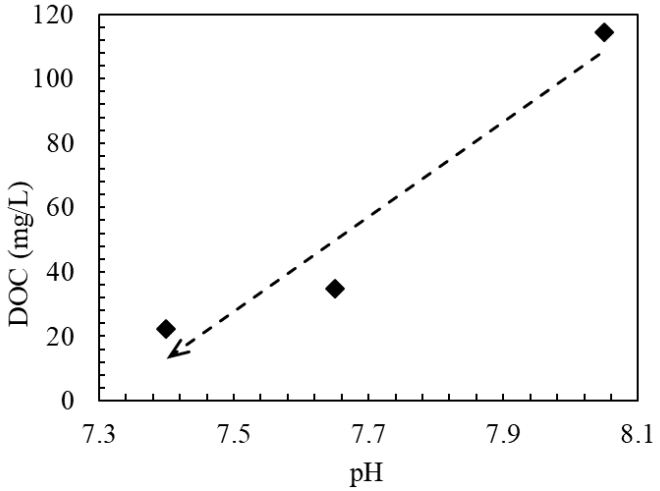

Figure 5.7 - Correlation between DOC and pH for site D4 showing that a decrease in DOC concentrations are accompanied by a decrease in the solution's pH.

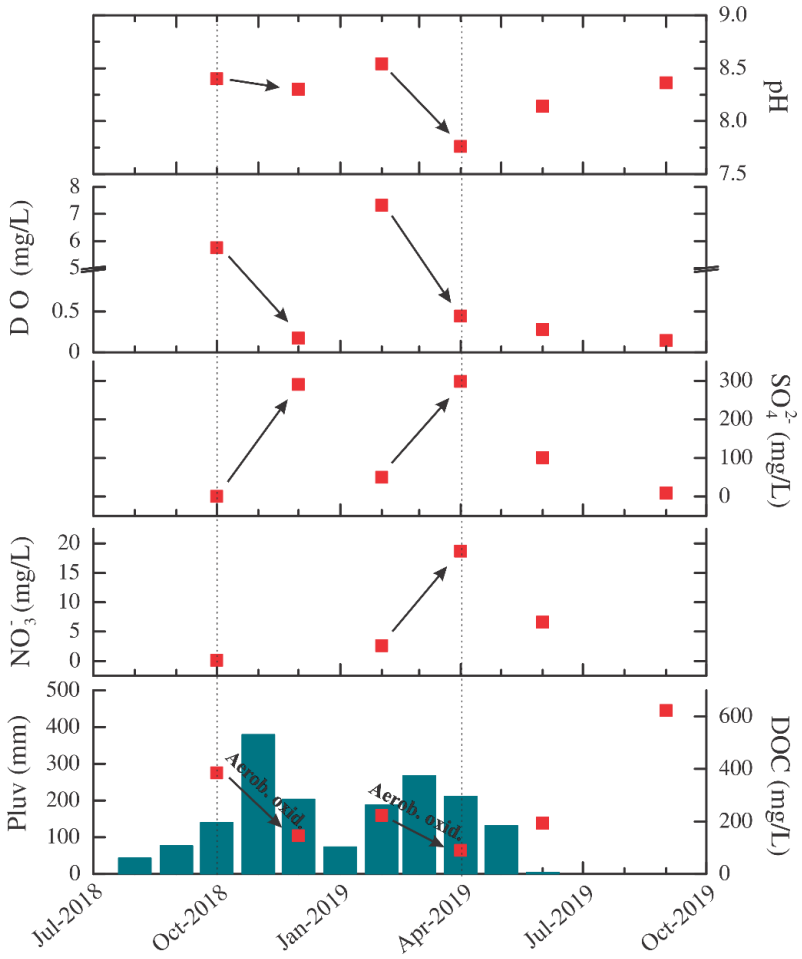

Figure 5.8 - Correlation among pluviometry (Pluv) and concentrations of DOC, NO_3^-, SO_4^{2-}, DO, and pH for site L1. Arrows demonstrate process of aerobic oxidation (Aerob. oxid.).

Sampling sites D3 and D5 have the most reduced environmental conditions, with negative Eh values even during the rainy season (Table 5.1; Figure 5.6). Sampling site D2 plot in Figure 5.6 between these two sites and L1. Sampling sites D3 and D5 present low concentrations of DO, with values ranging between 0.20 and 0.06 mg/L (except site D3 on October 2018, DO = 1.08 mg/L). These sampling sites also have high concentrations of NH_4^+ (from 127.6 to 1305.7 mg/L) and low concentrations of NO_3^- (below 0.1 mg/L). The high NH_4^+/NO_3^- ratio reinforces the low Eh conditions in which the redox agent NO_3^- is been reduced to NH_4^+, as previously described by Caschetto et al. (2018) and Rivett et al. (2008). Under more reducing conditions, iron and sulphate species may also participate in the organic matter oxidation processes. As indicated by reactions in Figure 5.6, Eh values of sites D3 and D5 favors iron over sulphate reduction. In this case, microorganisms use $Fe(OH)_3$ to consume organic carbon, releasing Fe^{2+} (as $FeCO_3$) and H_2O (Equation 4 in Figure 5.6) (Lovley and Phillips, 1988; et al., 2006). The wide variation range of Fe^{2+}/Fe^{3+} observed in D3 and D5 samples (Figure 5.9) supports this interpretation and indicates that the interaction between the landfill leachate and the local oxisol may have a major impact on Fe mobility. As shown in Figure 5.9, the increase in the Fe^{2+}/Fe^{3+} ratio in these sampling sites are accompanied by a slight depletion in DOC values, indicating an anaerobic degradation by iron reduction. This process is supported by the increase on Fe^{2+} over Fe^{3+} leading the ratio to values higher than zero. If the opposite direction of the reaction was taken and Fe^{2+} was been oxidized, the ratio Fe^{2+}/Fe^{3+} would reach lower values, close to zero.

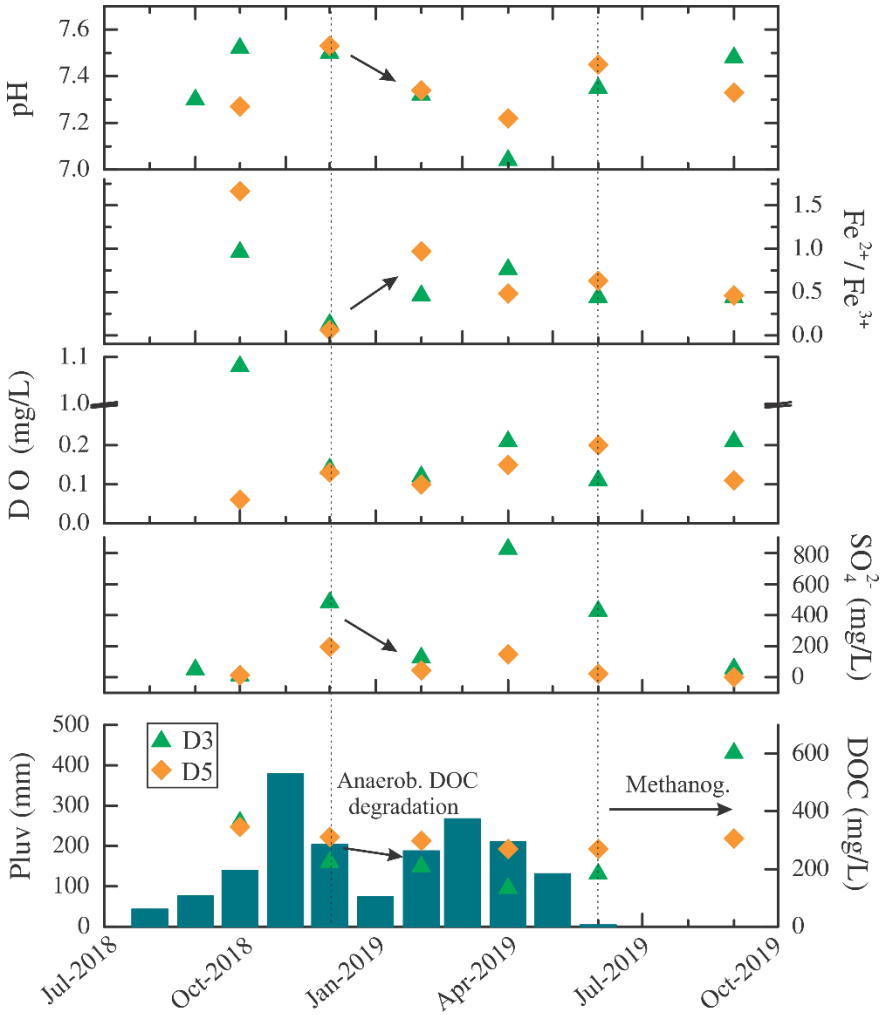

Figure 5.9 - Correlation between pluviometry (Pluv), DOC and availability of different electron acceptors for sites D3 and D5. Anaerob. = Anaerobic; Methanog. = Methanogenesis.

Other groups of microorganisms, such as sulfate reducing bacteria, may use SO_4^{2-} molecules to oxidize dissolved organic matter available in the system, releasing HS^-, HCO_3^-, H_2O and CO_2 (Equation 5 in Figure 5.6) (Liamleam and Annachhatre, 2007; Lovley and Phillips, 1988). These bacteria can also use H_2, for which they will compete with methanogenic and acetogenic bacteria under very reduced condition (Liamleam and Annachhatre, 2007). Although a such reduced environment was not observed in the JCBL, a decrease in SO_4^{2-} concentration combined with a decrease of DOC suggests that sulfate reduction process may also occur.

In the absence of oxygen and redox agents, methanogenesis is the main process of organic matter decomposition (Lovley and Phillips, 1988; Rivett et al., 2008). As shown by the Figure 5.5, methanogenesis is a widespread process in the JCBL, being responsible for most of organic matter degradation. The increase in DO during the rainy season may affect the methanogenesis

rate, when decomposition of organic matter can occur either by aerobic or anaerobic oxidation. We argue that the production rate of CH_4 depends on the confinement level of the sampling sites, reason why Figure 5.5 displays a wide range of gas concentrations.

4.3. δ^{13}C-DIC variations and the JCBL stabilization

The inorganic carbon (δ^{13}C-DIC) of leachate samples from the JCBL have a wide isotope composition range. Most studies argue that these variations are related to biochemical reactions within the landfill (Baedecker and Back, 1979; Conrad, 2005; Hackley et al., 1996; Mohammadzadeh and Clark, 2011; North et al., 2006; Wimmer et al., 2013). We here propose that, besides these biochemical reactions, rainfall plays an important role to carry oxygen into the landfill, leading to an increase of DO and a decrease in δ^{13}C-DIC values.

Organic matter degradation process is strongly dependent on biochemical reactions, which are related to variations in chemical and physical parameters of the environment. For instance, under aerobic conditions, CO_2 with low δ^{13}C values may be directly produced from the oxidation of organic matter. As demonstrated by Wimmer et al. (2013), during the initial aerobic phase of the landfill, δ^{13}C-DIC is mainly dependent on the δ^{13}C-DOC signature of the organic matter present in the refuse, resulting in values between -20 and -25‰. In contrast, in reduced conditions the fermentation of acetic acid (Equation 5.1) will result in the production of CO_2 and CH_4 with a molar ratio near 1:1.

Because of the high carbon isotope fractionation values between CO_2 and CH_4 at low temperatures (e.g. +68.2‰ at 25°C; Bottinga, 1969), mass balance indicates that CO_2 produced by methanogenesis will generally have a high δ^{13}C value (Grossman et al., 2002; Hackley et al., 1996; North et al., 2006; Porowska, 2015; van Breukelen et al., 2003; Wimmer et al., 2013). This is the case of most leachate samples from the JCBL, which have an average δ^{13}C values of +13.3‰. These results are in agreement with experimental values reported by Wimmer et al. (2013) for landfill under stable methanogenic condition. Compared to the DIC values, δ^{13}C-DOC signatures in JCBL vary from -32.45 to -22.40‰ (average of -25.87‰) and indicates that all sites have a similar kind of organic matter.

Biochemical reactions alone may not explain all carbon isotope variations observed in JCBL, particularly the high CH_4/CO_2 ratio of a few gas well and the strong relationship between rainfall and isotope values. The high CH_4/CO_2 ratios observed in Figure 5.5 may be related to CH_4 production by CO_2 reduction under very anoxic conditions. Because of the large carbon

isotope fractionation between methane and carbon dioxide (Bottinga, 1969), the residual CO_2 will be very enriched in ^{13}C, as indicated the high $\delta^{13}C$-DIC values (+15 to +19‰) observed in L1, D3, and D5 (Figure 5.10).

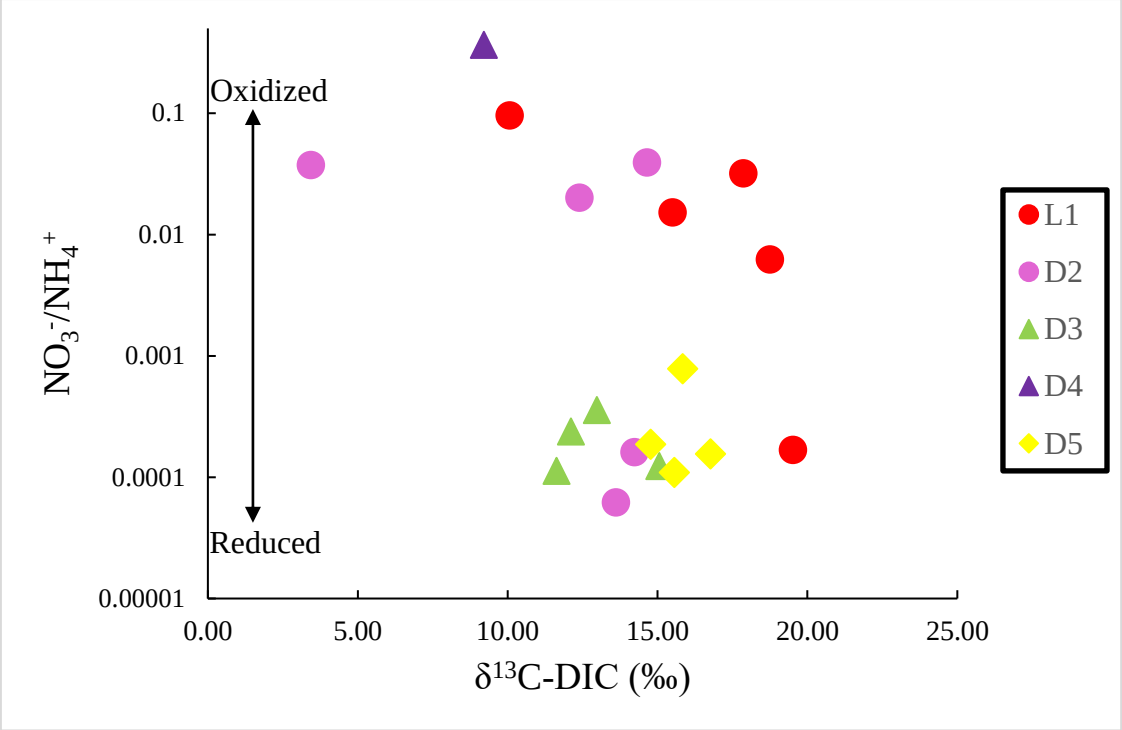

Figure 5.10 - $\delta^{13}C$-DIC values of sampling sites in comparison with the ratio NO_3^-/NH_4^+.

In contrast, there are isotopic variations on leachate samples that are strongly related to changes in rainfall regime and, consequently, on the input of oxygen into the landfill (Figure 5.11). For instance, Figure 5.10 shows that the increase in the NO_3^-/NH_4^+ ratio is accompanied by a decrease in the $\delta^{13}C$-DIC. Figure 5.11 further illustrates the correlation between rainfall and isotope variations in which, after a high pluviosity as observed on November 2018, DOC consumption is main related to aerobic oxidation. The oxidation of organic matter leads to an input of CO_2 with $\delta^{13}C$ similar to $\delta^{13}C$-DOC signature (average of -25.87‰), therefore decreasing $\delta^{13}C$-DIC values. Besides producing CO_2 directly from DOC oxidation, the increase in DO may also halt methanogenic reactions and change the CH_4/CO_2 ratio of carbon species in the system. An increase on $\delta^{13}C$-DIC values is notice in the beginning of the dry season (represented by the dashed line in Figure 5.11), when methane production starts to occur in this sampling site.

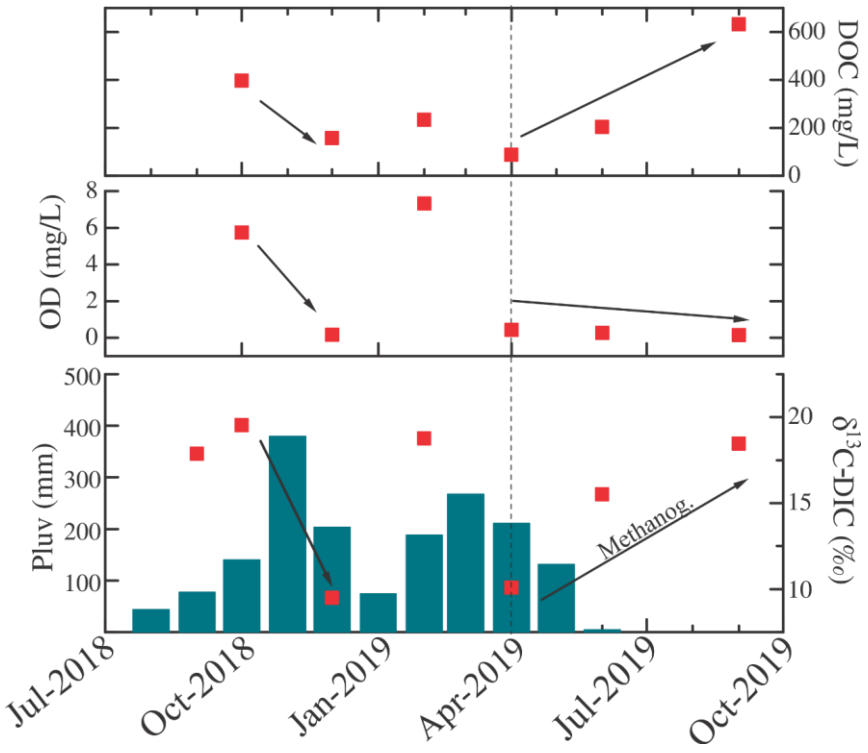

Figure 5.11 - δ^{13}C-DIC variations for sampling site L1 and their relation to OD and DOC availability.

5. Conclusion

The JCBL is a very heterogenic area and its stabilization stage can vary seasonally and spatially. As proposed by Kjeldsen et al. (2002) and Wimmer et al. (2013), the different stages of chemical evolution of landfill's stabilization process are (1) aeration and acid phase, (2) initial methanogenic phase, (3) stable methanogenic phase, (4) air intrusion, (5) CO_2 phase/aerobic, (6) background. These stages are characterized by specific chemical reactions and can be defined based on the variations of carbon isotopic signature and organic matter degradation phase (Wimmer et al., 2013).

Based on our data, rainwater plays an important role on carrying oxygen into the landfill and directly affect methane production. Oxygen controls the availability of electron acceptors, such as SO_4^{2-} and NO_3^-, and the addition of CO_2 with negative isotopic signature to the DIC pool. As demonstrated in Figure 5.8, rainfall events provide an increase in DO, which leads to aerobic oxidation of the available organic matter. This process is effective on reducing long-term emissions of contaminants and gases (van Turnhout et al., 2018; Wang et al., 2006). However, in terms of CH_4 production, oxygenation is not a good practice. Our data suggests that a depletion of CH_4 is either related to an oxidation process or it is not been produced due to the high availability of DO or redox agents such as NO_3^-, Fe^{3+} (as $Fe(OH)_3$), and SO_4^{2-}.

Isotopic data of leachate samples and gas measurements suggests that most of the JCBL is on the stable methanogenic phase. Variations on the CH_4/CO_2 ratio indicate that these gases are being produced or consumed within the landfill system. These processes are supported by chemical and isotopic data of leachate samples. For example, CO_2 reduction is indicated by the high δ^{13}C-DIC values (+15 to +19‰) observed in L1, D3, and D5.

The JCBL is a complex chemical system and processes of aerobic and anaerobic oxidation may affect different regions of the landfill depending on their confinement level. Therefore, there are a few improvements that could be made to increase the methane production in the JCBL: avoid rainwater inflow into the landfill and set a closed recirculation procedure of leachate.

Acknowledgments

The authors are thankful to the University of Brasília for the infrastructure and technical support. We also thank the financial support of the Coordination for the Improvement of Higher Education Personnel – Brazil (CAPES) - Finance Code 001.

5.2. ARTIGO 2: INORGANIC CARBON ISOTOPE COMPOSITION (δ^{13}C-DIC) AS AN INDICATOR OF CONTAMINATION LEVEL BY LANDFILL LEACHATE.

Authors:

1 - Giovanna Orletti Del Rey* [a] (*corresponding author: giovannaodelrey@gmail.com)

2 - Roberto Ventura Santos [a]

3 - Luciano Soares da Cunha [a]

[a] University of Brasília – UnB, Asa Norte, 70910-900, Brasília - DF, Brazil

Abstract:

Landfill leachate is a potential source of water resources contamination, especially when waste disposal sites lack engineered liners. Leachates have a very complex composition, with a range of organic and inorganic compounds that are harmful to human health and to the environment. When natural properties of aquifers are not enough to avoid the propagation of pollutants, a contamination plume is formed. In most instances, the concentrations of contaminants will vary according to the distance from the source. Depending on the stabilization stage of the landfill, the CO_2 produced by organic matter decomposition may have a characteristic $\delta^{13}C$ signatures that can be traced in the aquifer. This study uses the isotopic signature of the dissolved inorganic carbon together with other chemical parameters at evaluating the level of contamination of groundwater and surface water close to The Jockey Club of Brasília landfill (JCBL), a 50-year-old reclaimed landfill in Brasília, Federal District, Brazil. Because of methanogenesis, CO_2 within landfill leachate from the JCBL is highly enriched in heavy carbon isotopes (~ +13‰), thus contrasting with the low $\delta^{13}C$ values of local groundwater (~ -12‰). Based on the $\delta^{13}C$ - DIC values of shallow and deep groundwater wells, our results show that landfill leachate plume is affecting groundwater quality at shallow depths. Based on mass balance calculations, we have estimated that about 48% of dissolved CO_2 in the shallow aquifer are derived from the leachate. We argue that this is a minimum contamination value since the isotopic composition of dissolved CO_2 in the aquifer may had been derived from CH_4 oxidation, thus driving the $\delta^{13}C$-DIC to lower values. Contamination of the shallow groundwater by the reduced leachate also explains a high concentration of Fe^{2+} has been derived from reduction of Fe^{3+} present in the local Fe-rich soils.

Keywords:

Groundwater

Contamination

Landfill leachate

Carbon isotopes

Redox zones

1. Introduction

Landfilling is an effective and low-cost method to dispose refuse. However, landfills that lack engineered liners are potential source of groundwater contamination. Percolation of landfill leachate it is been highly reported in literature as a primary source of groundwater contamination around landfills (Adeolu et al., 2011; Engelmann et al., 2018; Hackley et al., 1996; Mohammadzadeh and Clark, 2011; Porowska, 2015; van Breukelen et al., 2003; Wimmer et al., 2013). Leachate forms as rainfall percolate through the refuse layers by leaching and biodegradation reactions, resulting in a very complex liquid composed of organic and inorganic compounds that are harmful to the human health and to environment (Adeolu et al., 2011; Lee and Ko, 2006). Microbiological and chemical compositions of leachates depends on the nature of the residues, landfill age, operational mode, mechanisms of organic matter degradation, and local environmental conditions (Engelmann et al., 2018; Kjeldsen et al., 2002).

Aquifers may attenuate landfill leachate contamination by different processes including adsorption, dilution, precipitations, volatilization, and ion exchange reactions. When attenuation processes are not sufficient to avoid the propagation of pollutants through the aquifers, a contamination plume forms irradiating away from the mixing zone (Adeolu et al., 2011; Engelmann et al., 2018; van Breukelen et al., 2003). In most instances, the concentration of contaminants decreases with distance from the mixing point due to dilution and reactions within the aquifer (MacFarlane et al., 1983). Isotopic variations in the contamination plume will be driven by equilibrium and kinetic reactions, related to natural attenuation occurring throughout the plume propagation (Conrad, 2005; Hoefs, 2009; Mohammadzadeh and Clark, 2008).

The initial stage of refuse decomposition is aerobic and involves the consumption of available oxygen within the residues. As oxygen is consumed and anaerobic phase starts, organic matter degradation takes place by redox agents (e.g. NO_3^-, SO_4^{2-}) and methanogenesis. This latter process involves the production of CH_4 and CO_2 in a proportion of 1:1 accompanied by an increase in the pH values of the leachate (Christensen et al., 2001; gooann et al., 2017; Kjeldsen et al., 2002; Porowska, 2015; Wimmer et al., 2013). Because of the large isotope fractionation factor between CO_2 and CH_4 (e.g. ~+68‰ at 25°C, Bottinga, 1969), the δ^{13}C-DIC of dissolved CO_2 in landfill leachate under methanogenic conditions usually have high isotopic values (~+13‰), thus being a powerful tracer of contamination.

The $\delta^{13}C$ variations of DIC within a landfill leachate plume have been characterized by a number of studies (Conrad, 2005; Hackley et al., 1996; Mohammadzadeh and Clark, 2008, 2011; North et al., 2006; Wimmer et al., 2013). Generally, the values of $\delta^{13}C$-DIC in non-contaminated groundwater may range from -4 to -30‰ depending on the source of carbon in the DIC pool. In leachate-contaminated groundwater, the isotopic composition of the inorganic carbon depend on the nature of organic matter and on biodegradation reactions (Porowska, 2015). In the initial aerobic stage of organic matter degradation, $\delta^{13}C$-DIC will have negative values, similar to the primary organic matter (between -20 and -25‰) (Wimmer et al., 2013). As the landfill reaches more advanced stages, $\delta^{13}C$-DIC values become positive (around + 20‰) due to CO_2 formed by methanogenesis (Grossman et al., 2002; Hackley et al., 1996; Lee and Ko, 2006; North et al., 2006; Porowska, 2015; van Breukelen et al., 2003; Wimmer et al., 2013).

The Jockey Club of Brasília landfill (JCBL), a 50-year-old reclaimed landfill in Brazilian Federal District, was the largest MSW landfill of Latin America, with an area of 200 ha and approximately 50 meters thick of residue (Barbosa et al., 2015; Koide and Bernardes, 1998). The estimated gravimetric composition grounded in the JCBL is about 40 to 50% composed by organic refuse, 20 to 25% by paper, 10 to 15% by plastic, 3 to 5% by metals, 1 to 3% by glass, and 10 to 20% by other materials. The JCBL operation mode involves leachate recirculation by pumping drained leachate from a treatment lagoon back to the trash dump. Analyses of $\delta^{13}C$-DIC for leachate from the JCBL point to values as high as +19‰ (Del Rey et al., in prep), indicating that the landfill has reached the methanogenesis stage. Since this landfill does not have a properly engineered liner, the leachate is potentially being transferred to the local oxisol over which it was built. Considering the redox nature of the leachate, it will imprint major biochemical changes in the local groundwater and soil.

In this study, we use the isotopic composition of dissolved inorganic carbon to evaluate the mixture between carbon derived from the landfill and carbon derived from deep and shallow groundwater reservoir. Besides carbon isotopes, we also present other chemical parameters (Cl^-, Na, K, NH_4^+, NO_3^-, Fe) determined during a hydrological cycle. The data indicate that the shallow aquifer has been strongly affected by carbon derived from the landfill, and that interaction between leachate and soil have a significant impact in the shallow groundwater chemistry. For instance, the reduced leachate is a powerful agent to remobilize iron in Fe-rich oxisol over which the landfill was constructed. The distribution of contaminants throughout the

plume and its redox species will also be addressed in order to understand attenuation processes that might occur in this environment.

2. Study area

The Jockey Club of Brasília Landfill (JCBL) is in the center-west of the Federal District, Brazil. The landfill is about 20 km far from the center of Brasília and can be accessed by the EPCL-DF-096/BR-070 road. The regional climate is characterized by strong seasonality, with distinct dry (May to September) and rainy (October to April) periods. About 90% of the rainfall occurs between October and April, and an average precipitation is about 350 mm per month (INMET, 2018). The landfill site is underlain by both shallow and deep aquifers. The shallow aquifer is about 30 meters thick and comprises an unconfined aquifer hostel in oxisol with high hydrological conductivity (Campos, 2004). The deeply fractured aquifer is confined and hosted by slates with few lenses of quartzite of the Paranoá Group (Barbosa et al., 2015; Campos, 2004; Campos et al., 2013).

The landfill was placed in a watershed at an elevation of 1,120 meters above the sea level. The Cabeceira do Valo stream borders its western side, while the Brasília National Park and the spring of the Acampamento stream border its eastern side (Figure 5.12). A district called "Vila Estrutural", which today has about 40,000 inhabitants, was built around the JCBL since the early days of the landfill. The JCBL operated continuously between 1977 and January 2018, and was the largest landfill in Latin America, with an area of 200 ha and approximately 50 meters of refuse (Barbosa et al., 2015; Koide and Bernardes, 1998).

3. Material and Methods

In this study we have sampled both the leachate and ground and surface water near the landfill. The samples of leachate were collected in five different sites in the JCBL area, while ground and surface water were sampled outside the landfill limits, respectively, at 130 and 210 meters far from its western border (Figure 5.12). Groundwater sampling was performed in a shallow and deep well from the monitoring network of the Regulatory Agency of Water, Energy and Basic Sanitation of the Federal District (ADASA). The shallow well is 30 meters deep and represents an unconfined aquifer hosted in an oxisol. The deep well is 130 meters deep and drains water from a confined aquifer hosted by fractured metasedimentary rocks (slates). Surface water samples were collected in the Cabeceira do Valo stream, in a site close to the multilevel wells (Figure 5.12). The sampling campaigns occurred every two months between September 2018 and September 2019.

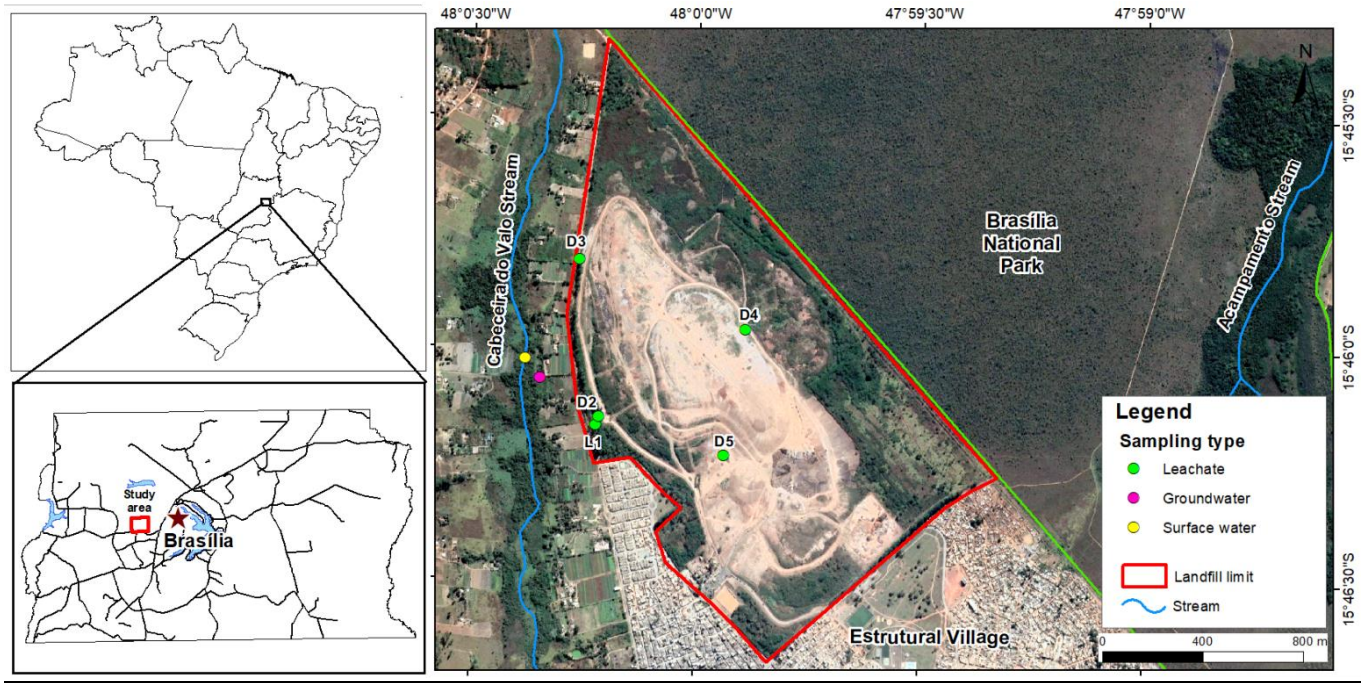

Figure 5.12 - Location of the JCBL landfill and the sampling sites.

Landfill leachate and surface water sampling were directly performed in 500mL polyethylene bottles (PE), 60mL pre-combusted amber glasses (for organic carbon analyses), and in a 30mL PE container for metal analyses. Groundwater samples were collected after pumping about three times the well's volume. The pumping procedure was not able to maintain a constant and low flow, which could have altered the concentration of some redox species, such as Fe^{2+}/Fe^{3+} and NH_4^+/NO_3^-. The samples were stored in cold conditions (4°C) until analysis. The pH, electrical conductivity (EC) and dissolved oxygen (OD) were measured in the field with different probes: a WTW Multi-parameter instrument logged with pH/Cond 340i to measures pH; an EUTECH Cond 6+ logged with the electrode EC-CONSEN91B (resolution of 1 µS/cm) to measure EC and; a Mettler Toledo FiveGo logged with OD probe (precision of 0.01 mg/L) to measure OD. Analysis of iron species, ammonium (NH_4^+), and alkalinity were performed in less than 3 hours after sampling. Samples for anions and metals analyses were stored in 4°C after been filtered with 0.45µm filter. The aliquot for metal analyses was preserved with 3 drops of pure HNO_3 (pH ≈ 2). The anions F^-, Cl^-, NO_3^-, PO_4^{3-} and SO_4^{2-} were determined by ion chromatography (IC) (Dionex ICS90). For metals, the filtered samples were preserved with 3 drops of concentrated HNO_3 (pH<2) and determined by Inductively Coupled Plasma Optical Emission Spectrophotometer (ICP-OES). Standard solutions of 1000 ppm from Vetec were used to prepare the IC and ICP calibration curves for each element analyzed. The analytic

control of the results was validated by international standard samples Canada NWRI (National Water Research Institute) ION-915 and MIRAMICHI-02, batch 0310 and 1109, respectively.

The determination of iron species were performed inside a glove box following a procedure adapted from Viollier et al. (2000). After filtering the samples in 0.45 µm membranes, a solution of ferrozine 10^{-2} N in ammonium acetate (CH_3COONH_4) 10^{-1} N was added to each sample as a Fe^{2+} complexing agent. The absorbance of the Fe^{2+} was measured at 562 nm. Afterward, 0.2 mL of hydroxylamine (H_2NOH HCl) 1.4 M in HCl 2M was added and left to rest for 10 minutes for the complete reduction of iron. After this time, 0.1 mL of buffer solution (CH_3COONH_4) 10M with adjusted pH to 9.5 was added. The determination of total iron (Fe total) was then measured at 562 nm. The absorbance was measured in a T60 UV/VIS spectrophotometer (PG Instruments). The NH_4^+ ion was measured by colorimetry using a HACH – DR 2000 equipment, set at 425 nm. An ammonium reaction kit (mineral stabilizer, Nessler reagent, and polyvinyl alcohol) was used for this determination. The bicarbonate alkalinity was determined in a Schott titulator (Titroline easy model) by titration method, adding H_2SO_4 to the solution until pH turned 4.2.

The samples for δ^{13}C-DIC determination were filtered in 0.45 µm filters. Prior the isotopic analyses, the borosilicate-glass vials were filled with three drops of H_3PO_4 and flushed with helium to remove atmospheric gases and other interferences. The samples aliquots were 0.1 ml for leachate samples and 1.0 mL for water samples, and each analysis was performed in duplicates. The CO_2 isotopic composition was determined with Gas Bench II device connected to a Delta V Plus mass spectrometer (IRMS - Thermo Fisher Scientific).

DOC determinations were performed after filtering samples in pre-combusted 0.70 µm glass filters (Whatman GF/F). Samples were diluted and acidified with HCl 2 M (pH ≈ 2) to remove DIC. Then, they were stored in pre-combusted 15 mL amber glasses in a cool environment until analysis (0 – 4°C). The DOC concentrations were determined by NPOC method, using high-temperature catalytic oxidation (HTCO) with infrared detection of CO_2 in a Total Carbon Analyzer (Shimadzu TOC-L CPH/CPN).

4. Results

Table 5.3 shows the average results of geochemical parameters for the leachate samples, water from the shallow and deep wells, as well as water from the Cabeceira do Valo stream. Leachate samples are characterized by high concentrations of inorganic components such as Cl^- (1,455.77

mg/L), Na (776.19 mg/L), K (762.53 mg/L), SO_4^{2-} (229.91 mg/L), and Ca (112.11 mg/L) (Table 5.3). They also have a slightly basic pH (7.66) as well as high electrical conductivity (9,226 µS/cm) and bicarbonate alkalinity (2,745.12 mg/L). The measured concentrations of DOC in leachate samples were often higher than 100 mg/L, with an average value of 284.53 mg/L. In contrast, concentrations of heavy metals were below the quantification limit (Table 5.3), except for Zn that presented values as high as 3 mg/L during the rainy months. The reduced nitrogen species NH_4^+ prevails over NO_3^-, with an average NO_3^-/NH_4^+ ratio of ~0.02 (Table 5.3), while the ferric (Fe^{3+}) concentrations are slightly higher than that of ferrous iron (Fe^{2+}) (Table 5.3). The average value of DO measured in the leachate samples was 1.08 mg/L, which characterizes an anoxic environment.

Table 5.3 - Average values of the physicochemical parameters for the sampling points. Species F^-, PO_4^{3-}, As, Ba, Cd, Co, Cu, Li, Mn, Mo, Ni, Ti, V, Zr were below quantification limit or presented deficient concentrations. 1) The average composition of all leachate samples; 2) Shallow well water representing the shallow unconfined aquifer; 3) Deep well water representing the fractured confined aquifer.

Parameter	**Leachate (1)**	**Shallow well (2)**	**Deep well (3)**	**River**
pH	7.66	6.19	6.80	6.11
Conductivity (µS/cm)	9226	1576	159.05	77.04
Temperature (°C)	26.68	25.65	25.50	20.25
DO (mg/L)	1.08	2.82	4.10	2.83
Alkalinity (mg/L HCO_3^-)	2745.12	161.69	87.54	18.25
DOC total (mg/L)	284.53	8.14	1.18	2.12
Isotopic analysis				
δ^{13}C-DIC (‰)	+ 13.83	+ 0.55	- 11.65	- 9.64
Inorganic components				
Cl^- (mg/L)	1455.77	220.35	1.02	16.55
SO_4^{2-} (mg/L)	229.91	13.03	0.38	0.44
NO_3^- (mg/L)	13.11	14.32	0.57	1.51
NH_4^+ (mg/L)	607.35	39.45	0.04	0.78
Ca (mg/L)	112.11	1.38	26.01	0.50
Mg (mg/L)	98.84	0.20	1.45	0.09
Na (mg/L)	776.19	140.37	0.69	8.88
K (mg/L)	762.53	46.21	0.56	1.23
Al (mg/L)	<0.17	0.56	<0.17	<0.17
P (mg/L)	1.02	<0.003	<0.003	<0.003
Si (mg/L)	16.01	0.94	5.49	1.99
Sr (mg/L)	2.13	<0.06	<0.06	<0.06

- *Iron species*				
Fe total (mg/L)	1.10	84.57	0.29	0.55
Fe^{2+} (mg/L)	0.44	67.96	0.04	0.09
Fe^{3+} (mg/L)	0.66	16.61	0.25	0.46
- *Heavy metals*				
Zn (mg/L)	3.21	<0.007	<0.007	<0.007

Water samples presented very different compositions when compared to the leachate (Table 5.3). Except for NO_3^- and Fe species, samples of surface and groundwater have lower concentration of metals and ions than the leachate ones. The geochemical data also reveal that the shallow unconfined aquifer has higher electrical conductivity and a high concentration of inorganic components (Cl^-, Fe, Na, K, NH_4^+, and NO_3^-) when compared to samples from the deep aquifer and the Cabeceira do Valo stream (Table 5.3). Water from the shallow well has the highest total iron (84.57 mg/L) and NO_3^- (14.32 mg/L) concentrations among all sampling sites. Fe^{2+} represents about 80% of the iron species in these samples. Other inorganic components are also relevant concentrations in the shallow well, such as Cl^- (220.35 mg/L), SO_4^{2-} (13.03 mg/L), Na (140.37 mg/L) and K (46.21 mg/L). These same components where observed in much lower concentrations in the deep well and the Cabeceira do Valo stream, which the average values were respectively 1.02 and 16.55 mg/L for Cl^-, 0.38 and 0.44 mg/L for SO_4^{2-}, 0.69 and 8.88 mg/L for Na, and 0.56 and 1.23 mg/L for K.

The sampling sites present quite distinct inorganic carbon isotopic composition (Table 5.3). The highest δ^{13}C-DIC was observed in the leachate (+13.83‰), followed by the shallow aquifer (+0.55‰), and then by the stream (-9.64‰) and deep aquifer (-11.65‰). The DOC content of water samples also presented very different values when compared to the leachate. The shallow well have the highest concentrations of dissolved organic carbon (8.14 mg/L), followed by the stream (2.12 mg/L), and then by the deep well (1.18 mg/L).

The heads (water level) of both the shallow and deep aquifers showed different variation pattern among the sampling period (Figure 5.13). The shallow well head measured during the study

period varied from 2.07 to 3.69 meters below the surface, while the same parameter in the deep well varied from 1.08 to 2.25 meters (Figure 5.13).

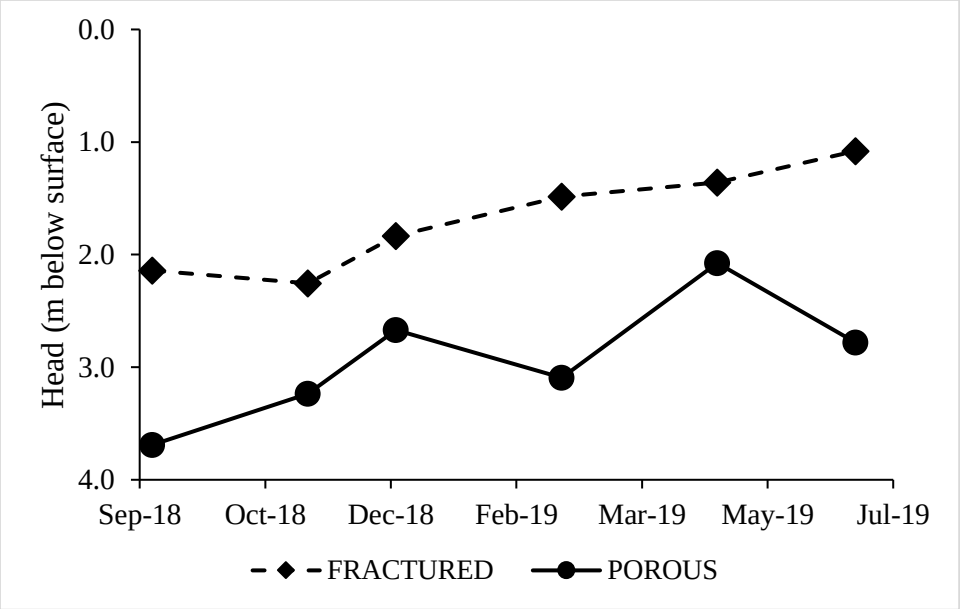

Figure 5.13 - Correlation between heads in both aquifers during the studied period. Heads are expressed in meters below the surface.

5. Discussion

5.1. Landfill leachate plume geochemistry

The development of a landfill leachate plume and migration of different pollutants through the saturated zone will be strongly dependent on the local geological setting and hydrogeological flow directions (Christensen et al., 2001). As the plume develops, leachate compounds will be subjected to attenuation mechanisms due to interactions with the environment (Christensen et al., 2001). In most instances, dilution will be the first attenuation process to affect leachate compounds in groundwater. The role of other mechanisms such as absorption, ion exchange, and adsorption will depend on soil and pollutant's chemical properties (Christensen et al., 2001; Lisk, 1991). Additionally, the mixing of reduced leachate with an often-oxidized aquifer will set environmental conditions for redox-dependent species. Tracing the propagation of the landfill leachate plume through the saturated zone requires a comprehensive monitoring network that covers different groundwater depths and flow directions. In the present study, the geochemical data reveals significant variations across the JCBL landfill-groundwater-surface water system. While the leachate is a highly reduced solution, ground and surface waters are highly oxidized, thus forming a robust geochemical gradient. The following main points arise from the geochemical data: how far does the leachate plume migrate near the JCBL, and how

does it interact with a highly oxidized oxisol in which the main components are Fe and Al? How do the different water compartments (i.e., shallow and deep groundwater and surface water) interact with each other? These questions are essential to define the main controls of groundwater-leachate interaction, which are important to understand chemical processes that may occur as the plume migrates in the oxisol.

Geochemical data presented in Table 5.3 indicate that the shallow aquifer is being significantly contaminated by reduced solutions derived from the landfill. These effects are not clearly observed in deep groundwater nor in surface waters from the Cabeceira do Valo stream, suggesting that the plume is restricted to the shallow aquifer. The leachate from the landfill promotes major geochemical alterations in the shallow groundwater, being the most important: changes on physicochemical water parameters (conductivity, alkalinity, and DOC), and alterations on the concentration chemical species, particularly those that are redox-dependent. There are also significant alterations in the carbon isotopic composition of dissolved CO_2, which will be addressed in the next topic.

Among the physicochemical parameters, there is a significant contrast in conductivity, DO, and DOC between the shallow and deep aquifers. A linear increase in conductivity, alkalinity, and DOC with chloride (Cl^-) content is observed from the deep aquifer toward the stream, the shallow aquifer and the landfill leachate. The DO behaves the opposite way, presenting a linear decrease in the same direction. As Cl^- behaves as conservative or inert specie, we argue that the linear behavior of these physicochemical parameters indicates they are also nearly conservative. In this case, dilution will be the most critical attenuation mechanism in such environment as previously suggested by Christensen et al. (2001). As demonstrated in Figure 5.14, Cl^- plume possibly has a vertical and horizontal propagation front in the area, reaching the confined aquifer with deficient concentrations (approximately 1.0 mg/L). It is also expected that the horizontal dispersion velocity of this pollutant is faster in shallower depths due to the high hydraulic conductivity of the oxisol (Campos, 2004). Sodium (Na^+) will also behave as a conservative parameter in the JCBL leachate plume (Figure 5.14), since it is not affected by ion exchange interaction with soil components (Christensen et al., 2001).

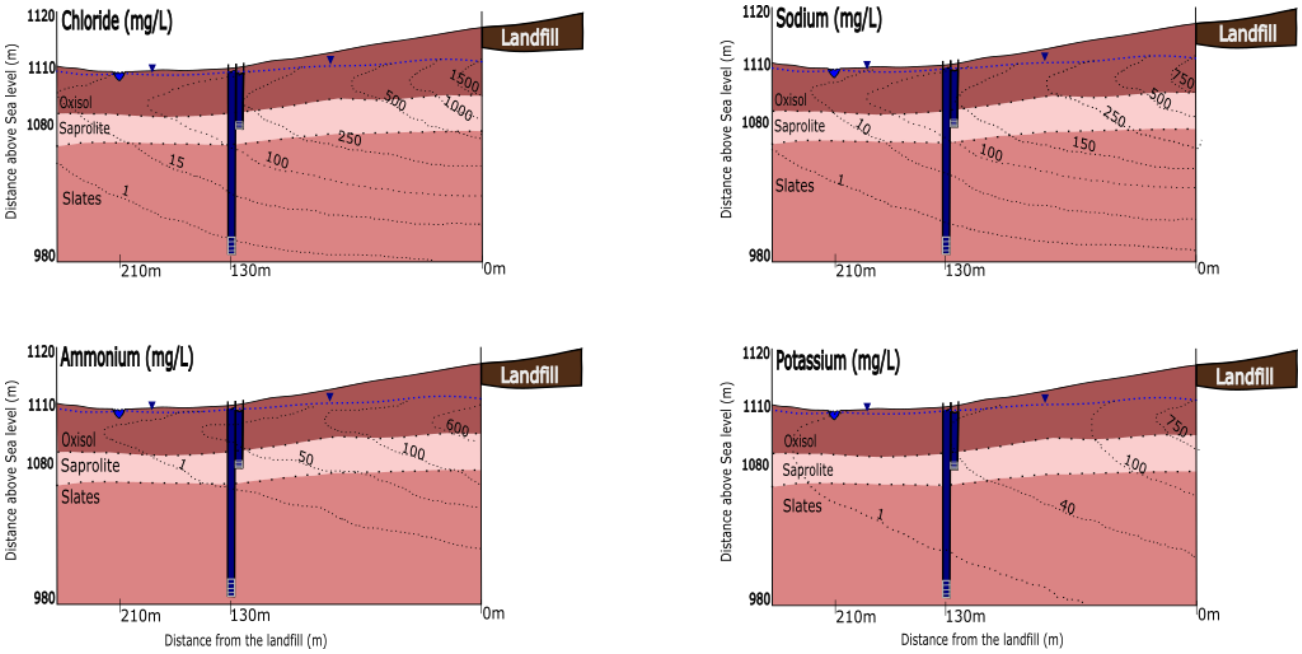

Figure 5.14 - Estimation of the propagation of chloride, sodium, ammonium, and potassium plume in the saturated zone based on concentrations of the sampling sites and literature (Christensen et al., 2001). Grey lines on the base of the monitoring well indicate the filter position. Soil profile and thickness were estimated based on the well's drilling samples.

The assessment of chloride and sodium concentrations throughout the plume helped to identify that pollutants are unlikely to be found further than 300 meters from the landfill and deeper than 150 meters (Figure 5.14). Furthermore, the shallower water level of the deep aquifer well indicates that we may have an upward groundwater migration, thus suggesting that the shallow aquifer water is probably sourced from the deep fractured one (Figure 5.13). This vertical drainage may also function as a hydraulic barrier that avoids migration of contaminants to the fractured aquifer. This fact has also a direct impact in the isotopic analysis, especially when considering that the background of δ^{13}C-DIC in region is similar to the values measured in the deep aquifer.

Other parameters such as Ca, Mg, and K behave as non-conservative cations, suggesting that interactions between the contaminated shallow aquifer and the oxisol lead to depletion of these elements in the groundwater. Previous studies suggest that the propagation of K^+, Ca^{2+} and Mg^{2+} can be attenuated by ion exchange with clay minerals from the soil, or precipitation (Christensen et al., 2001). The propagation of the K-plume in the studied site has been estimated to reach the confined aquifer in deficient concentrations (approximately 0.5 mg/L) (Figure 5.14). However, this low concentration of K^+ in groundwater can also be characteristic of the aquifer geochemistry, disregarding this data as an indication of plume propagation.

Chemical species that are redox dependent have different concentrations in the leachate and in the shallow aquifer. For instance, the shallow aquifer has an anomalously high concentration of total Fe, especially the species Fe^{2+}. We argue that this anomaly results from the interaction between the leachate and iron-rich oxisol, which brings to solution Fe^{2+} initially present as Fe^{3+} in soil minerals (e.g., hematite, goethite, and iron-bearing clays). Soils around the landfill are particularly enriched in Fe and Al, which are elements concentrated in tropical zones by laterization (Bockheim and Gennadiyev, 2000). Table 5.3 shows that the leachate has a low concentration of Fe, reinforcing the above interpretation. Aluminum is also observed in the shallow aquifer with an average value of 0.56 mg/L which, despite its inert property, it possibly being associated to water as well.

The difference in redox conditions between the leachate and the shallow aquifer also affects the nitrogen species distribution. While NH_4^+ is the main N-specie in the leachate (average $NO_3^-/NH_4^+ \sim 0.02$), both NO_3^- and NH_4^+ are important species in the shallow aquifer. We argue that part of the NH_4^+ present in the leachate is oxidized to NO_3^- when it mixes the more oxidized shallow groundwater. The correlation between Cl and the molar sum of nitrogen species indicates that nitrogen is not conservative, being probably partially lost as N_2 or by other processes (Figure 5.14). For instance, NH_4^+ may be incorporated by clay minerals present in oxisol, as reported by Böhlke et al. (2006), Christensen et al. (2001) and Gooddy et al. (2014).

5.2. Estimation of carbon sources in contaminated groundwater

As indicated by the geochemical data, the shallow unconfined aquifer presented higher concentrations of different pollutants, which are probably sourced from the landfill. Because the sampling sites are in an urbanized area, other possible sources of groundwater contamination cannot be ruled out. Previous studies have shown that the isotopic composition of dissolved inorganic carbon may be a robust tracer of groundwater contamination by landfill leachate (Castañeda et al., 2012; Engelmann et al., 2018; North et al., 2004; Porowska, 2015). This is particularly true when the organic matter is consumed by methanogenesis, as shown by Equations 5.3 and 5.4 below:

5.3) $CH_3COOH \rightarrow CO_2 + CH_4$

5.4) $CO_2 + 4H_2 \rightarrow CH_4 + 2H_2O$

These reactions will increase the solution pH and release a mixture of CH_4 and CO_2 (Christensen et al., 2001; Engelmann et al., 2017; Kjeldsen et al., 2002; Porowska, 2015; Wimmer et al.,

2013). Because of the large carbon isotope fractionation values between CO_2 and CH_4 at low temperatures (e.g., +68.2‰ at 25°C; Bottinga, 1969), mass balance indicates that CO_2 produced by methanogenesis will generally have a high $\delta^{13}C$ value (Grossman et al., 2002; Hackley et al., 1996; North et al., 2006; Porowska, 2015; van Breukelen et al., 2003; Wimmer et al., 2013). Hence, stable carbon isotope studies can provide valued information about carbon transfer from a landfill that has reached the methanogenesis stage to the natural environment due to the distinct isotope signature of these sources (Engelmann et al., 2018; Grossman et al., 2002; Porowska, 2015; van Breukelen et al., 2003; Wimmer et al., 2013). The transformations of the released CO_2 in DIC depend on by acid-base and redox reactions; therefore, the analysis of the isotopic composition of these species plays an essential role in the understanding of the carbon cycle, biogeochemical processes, and contaminants flow to water resources (Engelmann et al., 2018; Zhou et al., 2015).

Dissolved CO_2 in groundwater is commonly expressed as alkalinity, in which the most abundant specie is the bicarbonate ion (HCO_3^-). This ion may have different sources (e.g., soil respiration, atmosphere, contaminants, carbonate rocks) and can be attenuated by complexation and precipitation reactions with metals such as Ca, Mg, Na, Fe, and Mn (Christensen et al., 2001). The data from Table 5.3 indicate very high alkalinity values in the leachate and quite high values in the shallow and deep aquifers. As indicated by the $\delta^{13}C$-DIC and nitrogen species, the high alkalinity observed in the shallow aquifer is probably related to contamination from the leachate. However, it is not clear the origin of the high alkalinity observed in the deep aquifer since there is no evidence of the leachate plume contamination. Because of the high values of Ca and Mg (Table 5.3), the observed alkaline values could be related to interactions with carbonate minerals present within the rocks of the host aquifer.

The interpretation above is fully supported by the isotopic composition of dissolved inorganic carbon ($\delta^{13}C$). Leachate samples from the JCBL have a highly positive $\delta^{13}C$ (~ +13‰), indicating fermentation of acetic acid as the primary methanogenic process in the landfill (Del Rey et al. in prep.). In contrast, dissolved inorganic carbon in ground and surface waters near the landfill is much more negative. The shallow groundwater has an average $\delta^{13}C$ value of +0.55‰, deep groundwater has an average value of -11.65‰, and surface water has an average value of -9.64‰. Available regional groundwater $\delta^{13}C$ values range between -12.27 and -18.03 (Pacheco, 2012), indicating that the deep aquifer and the Cabeceira do Valo stream do not clearly show the effects of leachate derived from the landfill. It further supports the

interpretation that the alkalinity observed in the deep groundwater is not related to contamination from the landfill. In contrast, the shallow groundwater presents average isotope values that fall in between the leachate and uncontaminated groundwater (Figure 5.15). These high values observed in the shallow well indicate a contribution of carbon from leachate (North et al., 2006; van Breukelen et al., 2003), which is also supported by other geochemical parameters such as the concentrations of Fe and N species discussed above.

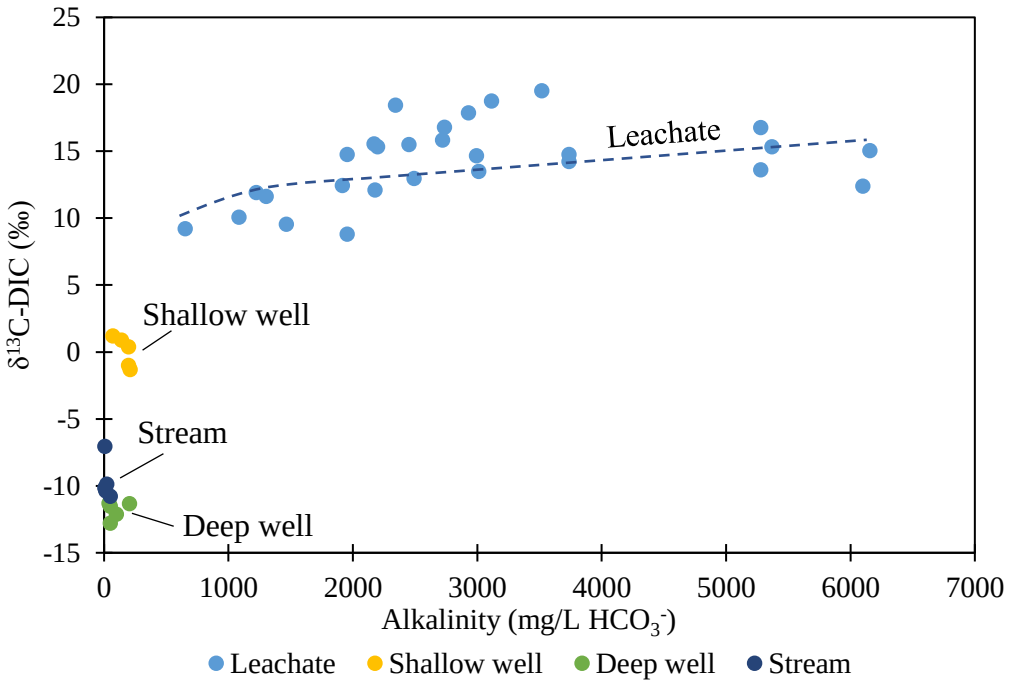

Figure 5.15 - Cross-plot Alkalinity (mg/L HCO_3^-) *versus* δ^{13}C-DIC (‰) indicating the values for the shallow well (Porous aquifer) relative to leachate samples, deep well and surface water. See Figure 1 for location of the sampling sites.

The high $\delta^{13}C$ value of CO_2 produced by methanogenesis may be used as a tracer to evaluate groundwater contamination by the landfill leachate. This evaluation can be assessed if considering that the DIC has two main sources: the leachate and groundwater. The isotopic mass balance (Equation 5.5) implies that $\delta^{13}C_{total}$ measured in the water sample is the result of these two different sources with distinct $\delta^{13}C$ values (Engelmann et al., 2018; Hackley et al., 1996; Mohammadzadeh and Clark, 2011; Porowska, 2015)

5.5) $$\delta^{13}C_{total} = X_{BG} \times \delta^{13}C_{BG} + X_{leachate} \times \delta^{13}C_{leachate}$$

In the Equation 5.5, X represents the fraction of carbon from each source, being $X_{BG} + X_{leachate} = 100\%$. BG represents the uncontaminated background water, which is assumed to have the same δ^{13}C-DIC of deep groundwater ($\delta^{13}C_{BG}$ = -11.65 ‰). The $\delta^{13}C_{leachate}$ was assumed to be

+13.83 ‰ (Table 5.3). Based on the δ^{13}C-DIC of the shallow well, which is the result of the mixture between the two sources, we have calculated the fraction of CO_2 derived from the pristine groundwater and from the leachate. Our calculations indicate that about 48% of the CO_2 in the shallow aquifer is derived from the leachate. This is a minimum value, considering that part of the CO_2 may be derived from oxidation of the CH_4, thus driving the δ^{13}C-DIC to lower values. Figure 5.16 illustrates the relationship between the fraction of methanogenic CO_2 and the head of the shallow well. An increase in of the shallow well's head is accompanied by an increase in the fraction of methanogenic derived CO_2, which indicates that the arrival of methanogenic CO_2 is not affected by dilution, therefore, its attenuation seams dependent on complexation and precipitation reactions.

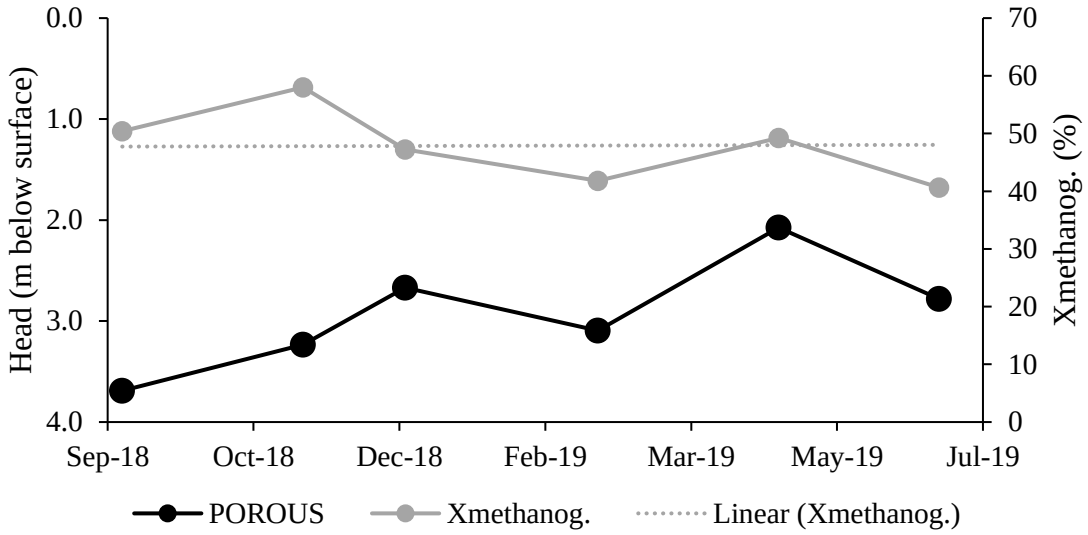

Figure 5.16 - Variations on the contributions of methanogenic CO_2 as the phreatic level changes in the porous aquifer. Linear (Xmethanog.) shows the average value of the contribution of methanogenic CO_2 in porous aquifer, which is about 48%.

6. Conclusion

The dissolved carbon isotopic composition and other geochemical data indicate that landfill leachate is affecting water quality in the surroundings of the JCBL, especially of the shallow unconfined aquifer. There is also evidence that attenuation processes in the saturated zone decrease the horizontal and vertical dispersion of these contaminants. The pH, δ^{13}C-DIC, and OD data point to anoxic condition of the leachate and that organic matter decomposition in the landfill has reached the methanogenic stage. The concentration of redox species such as NH_4^+ and Fe^{2+} in groundwater samples suggest that there is a redox zonation in the contamination plume. Furthermore, the interaction between the leachate and the Fe-rich oxisol affects groundwater geochemistry as indicated by the high levels of Fe^{2+} in the shallow aquifer.

6. CONSIDERAÇÕES FINAIS E SUGESTÕES

Este trabalho teve como principal objetivo definir o estágio de estabilização do ACJC com base em parâmetros geoquímicos. Desta forma, o primeiro artigo apresentado nesta dissertação, intitulado "*Seasonal variations of geochemical parameters for a tropical landfill: Implications for landfill stabilization*", cumpre o primeiro objetivo específico desta dissertação ao abordar como variações sazonais (ex. regime de chuvas) alteram parâmetros geoquímicos que acabam influenciando na estabilidade biológica do ACJC. As principais conclusões deste artigo foram:

- Os dados de concentrações dos gases CO_2 e CH_4 medidos nos queimadores explicitam a heterogeneidade espacial do ACJC, porém, pode se dizer que o principal processo atuante na produção de gases é a metanogênese por fermentação do ácido acético (CH_3COOH);

- A comparação de parâmetros físicos e químicos (OD, pH, NO_3^-, NH_4^+, SO_4^{2-}, Fe) e isotópicas (δ^{13}C-DIC) suporta evidências de que o processo de metanogênese é dominante no ACJC;

- A água da chuva atua como o principal mecanismo de entrada de oxigênio no sistema, favorecendo a oxidação aeróbica da matéria orgânica, aumento a concentração de espécies redox, e afetando a produção de metano;

- A decomposição anaeróbica da matéria orgânica por oxirredução foi identificada em locais mais confinados do ACJC, onde o consumo do carbono orgânico dissolvido ocorre em paralelo à diminuição na concentração dos íons SO_4^{2-}, NO_3^- e Fe^{3+}.

- Outros processos secundários como oxidação do CH_4 e redução do CO_2 também são observados no ACJC.

O segundo artigo produzido nesta dissertação, intitulado "I*norganic carbon isotope composition (δ^{13}C-DIC) as an indicator of contamination level by landfill leachate*", cumpre o segundo objetivo específico desta dissertação ao demonstrar por meio de dados químicos e isotópicos que a percolação de lixiviado tem afetado a qualidade dos aquíferos da região adjacente ao ACJC, especialmente em profundidades mais rasas. Além disso, a interação lixiviado (reduzido) com o aquífero (oxidado) leva a formação de zonas de oxirredução, identificadas pela presença de espécies reduzidas como NH_4^+ e Fe^{2+} no aquífero mais raso. A interação do lixiviado com o latossolo também afeta a geoquímica da água subterrânea, indicada

pela alta concentração de Fe^{2+} observada no poço raso. A ocorrência de uma drenança vertical do aquífero fraturado para o intergranular atua como um mecanismo de atenuação da propagação da pluma de contaminação para maiores profundidades.

Como forma de dar prosseguimento às indagações aqui levantadas, sugere-se que se continue o monitoramento geoquímico do ACJC para que se detalhe, assim, a atuação dos processos de metanogênese e oxidações aeróbica e anaeróbica em relação à produção de gases no aterro. Também seria de grande relevância a investigação da zona de oxirredução causada pela mistura lixiviado+água subterrânea, principalmente no que tange a remobilização de ferro no sistema.

PROPOSTA DE MONITORAMENTO GEOQUÍMICO

Sugere-se que seja realizado um monitoramento geoquímico para um melhor gerenciamento dos gases e lixiviados produzidos no ACJC. Primeiramente, para que se amplie a produção de CH_4 no ACJC deve-se evitar a entrada de água de chuva no sistema e definir um procedimento fechado de recirculação de lixiviado.

O monitoramento geoquímico deve contemplar as seguintes atividades:

- Avaliação da qualidade do lixiviado. Este monitoramento tem como objetivo avaliar o processo de produção de metano por meio da degradação da matéria orgânica que se encontra disponível em solução. Para isto, os principais parâmetros a serem quantificados são:

- pH, Eh (ou ORP), alcalinidade, oxigênio dissolvido (OD);

- DBO (demanda bioquímica de oxigênio) e DQO (demanda química de oxigênio): a razão DBO/DQO auxiliam na avaliação da atividade biológica do sistema e, consequentemente, uma melhor avaliação do estágio de estabilização do aterro;

- DOC (carbono orgânico dissolvido): quantificar as diferentes espécies e suas composições isotópicas (Mohammadzadeh e Clark, 2008) como forma de aprofundar o conhecimento sobre mecanismos de degradação da matéria orgânica;

- DIC (carbono inorgânico dissolvido): Quantificar as diferentes espécies, principalmente CO_2 e HCO_3^- (alcalinidade) e a concentração de CH_4 dissolvido. Avaliar também as composições isotópicas do DIC e CH_4;

- Medir a concentração de DIC e DOC em profundidades distintas no aterro;

- Concentração das espécies redox (NO_3^-, NO_2^-, NH_4^+, N_2, MnO_2, $MnCO_3$, Fe^{3+}, Fe^{2+}, SO_4^{2-}, e HS^-) em diferentes profundidades no aterro;

- Realizar ensaios de *Biochemical methane potential* (BMP), ou potencial bioquímico de metano (Filer et al., 2019).

- Quantificação dos gases gerados: monitorar as concentrações de gases emitidos pelo aterro e diferentes áreas. Sugere-se prioritariamente que os seguintes gases sejam quantificados de forma periódica: CO_2, CH_4 e H_2S. A importância na quantificação dos dois primeiros está relacionada ao processo de degradação aeróbica e anaeróbica que podem ocorrer no sistema. Quanto a quantificação do H_2S serve de ferramenta auxiliar na avaliação da idade do aterro e, consequentemente, seu potencial de emissão de poluentes a longo prazo (Kim, 2006; Porowska, 2016).

REFERÊNCIAS BIBLIOGRÁFICAS

Adeolu, A.O., Ada, O. V, Gbenga, A.A., Adebayo, O.A., 2011. Assessment of groundwater contamination by leachate near a municipal solid waste landfill. African Journal of Environmental Science and Technology 5 (11), 933-940.

Aghdam, E.F., Scheutz, C., Kjeldsen, P., 2018. Impact of meteorological parameters on extracted landfill gas composition and flow. Waste Management 87, 905-914.

Albrechtsen, H.J., Bjerg, P.L., Ludvigsen, L., Rügge, K., Christensen, T.H., 1999. An anaerobic field injection experiment in a landfill leachate plume, Grindsted, Denmark. 2. Deduction of anaerobic (methanogenic, sulfate-, and Fe(III)-reducing) redox conditions. Water Resources Research 35 (4), 1247-1256.

Amorim, V.P., Aguiar, M.I.O., 1978. As Características Físicas e Químicas do Lixo do Distrito Federal – SLU/GDF. Relatório Técnico, Brasília, DF, 31p.

Araújo, R.N.G. 1996. Estudos Geoquímicos da Contaminação dos Recursos Hídricos e sua Propagação nas Adjacências do Aterro de Resíduos Sólidos Jockey Club-DF. Dissertação de Mestrado, Instituto de Geociências, Universidade de Brasília, Brasília, DF, 74 p.

Atekwana, E.A., Krishnamurthy, R. V., 2004. Investigating landfill-impacted groundwater seepage into headwater streams using stable carbon isotopes. Hydrological Processes 18 (10), 1915-1926.

Baedecker, M.J., Back, W., 1979. Hydrogeological Processes and Chemical Reactions at a Landfill. Ground Water 17 (5), 429-437.

Barbosa, L.Q., Bernardes, R.S., Brito, A.J., 2015. Propostas de Remediação de Área Degradada por Resíduos Sólidos Urbanos – Estudo de Caso Aterro Jokey Club Brasília, DF, in: XXI Simpósio Brasileiro de Recursos Hídricos. pp. 1-10.

Barella, C.F., Bacellar, L. de A.P., Nalini, H.A., 2013. Influence of the natural oxidation of the leachate organic fraction from a landfill on groundwater quality, Belo Horizonte: Minas Gerais, south-eastern Brazil. Environmental Earth Sciences 70 (5), 2283-2292.

Barlaz, M.A., Ham, R.K., 1993. Leachate and gas generation, in: Daniel D.E. (Eds.), Geotechnical Practice for Waste Disposal. Springer, Boston, pp. 113–136.

Bockheim, J.G., Gennadiyev, A.N., 2000. The role of soil-forming processes in the definition of taxa in Soil Taxonomy and the World Soil Reference Base. Geoderma 95, 53-72.

Böhlke, J.K., Smith, R.L., Miller, D.N., 2006. Ammonium transport and reaction in contaminated groundwater: Application of isotope tracers and isotope fractionation studies. Water Resources Research 42 (5), 1-19.

Bottinga, Y., 1969. Calculated fractionation factors for carbon and hydrogen isotope exchange in the system calcite-CO_2-graphite-methane-hydrogen and water vapour. Geochimica et Cosmochimica Acta 33, 49-64.

Botz, R., Pokojski, H.-D., Schmitt, M., Thomm, M., 1996. Carbon isotope fractionation during bacterial methanogenesis by CO_2 reduction. Organic Geochemistry 25 (3-4), 255-262.

Bozkurt, S., Moreno, L., Neretnieks, I., 1999. Long-term fate of organics in waste deposits and its effect on metal release. Science of the Total Environment 228 (2-3), 135-152.

Campos, J.E.G., 2004. Hidrogeologia do Distrito Federal: Bases para a Gestão dos Recursos Hídricos Subterrâneos. Revista Brasileira de Geociências 34 (1), 41-48.

Campos, J.E.G., Dardenne, M.A., Freitas-Silva, F.H., Martins-Ferreira, M.A.C., 2013. Geologia do Grupo Paranoá na porção externa da Faixa Brasília. Brazilian Journal of Geology 43 (3), 461-476.

Campos, J.E.G., Gonçalves, T.D., 2015. Diretrizes para o desenvolvimento de recarga artificial de aquíferos no Distrito Federal. Relatório de consulta técnica, ADASA, Brasília, DF, 70 p.

Campos, H.K.T., 2018. Como fechamos o segundo maior lixão do mundo. Revista Brasileira de Planejamento e Orçamento 8 (2), 204-253.

Carneiro, G.A., 2002. Estudo de Contaminação do Lençol Freático Sob a Área do Aterro de Lixo do Jockey Club-DF e Suas Adjacências. Dissertação de Mestrado, Departamento de Engenharia Civil e Ambiental, Universidade de Brasília, Brasília, DF, 140 p.

Caschetto, M., Robertson, W., Petitta, M., Aravena, R., 2018. Partial nitrification enhances natural attenuation of nitrogen in a septic system plume. Science of the Total Environment 625, 801-808.

Castañeda, S.S., Sucgang, R.J., Almoneda, R. V, Mendoza, N.D.S., David, C.P.C., 2012. Environmental isotopes and major ions for tracing leachate contamination from a municipal land fi ll in Metro Manila , Philippines. Journal of Environmental Radioactivity 110, 30-37.

Cavalcanti, M.M., 2013. Aplicação De Métodos Geoelétricos No Limites Do Aterro Controlado Do Jokey Clube De Brasília. Dissertação de Mestrado, Instituto de Geociências, Universidade de Brasília, Brasília, DF, 128p.

Christensen, T.H., Kjeldsen, P., Bjerg, P.L., Jensen, D.L., Christensen, J.B., Baun, A., Albrechtsen, H., Heron, G., 2001. Biogeochemistry of landfill leachate plumes. Applied Geochemistry 16, 659–718.

Companhia de Planejamento do Distrito Federal – CODEPLAN, 2017. Atlas do Distrito Federal. Brasília, DF, 114 p.

Companhia de Saneamento Ambiental do Distrito Federal – CAESB, 2018. Banco de dados hidrológicos.

Conrad, R., 2005. Quantification of methanogenic pathways using stable carbon isotopic signatures: A review and a proposal. Organic Geochemistry 36, 739-752.

Cossu R., Morello L., Raga R., Cerminara G., 2016. Biogas production enhancement using

semi-aerobic pre-aeration in a hybrid bioreactor landfil. Waste Management 55, 83-92.

Diamond, L.W., Akinfiev, N.N., 2003. Solubility of CO_2 in water from -1.5 to 100°C and from 0.1 to 100 MPa: evaluation of literature data and thermodynamic modelling. Fluid Phase Equilibria 208, 265-290.

Distrito Federal, 2018. Plano Distrital de Gestão Integrada de Resíduos Sólidos. Brasília, DF, 409 p.

Empresa Brasileira de Pesquisa Agropecuária – EMBRAPA, 1978. Levantamento de Reconhecimento dos Solos do Distrito Federal. Boletim Técnico, EMBRAPA/SNLCS, Rio de Janeiro, 455 p.

Engelmann, P. de M., dos Santos, V.H.J.M., Moser, L.I., do Canto Bruzza, E., Barbieri, C.B., Barela, P.S., de Moraes, D.P., Augustin, A.H., Goudinho, F.S., Melo, C.L., Ketzer, J.M.M., Rodrigues, L.F., 2017. Environmental monitoring of water resources around a municipal landfill of the Rio Grande do Sul state, Brazil. Environmental Science and Pollution Research 24 (26), 1-14.

Engelmann, P.M., Santos, V.H.J.M., Barbieri, C.B., Augustin, A.H., Ketzer, J.M.M., Rodrigues, L.F., 2018. Environmental monitoring of a landfill area through the application of carbon stable isotopes, chemical parameters and multivariate analysis. Waste Management 76, 591-605.

Filer J., Ding H.H., Chang S., 2019. Biochemical Methane Potential (BMP) Assay Method for Anaerobic Digestion Research. Water 11 (5), 921.

Gooddy, D.C., Macdonald, D.M.J., Lapworth, D.J., Bennett, S.A., Griffiths, K.J., 2014. Nitrogen sources, transport and processing in peri-urban floodplains. Science of the Total Environment 494–495, 28-38.

Greentec, 2012. Plano de Manejo ARIE da Cabeceira do Valo. Brasília, DF. 440 p.

Grossman, E.L., Cifuentes, L.A., Cozzarelli, I.M., 2002. Anaerobic methane oxidation in a landfilll-leachate plume. Environmental Science & Technology 36 (11), 2436-2442.

Gurijala, K.R., Suflita, J.M., 1993. Environmental Factors Influencing Methanogenesis from Refuse in Landfill Samples. Environmental Science & Technology 27 (6), 1176-1181.

Haarstad, K., Mæhlum, T., 2013. Tracing solid waste leachate in groundwater using $\delta^{13}C$ from dissolved inorganic carbon. Isotopes in Environmental and Health Studies 49 (1), 48-61.

Hackley, K.C., Liu, C.L., Coleman, D.D., 1996. Environmental Isotope Characteristics of Landfill Leachates and Gases. Ground Water 34 (5), 827-836.

Han, D., Tong, X., Currell, M.J., Cao, G., Jin, M., Tong, C., 2014. Evaluation of the impact of an uncontrolled landfill on surrounding groundwater quality, Zhoukou, China. Journal of Geochemical Exploration 136, 24-39.

He, X., Xi, B., Wei, Z., Jiang, Y., Geng, C., Yang, Y., 2011. Physicochemical and spectroscopic characteristics of dissolved organic matter extracted from municipal solid waste (MSW)

and their influence on the landfill biological stability. Bioresource Technology 102 (3), 2322-2327.

Hoefs, J., 2009. Stable Isotope Geochemistry, sixth ed. Springer, Göttingen.

Instituto Nacional de Meteorologia – INMET, 2018. http://www.inmet.gov.br/portal/ (acesso em 12 de abril de 2018)

Junqueira, F.F., 1995. Relatório Individual Final. Programa RHAE/CNPq/MCT, Brasília, DF, 90p.

Kim, K., 2006. Emissions of reduced sulfur compounds (RSC) as a landfill gas (LFG): A comparative study of young and old landfill facilities. Atmospheric Environment 40, 6567-6578.

Kjeldsen, P., Barlaz, M.A., Rooker, A.P., Baun, A., Ledin, A., Christensen, T.H., 2002. Present and long-term composition of MSW landfill leachate: A review. Critical Reviews in Environmental Science and Technology 32(4), 297-336.

Koide, S., Bernardes, R.S., 1998. Contaminação do Lençol Freático sob a Área do Aterro do Jockey Club, Distrito Federal, in: X Congresso Brasileiro de Águas Subterrâneas. pp. 1–11.

Kulikowska, D., Klimiuk, E., 2008. The effect of landfill age on municipal leachate composition. Bioresource Technology 99, 5981-5985.

Lee, K., Ko, K., 2006. Stable isotopic evidence of biodegradation in a landfill site. Geochimica et Cosmochimica Acta 70, A349.

Lee, G.F., Jones-Lee, A., 2004. Flawed technology of Subtitle D Landfilling of Municipal Solid Waste.

Liamleam, W., Annachhatre, A.P., 2007. Electron donors for biological sulfate reduction. Biotechnology Advances 25, 452-463.

Lisk, D.J., 1991. Environmental effects of landfills. Science of the Total Environment 100, 415-468.

Loizidou, M., Kapetanios, E.G., 1993. Effect of leachate from landfills on underground water quality. Science of the Total Environment 128, 69-81.

Lovley, D.R., Phillips, E.J.P., 1988. Novel Mode of Microbial Energy Metabolism : Organic Carbon Oxidation Coupled to Dissimilatory Reduction of Iron or Manganese. Applied and Environmental Microbiology 54 (6), 1472-1480.

MacFarlane, D.S., Cherry, J.A., Gillham, R.W., Sudicky, E.A., 1983. Migration of contaminants in groundwater at a landfill: a case study. 1) Groundwater flow and plume delineation. Journal of Hydrology 63, 1-29.

Matsufuji, Y., Hanashima, M., Nagano, S., Tanaka, A., 1993. Generation of greenhouse effect gases from different landfill types. Engineering Geology 34, 181-187.

Mohammadzadeh, H., Clark, I., 2008. Degradation pathways of dissolved carbon in landfill leachate traced with compound-specific ^{13}C analysis of DOC. Isotopes in Environmental and Health Studies 44 (3), 267-294.

Mohammadzadeh, H., Clark, I., 2011. Bioattenuation in Groundwater Impacted by Landfill Leachate Traced with $\delta^{13}C$. Ground Water 49 (6), 880-890.

Nag, M., Shimaoka, T., Komiya, T., 2016. Impact of intermittent aerations on leachate quality and greenhouse gas reduction in the aerobic – anaerobic landfill method. Waste Management 55, 71-82.

Nag, M., Shimaoka, T., Komiya, T., 2018. Influence of operations on leachate characteristics in the Aerobic-Anaerobic Landfill Method. Waste Management 78, 698-707.

Nisiyama, F.L., 2019. Ferramenta computacional para avaliação de risco à saúde humana em áreas contaminadas - Caso de Estudo: Aterro Controlado do Jóquei Clube de Brasília/DF. Dissertação de Mestrado, Departamento de Engenharia Civil e Ambiental, Universidade de Brasília, Brasília, DF, 202 p.

Nordstrom, D.K., Wilde, F.D., 2005. Reduction- 6.5 Oxidation potential (electrode method), in: Reduction-Oxidation Potential, Version 1.2. pp. 1–21

North, J.C., Frew, R.D., Peake, B.M., 2004. The use of carbon and nitrogen isotope ratios to identify landfill leachate contamination: Green Island Landfill, Dunedin, New Zealand. Environmental International 30 (5), 631-637.

North, J.C., Frew, R.D., Van Hale, R., 2006. Can stable isotopes be used to monitor landfill leachate impact on surface waters?. Journal of Geochemical Exploration 88, 49-53.

Novaes-Pinto, M., 1994. Caracterização geomorfológica do Distrito Federal. In. Novaes-Pinto, M. (Eds.), Cerrado: caracterização, ocupação e perspectivas. UnB, Brasília pp. 285-344.

O'Leary, M.H., 1988. Carbon Isotopes in Photosynthesis. BioScience 38(5), 328-336.

Pacheco, W.L., 2012. Águas Subterrâneas Do Distrito Federal - Efeito De Sazonalidade E Características Associadas Aos Isótopos De Deutério, Oxigênio e Carbono. Dissertação de Mestrado, Instituto de Geociências, Universidade de Brasília, Brasília, DF, 145 p.

Pereira, J.H.F., Pastore, E.L., Bernardes, R.S., Souza, N.M., Carvalho, J.C., 1997. Estudos Geológico-Geotécnicos para o Planejamento e Projeto de Disposição de Resíduos Urbanos do Aterro de Lixo do Jóquei. Relatório Final, Universidade de Brasília, Brasília, DF, 17 p.

Pesquisa Distrital por Amostra de Domicílios – PDAD, 2015. SCIA-Estrutural, Brasília, DF, 54 p.

Plano Nacional de Resíduos Sólidos – PNRS, 2011. Versão Preliminar para Consulta Pública. Brasília, DF, 109 p.

Porowska, D., 2015. Determination of the origin of dissolved inorganic carbon in groundwater around a reclaimed landfill in Otwock using stable carbon isotopes. Waste Management 39, 216-225.

Porowska, D., 2016. Assessment of a degree of geochemical maturation and activity of a closed landfill site in Poland. Environmental Earth Science 75 (4), 1-8.

Reinhart, D., McCreanor, P.T., Townsend, T.G., 2002. The bioreactor landfill: Its status and future. Waste Management & Research 20, 172-186.

Rivett, M.O., Buss, S.R., Morgan, P., Smith, J.W.N., Bemment, C.D., 2008. Nitrate attenuation in groundwater: A review of biogeochemical controlling processes. Water Research 42 (16), 4215–4232.

Santos, P.C.V., 1996. Estudos da Contaminação de Água Subterrânea por Percolado de Aterro de Resíduos Sólidos do Jockey Club. Dissertação de Mestrado, Departamento de Engenharia Civil e Ambiental, Universidade de Brasília, Brasília, DF, 137 p.

Serviço de Limpeza Urbana do Distrito Federal – SLU, 2016. Relatório sobre a situação de emergência no âmbito da limpeza urbana jóquei (23.05 a 29.11.15). Relatório Técnico, Brasília, DF, 138 p.

Serviço de Limpeza Urbana do Distrito Federal – SLU, 2018. Relatório de atividades SLU – 1° trimestre 2018. Brasília, DF, 98 p.

Serviço de Limpeza Urbana do Distrito Federal – SLU, 2019. Relatório de atividades SLU – Janeiro a Setembro de 2019. Brasília, DF, 176 p.

Shalini, S.S., Karthikeyan, O.P., Joseph, K., 2010. Bioresource Technology Biological stability of municipal solid waste from simulated landfills under tropical environment. Bioresource Technology 101 (3), 845-852.

Tchobanoglous, G., O'Leary, P.R., 2002. Landfilling, in: Tchobanoglous G., Kreith F. (Eds.), Handbook of Solid Waste Management. McGraw-Hill, New York, pp. 14.1-14.93.

van Breukelen, B.M., Röling, W.F.M., Groen, J., Griffioen, J., Van Verseveld, H.W., 2003. Biogeochemistry and isotope geochemistry of a landfill leachate plume. Journal of Contaminant Hydrology 65, 245-268.

van Turnhout, A.G., Brandstätter, C., Kleerebezem, R., Fellner, J., Heimovaara, T.J., 2018. Theoretical analysis of municipal solid waste treatment by leachate recirculation under anaerobic and aerobic conditions. Waste Management 71, 246-254.

Viollier, E., Inglett, P.W., Hunter, K., Roychoudhury, a N., Van Cappellen, P., 2000. The Ferrozine Method Revisited: Fe (II)/Fe (III) Determination in Natural Waters. Applied Geochemistry 15 (6), 785-790.

Wang, Q., Matsufuji, Y., Dong, L., Huang, Q., Hirano, F., Tanaka, A., 2006. Research on leachate recirculation from different types of landfills. Waste Management 26, 815-824.

Warith, M. A., 2003. Solid waste management – New trends in landfill design. Emirates Journal for Engineering Research 8 (1), 61-70.

Weber, K.A., Achenbach, L.A., Coates, J.D., 2006. Microorganisms pumping iron: anaerobic microbial iron oxidation and reduction. Nature Reviews 4, 752-764.

Wimmer, B., Hrad, M., Huber-Humer, M., Watzinger, A., Wyhlidal, S., Reichenauer, T.G., 2013. Stable isotope signatures for characterising the biological stability of landfilled municipal solid waste. Waste Management 33 (10), 2083-2090.

Yamamoto, S., Alcauskas, J.B., Crozier, T.E., 1976. Solubility of Methane in Distilled Water and Seawater. Journal of Chemical and Engineering Data 21 (1), 78-80.

Zhou, Y., Guo, H., Lu, H., Mao, R., Zheng, H., Wang, J., 2015. Analytical methods and application of stable isotopes in dissolved organic carbon and inorganic carbon in groundwater. Rapid Communications in Mass Spectrometry 29 (19), 1827-1835.

Zmora-nahum, S., Markovitch, O., Tarchitzky, J., Chen, Y., 2005. Dissolved organic carbon (DOC) as a parameter of compost maturity. Soil Biology & Biochemistry 37, 2109-2116.

Zoneamento Ecológico e Econômico do Distrito Federal – ZEE, 2011. Relatório do Meio Físico e Biótico, Subproduto 3.1, Volume 2. Relatório técnico, Brasília, DF, 172 p.

ANEXO 1 – DATAS DAS CAMPANHAS DE AMOSTRAGEM, TIPO DE AMOSTRA COLETADA E PERÍODO SAZONAL REPRESENTATIVO

DATA DE AMOSTRAGEM	TIPO DE AMOSTRA	PERÍODO SAZONAL
31/08/2018	LIXIVIADO	SECA
12/09/2019	ÁGUA SUBTERRÂNEA; ÁGUA SUPERFICIAL	SECA
17/10/2018	LIXIVIADO	SECA
13/11/2018	ÁGUA SUBTERRÂNEA	SECA
12/12/2018	LIXIVIADO	CHUVA
18/12/2018	ÁGUA SUBTERRÂNEA; ÁGUA SUPERFICIAL	CHUVA
19/02/2019	LIXIVIADO	CHUVA
22/02/2019	ÁGUA SUBTERRÂNEA; ÁGUA SUPERFICIAL	CHUVA
11/04/2019	LIXIVIADO	CHUVA
25/04/2019	ÁGUA SUBTERRÂNEA; ÁGUA SUPERFICIAL	CHUVA
12/06/2019	LIXIVIADO	SECA
19/06/2019	ÁGUA SUBTERRÂNEA; ÁGUA SUPERFICIAL	SECA
06/09/2019	LIXIVIADO	SECA

ANEXO 2 – DADOS DAS CAMPANHAS DE AMOSTRAGEM

AMOSTRAS DE LIXIVIADO/LEACHATE SAMPLES:

								Colorimetric method (mg/L)			
SITE	**SAMPLING**	**pH**	**Cond. (µS/cm)**	**T °C**	**O.D. (mg/L)**	**Eh (mV)**	**ORP (mV)**	**Fe 2+**	**Fe 3+**	**Fe total**	**NH_4+ (mg/L)**
L1	31/08/2018	8.37	11,040.00	n.m.	n.m.	n.m.	n.m.	n.m.	n.m.	n.m.	612.50
L1	17/10/2018	8.40	11,030.00	n.m.	5.75	176.20	-32.80	0.74	0.63	1.37	596.90
L1	11/12/2018	8.30	6,920.00	25.20	0.17	n.m.	n.m.	0.26	1.01	1.26	302.77
L1	19/02/2019	8.54	8,900.00	26.10	7.32	n.m.	n.m.	0.39	0.65	1.04	413.45
L1	11/04/2019	7.76	5,520.00	24.40	0.44	276.50	67.50	0.17	1.57	1.74	195.95
L1	12/06/2019	8.14	10,520.00	21.20	0.28	n.m.	n.m.	0.31	0.89	1.20	434.19
L1	06/09/2019	8.36	12,040.00	20.90	0.14	n.m.	n.m.	0.41	0.96	1.36	883.88
D2	31/08/2018	7.64	12,730.00	n.m.	n.m.	n.m.	n.m.	n.m.	n.m.	n.m.	728.2
D2	17/10/2018	7.59	7,190.00	n.m.	0.41	-66.10	-275.10	1.14	0.27	1.41	1,622.30
D2	11/12/2018	8.00	8,160.00	25.40	2.85	n.m.	n.m.	0.51	2.04	2.56	487.60
D2	19/02/2019	7.76	6,950.00	28.50	0.32	n.m.	n.m.	0.19	0.69	0.88	624.51
D2	11/04/2019	7.22	4,850.00	25.80	1.44	167.50	-41.50	0.10	0.80	0.90	694.46
D2	12/06/2019	7.88	6,720.00	22.40	0.56	n.m.		0.29	1.21	1.50	329.97
D2	06/09/2019	7.63	14,030.00	25.30	0.76	n.m.		0.86	n.m.	n.m.	1,255.61
D3	31/08/2018	7.30	12,240.00	n.m.	n.m.	n.m.	n.m.	n.m.	n.m.	n.m.	484.69
D3	17/10/2018	7.52	12,540.00	n.m.	1.08	206.30	-2.70	1.19	0.38	1.57	807.72
D3	11/12/2018	7.50	9,300.00	27.40	0.14	n.m.	n.m.	0.05	0.15	0.20	638.71
D3	19/02/2019	7.32	10,080.00	30.10	0.12	n.m.	n.m.	0.13	0.31	0.44	280.49
D3	11/04/2019	7.04	7,690.00	28.20	0.21	-90.50	-299.50	0.79	1.25	2.04	887.85
D3	12/06/2019	7.35	9,990.00	25.60	0.11	n.m.	n.m.	0.18	0.40	0.57	419.20
D3	06/09/2019	7.48	5,640.00	27.00	0.21	n.m.	n.m.	0.96	0.97	1.93	920.33
D4	11/12/2018	8.05	5,620.00	27.00	2.95	n.m.	n.m.	0.00	0.06	0.06	290.54
D4	19/02/2019	7.40	1,940.00	27.00	1.06	n.m.	n.m.	0.02	0.00	0.02	31.95
D4	11/04/2019	7.65	2,430.00	28.00	2.87	332.00	123.00	0.00	0.58	0.58	130.15
D5	17/10/2018	7.27	12,080.00	n.m.	0.06	-92.05	-301.05	1.25	0.35	1.60	644.08
D5	11/12/2018	7.53	10,560.00	n.m.	0.13	n.m.	n.m.	0.02	0.24	0.26	547.38
D5	19/02/2019	7.34	12,070.00	33.00	0.10	n.m.	n.m.	0.31	0.10	0.41	536.54
D5	11/04/2019	7.22	11,570.00	29.50	0.15	-114.00	-323.00	0.31	0.61	0.92	915.92
D5	12/06/2019	7.45	11,510.00	26.50	0.20	n.m.	n.m.	0.33	0.53	0.86	127.63
D5	06/09/2019	7.33	12,870.00	30.20	0.11	n.m.	n.m.	1.07	1.09	2.16	1,305.74

SITE	**SAMPLING**	**Alk. (mg/L HCO3-)**	**δ13C-DIC**	**δ13C-DOC**	**DOC (mg/L)**	**F (mg/L)**	**Cl (mg/L)**	**NO3 (mg/L)**	**PO4 (mg/L)**	**SO4 (mg/L)**
L1	31/08/2018	2,928.00	17.87	-25.06	n.m.	<LQ	146.74	19.45	<LQ	39.32
L1	17/10/2018	3,518.02	19.53	-26.41	385.59	<LQ	1,790.90	<LQ	<LQ	<LQ
L1	11/12/2018	1,465.84	9.56	-26.19	145.34	<LQ	792.65	contamination	<LQ	290.21
L1	19/02/2019	3,114.92	18.76	-24.36	222.73	<LQ	2,119.81	2.57	<LQ	49.44
L1	11/04/2019	1,084.72	10.08	-24.87	89.07	<LQ	721.01	18.68	<LQ	298.30
L1	12/06/2019	2,449.42	15.51	-24.76	192.80	<LQ	1,457.08	6.60	<LQ	100.29
L1	06/09/2019	2,342.22	18.45	-29.10	622.25	<LQ	2,347.97	contamination	8.61	8.86
D2	31/08/2018	6,100.00	12.4	-26.12	n.m.	<LQ	119.49	14.65	<LQ	31.86
D2	17/10/2018	5,277.04	13.62	-27.04	394.71	<LQ	1,779.55	<LQ	<LQ	<LQ
D2	11/12/2018	1,954.46	8.82	-25.63	220.57	<LQ	836.74	contamination	<LQ	253.47
D2	19/02/2019	3,737.90	14.24	-22.40	506.50	<LQ	2,902.36	<LQ	<LQ	31.43
D2	11/04/2019	1,084.72	3.45	-25.12	74.96	<LQ	612.09	25.92	<LQ	657.94
D2	12/06/2019	2,993.74	14.66	-26.21	265.86	<LQ	1,764.12	12.91	<LQ	28.67
D2	06/09/2019	3,009.86	13.50	-32.45	932.95	<LQ	2,245.72	contamination	<LQ	7.87
D3	31/08/2018	5,368.00	15.34	-25.76	n.m.	<LQ	934.67	<LQ	<LQ	48.88
D3	17/10/2018	6,156.54	15.06	-25.73	362.94	<LQ	2,085.18	<LQ	<LQ	10.17
D3	11/12/2018	1,954.46	14.76	-26.05	224.85	<LQ	1,110.50	contamination	<LQ	481.87
D3	19/02/2019	2,491.93	12.98	-23.19	208.22	<LQ	1,887.94	<LQ	<LQ	124.88
D3	11/04/2019	1,301.67	11.63	-25.28	133.95	<LQ	1,395.20	<LQ	<LQ	826.08
D3	12/06/2019	2,177.27	12.12	-23.92	182.42	<LQ	1,400.07	<LQ	<LQ	425.31
D3	06/09/2019	1,915.37	12.46	-27.47	603.40	<LQ	1,697.68	contamination	<LQ	55.37
D4	11/12/2018	1,221.54	11.93	-25.81	114.50	<LQ	534.55	contamination	<LQ	402.35
D4	19/02/2019	244.31	-2.28	-25.85	22.11	<LQ	164.68	109.03	<LQ	683.28
D4	11/04/2019	650.83	9.21	-25.06	34.91	<LQ	189.32	47.58	<LQ	590.75
D5	17/10/2018	5,277.04	16.77	-26.48	346.33	<LQ	1,929.93	<LQ	<LQ	11.94
D5	11/12/2018	2,198.76	15.34	-26.23	311.59	<LQ	1,654.93	contamination	<LQ	195.44
D5	19/02/2019	3,737.90	14.77	-26.63	297.62	<LQ	2,639.06	<LQ	<LQ	43.20
D5	11/04/2019	2,169.45	15.56	-25.93	270.22	<LQ	2,198.10	<LQ	<LQ	147.96
D5	12/06/2019	2,721.58	15.84	-25.05	269.07	<LQ	2,304.94	<LQ	<LQ	22.26
D5	06/09/2019	2,736.24	16.80	-25.89	306.28	<LQ	2,012.32	contamination	<LQ	<LQ

SITE	SAMPLING	Ca (mg/L)	Mg (mg/L)	Na (mg/L)	K (mg/L)	Al (mg/L)	As (mg/L)	Ba (mg/L)	Cd (mg/L)	Co (mg/L)
L1	31/08/2018	37.21	79.31	1,036.46	n.m.	n.m.	n.m.	n.m.	n.m.	n.m.
L1	17/10/2018	50.34	88.30	1,093.67	1,120.70	<LQ	<LQ	<LQ	<LQ	<LQ
L1	11/12/2018	124.41	64.81	458.76	448.95	<LQ	<LQ	n.m.	<LQ	<LQ
L1	19/02/2019	70.42	85.29	1,056.14	1,022.54	<LQ	<LQ	n.m.	<LQ	<LQ
L1	11/04/2019	148.63	57.37	374.64	379.21	<LQ	<LQ	n.m.	<LQ	<LQ
L1	12/06/2019	80.20	78.27	798.18	799.56	<LQ	<LQ	0.34	<LQ	<LQ
L1	06/09/2019	44.90	89.61	1,172.03	1,060.98	<LQ	<LQ	<LQ	<LQ	<LQ
D2	31/08/2018	45.30	83.04	997.80	n.m.	n.m.	n.m.	n.m.	n.m.	n.m.
D2	17/10/2018	47.27	85.70	1,066.02	1,086.03	<LQ	<LQ	<LQ	<LQ	<LQ
D2	11/12/2018	148.38	67.30	522.95	508.70	<LQ	<LQ	n.m.	<LQ	<LQ
D2	19/02/2019	72.22	89.91	1,139.43	1,094.87	<LQ	<LQ	n.m.	<LQ	<LQ
D2	11/04/2019	243.12	67.52	279.05	274.29	<LQ	<LQ	n.m.	<LQ	<LQ
D2	12/06/2019	73.12	81.99	931.69	924.56	<LQ	<LQ	0.43	<LQ	<LQ
D2	06/09/2019	46.63	77.33	1,032.79	981.04	<LQ	<LQ	<LQ	<LQ	<LQ
D3	31/08/2018	84.69	104.04	965.09	n.m.	n.m.	n.m.	n.m.	n.m.	n.m.
D3	17/10/2018	98.46	131.80	1,128.02	1,192.35	<LQ	<LQ	<LQ	<LQ	<LQ
D3	11/12/2018	159.11	122.46	603.51	642.92	<LQ	<LQ	n.m.	<LQ	<LQ
D3	19/02/2019	122.44	129.51	766.04	798.60	<LQ	<LQ	n.m.	<LQ	<LQ
D3	11/04/2019	201.86	122.01	493.54	517.71	<LQ	<LQ	n.m.	<LQ	<LQ
D3	12/06/2019	179.55	135.93	693.23	756.01	<LQ	<LQ	0.47	<LQ	<LQ
D3	06/09/2019	83.90	98.13	672.65	715.31	<LQ	<LQ	<LQ	<LQ	<LQ
D4	11/12/2018	153.12	104.04	341.77	400.98	<LQ	<LQ	n.m.	<LQ	<LQ
D4	19/02/2019	241.31	48.35	131.83	155.07	<LQ	<LQ	n.m.	<LQ	<LQ
D4	11/04/2019	210.71	73.63	95.80	130.81	<LQ	<LQ	n.m.	<LQ	<LQ
D5	17/10/2018	90.59	164.69	1,150.15	1,163.30	<LQ	<LQ	<LQ	<LQ	<LQ
D5	11/12/2018	115.69	140.47	730.23	743.65	<LQ	<LQ	n.m.	<LQ	<LQ
D5	19/02/2019	89.97	139.30	1,125.93	1,139.20	<LQ	<LQ	n.m.	<LQ	<LQ
D5	11/04/2019	68.77	104.26	790.23	785.61	<LQ	<LQ	n.m.	<LQ	<LQ
D5	12/06/2019	61.52	105.30	793.36	850.75	0.38	<LQ	0.42	<LQ	<LQ
D5	06/09/2019	49.02	104.27	879.65	891.65	<LQ	<LQ	<LQ	<LQ	<LQ

SITE	SAMPLING	Cr (mg/L)	Cu (mg/L)	Fe (mg/L)	Li (mg/L)	Mn (mg/L)	Mo (mg/L)	Ni (mg/L)	P (mg/L)	Pb (mg/L)
L1	31/08/2018	n.m.	n.m.	1.34	n.m.	n.m.	n.m.	n.m.	n.m.	n.m.
L1	17/10/2018	<LQ	<LQ	1.43	<LQ	<LQ	<LQ	<LQ	0.34	<LQ
L1	11/12/2018	<LQ	<LQ	1.48	n.m.	<LQ	<LQ	<LQ	<LQ	<LQ
L1	19/02/2019	<LQ	<LQ	1.23	n.m.	<LQ	<LQ	<LQ	1.03	<LQ
L1	11/04/2019	<LQ	<LQ	1.29	n.m.	<LQ	<LQ	<LQ	<LQ	<LQ
L1	12/06/2019	<LQ	<LQ	0.67	n.m.	<LQ	<LQ	0.08	0.87	<LQ
L1	06/09/2019	<LQ	<LQ	4.03	n.m.	<LQ	0.27	n.m.	0.52	<LQ
D2	31/08/2018	n.m.	n.m.	1.29	n.m.	n.m.	n.m.	n.m.	n.m.	n.m.
D2	17/10/2018	<LQ	<LQ	1.64	<LQ	<LQ	<LQ	<LQ	1.45	<LQ
D2	11/12/2018	<LQ	<LQ	2.59	n.m.	<LQ	<LQ	<LQ	0.78	<LQ
D2	19/02/2019	<LQ	<LQ	0.93	n.m.	<LQ	<LQ	<LQ	2.51	<LQ
D2	11/04/2019	<LQ	<LQ	0.77	n.m.	<LQ	<LQ	<LQ	<LQ	<LQ
D2	12/06/2019	<LQ	<LQ	1.00	n.m.	<LQ	<LQ	0.11	1.61	<LQ
D2	06/09/2019	<LQ	<LQ	3.43	n.m.	<LQ	<LQ	n.m.	1.42	<LQ
D3	31/08/2018	n.m.	n.m.	2.09	n.m.	n.m.	n.m.	n.m.	n.m.	n.m.
D3	17/10/2018	<LQ	<LQ	2.42	<LQ	<LQ	<LQ	<LQ	2.71	<LQ
D3	11/12/2018	<LQ	<LQ	0.46	n.m.	<LQ	<LQ	<LQ	0.76	<LQ
D3	19/02/2019	<LQ	<LQ	0.40	n.m.	<LQ	<LQ	<LQ	0.73	<LQ
D3	11/04/2019	<LQ	<LQ	1.83	n.m.	<LQ	<LQ	<LQ	0.93	<LQ
D3	12/06/2019	<LQ	<LQ	0.11	n.m.	0.08	<LQ	<LQ	1.38	<LQ
D3	06/09/2019	<LQ	<LQ	3.10	n.m.	<LQ	<LQ	n.m.	0.45	<LQ
D4	11/12/2018	<LQ	<LQ	0.21	n.m.	0.10	<LQ	<LQ	<LQ	<LQ
D4	19/02/2019	<LQ	<LQ	0.04	n.m.	<LQ	<LQ	<LQ	0.50	<LQ
D4	11/04/2019	<LQ	<LQ	0.68	n.m.	<LQ	<LQ	<LQ	<LQ	<LQ
D5	17/10/2018	<LQ	<LQ	2.01	<LQ	<LQ	<LQ	<LQ	<LQ	<LQ
D5	11/12/2018	<LQ	<LQ	0.28	n.m.	0.10	<LQ	<LQ	0.53	<LQ
D5	19/02/2019	<LQ	<LQ	0.63	n.m.	<LQ	<LQ	<LQ	0.60	<LQ
D5	11/04/2019	<LQ	<LQ	0.97	n.m.	<LQ	<LQ	<LQ	<LQ	<LQ
D5	12/06/2019	<LQ	<LQ	0.46	n.m.	0.06	<LQ	0.06	0.69	<LQ
D5	06/09/2019	<LQ	<LQ	3.38	n.m.	<LQ	<LQ	n.m.	0.76	<LQ

SITE	SAMPLING	Si (mg/L)	Sr (mg/L)	Ti (mg/L)	V (mg/L)	Zn (mg/L)	Zr (mg/L)
L1	31/08/2018	n.m.	1.44	n.m.	n.m.	n.m.	n.m.
L1	17/10/2018	17.50	1.49	<LQ	<LQ	<LQ	<LQ
L1	11/12/2018	n.m.	1.72	<LQ	<LQ	<LQ	<LQ
L1	19/02/2019	n.m.	1.69	<LQ	<LQ	<LQ	<LQ
L1	11/04/2019	9.46	1.76	<LQ	<LQ	3.09	<LQ
L1	12/06/2019	13.13	1.62	<LQ	<LQ	<LQ	<LQ
L1	06/09/2019	30.01	<LQ	<LQ	0.12	<LQ	<LQ
D2	31/08/2018	n.m.	1.59	n.m.	n.m.	n.m.	n.m.
D2	17/10/2018	17.49	1.49	<LQ	<LQ	<LQ	<LQ
D2	11/12/2018	n.m.	1.89	<LQ	<LQ	<LQ	<LQ
D2	19/02/2019	n.m.	1.82	<LQ	<LQ	<LQ	<LQ
D2	11/04/2019	9.36	2.47	<LQ	<LQ	3.43	<LQ
D2	12/06/2019	13.61	1.65	0.06	<LQ	<LQ	0.05
D2	06/09/2019	15.95	<LQ	<LQ	0.12	<LQ	<LQ
D3	31/08/2018	n.m.	1.94	n.m.	n.m.	n.m.	n.m.
D3	17/10/2018	22.58	2.32	<LQ	<LQ	<LQ	<LQ
D3	11/12/2018	n.m.	2.82	<LQ	<LQ	<LQ	<LQ
D3	19/02/2019	n.m.	2.62	<LQ	<LQ	<LQ	<LQ
D3	11/04/2019	11.24	3.14	<LQ	<LQ	3.20	<LQ
D3	12/06/2019	13.37	3.10	<LQ	<LQ	<LQ	<LQ
D3	06/09/2019	12.05	1.80	<LQ	0.10	<LQ	<LQ
D4	11/12/2018	n.m.	2.01	<LQ	<LQ	<LQ	<LQ
D4	19/02/2019	n.m.	1.95	<LQ	<LQ	<LQ	<LQ
D4	11/04/2019	8.13	2.20	<LQ	<LQ	3.22	<LQ
D5	17/10/2018	26.31	2.42	<LQ	<LQ	<LQ	<LQ
D5	11/12/2018	n.m.	2.58	<LQ	<LQ	<LQ	<LQ
D5	19/02/2019	n.m.	2.62	<LQ	<LQ	<LQ	<LQ
D5	11/04/2019	14.03	1.97	<LQ	<LQ	3.14	<LQ
D5	12/06/2019	17.43	1.90	<LQ	<LQ	<LQ	<LQ
D5	06/09/2019	17.29	<LQ	<LQ	0.15	<LQ	<LQ

AMOSTRAS DE ÁGUA SUBTERRÂNEA (POÇOS RASO E PROFUNDO)/GROUNDWATER SAMPLES (SHALLOW AND DEEP WELLS)

WELL	SAMPLING	Water level (m)	pH	Cond. (µS/cm)	T °C	O.D. (mg/L)	Fe2+	Fe3+	Fe total	NH_4^+ (mg/L)
SHALLOW	12/09/2018	3.69	5.99	1,429.00	n.m.	n.m.	n.m.	n.m.	n.m.	28.75
SHALLOW	13/11/2018	3.24	6.29	1,363.00	n.m.	n.m.	117.32	-9.87	107.45	32.28
SHALLOW	18/12/2018	2.67	6.09	1,339.00	26.8	2.36	44.98	8.04	53.02	43.67
SHALLOW	22/02/2019	1.48	6.4	1,366.00	n.m.	n.m.	98.31	30.20	128.50	43.61
SHALLOW	25/04/2019	2.08	6.32	1,333.00	n.m.	2.83	45.77	22.58	68.35	44.79
SHALLOW	19/06/2019	2.78	6.07	2,630.00	24.5	2.8	33.40	32.15	65.55	43.59
DEEP	12/09/2018	2.14	6.76	136.00	n.m.	n.m.	n.m.	n.m.	n.m.	0.02
DEEP	13/11/2018	2.26	7.06	138.40	n.m.	n.m.	0.00	0.00	0.00	0.00
DEEP	18/12/2018	1.84	7.27	136.00	24.7	4.18	0.05	0.01	0.06	0.06
DEEP	22/02/2019	3.09	7.14	135.3	n.m.	n.m.	0.08	0.39	0.48	0.19
DEEP	25/04/2019	1.36	6.62	139.6	n.m.	3.79	0.07	0.46	0.52	0.02
DEEP	19/06/2019	1.08	5.96	269	26.3	4.42	0.00	0.42	0.42	0.00

WELL	SAMPLING	Alk. (mg/L HCO3-)	δ13C-DIC	δ13C-DOC	DOC (mg/L)	F (mg/L)	Cl (mg/L)	NO3 (mg/L)	PO4 (mg/L)	SO4 (mg/L)
SHALLOW	12/09/2018	70.88	1.20	n.m.	10.60	n.m.	n.m.	n.m.	n.m.	n.m.
SHALLOW	13/11/2018	3,518.02	3.13	-5.70	8.66	<LQ	227.84	0.10	<LQ	11.17
SHALLOW	18/12/2018	195.4458	0.39	-27.27	8.28	<LQ	237.03	contamination	<LQ	<LQ
SHALLOW	22/02/2019	195.4458	-1.00	-14.75	6.76	<LQ	245.75	49.50	<LQ	14.90
SHALLOW	25/04/2019	139.0352	0.90	-25.78	6.78	<LQ	173.16	7.58	<LQ	<LQ
SHALLOW	19/06/2019	207.6611	-1.30	-26.41	7.73	<LQ	217.95	0.1	<LQ	<LQ
DEEP	12/09/2018	202.52	-11.32	n.m.	2.31	n.m.	n.m.	n.m.	n.m.	n.m.
DEEP	13/11/2018	1,759.01	-10.90	n.m.	1.59	<LQ	1.24	0.94	<LQ	0.24
DEEP	18/12/2018	48.86	-11.52	n.m.	0.97	<LQ	1.01	contamination	<LQ	0.35
DEEP	22/02/2019	48.86	-12.77	n.m.	0.26	<LQ	0.84	<LQ	<LQ	0.43
DEEP	25/04/2019	39.72	-11.29	-25.25	0.34	<LQ	0.97	0.2	<LQ	0.46
DEEP	19/06/2019	97.72	-12.12	-27.21	1.62	<LQ	1.00	<LQ	<LQ	0.42

WELL	SAMPLING	Ca (mg/L)	Mg (mg/L)	Na (mg/L)	K (mg/L)	Al (mg/L)	As (mg/L)	Ba (mg/L)	Cd (mg/L)	Co (mg/L)
SHALLOW	12/09/2018	n.m.	n.m.	n.m.	n.m.	n.m.	n.m.	n.m.	n.m.	n.m.
SHALLOW	13/11/2018	1.32	0.36	144.49	70.60	1.93	<LQ	<LQ	<LQ	<LQ
SHALLOW	18/12/2018	1.54	0.13	140.23	34.68	0.32	<LQ	n.m.	<LQ	<LQ
SHALLOW	22/02/2019	1.16	<LQ	142.70	40.85	<LQ	<LQ	n.m.	<LQ	<LQ
SHALLOW	25/04/2019	<LQ	<LQ	134.63	42.00	<LQ	<LQ	<LQ	<LQ	<LQ
SHALLOW	19/06/2019	1.51	0.11	139.78	42.93	<LQ	<LQ	<LQ	<LQ	<LQ
DEEP	12/09/2018	n.m.	n.m.	n.m.	n.m.	n.m.	n.m.	n.m.	n.m.	n.m.
DEEP	13/11/2018	26.25	1.47	0.60	0.45	<LQ	<LQ	<LQ	<LQ	<LQ
DEEP	18/12/2018	25.05	1.41	0.73	0.52	<LQ	<LQ	n.m.	<LQ	<LQ
DEEP	22/02/2019	25.20	1.42	0.72	0.76	<LQ	<LQ	n.m.	<LQ	<LQ
DEEP	25/04/2019	25.43	1.42	0.70	0.48	<LQ	<LQ	<LQ	<LQ	<LQ
DEEP	19/06/2019	28.14	1.55	0.70	0.60	<LQ	<LQ	0.03	<LQ	<LQ

WELL	SAMPLING	Cr (mg/L)	Cu (mg/L)	Fe (mg/L)	Li (mg/L)	Mn (mg/L)	Mo (mg/L)	Ni (mg/L)	P (mg/L)	Pb (mg/L)
SHALLOW	12/09/2018	n.m.	n.m.	n.m.	n.m.	n.m.	n.m.	n.m.	n.m.	n.m.
SHALLOW	13/11/2018	<LQ	<LQ	43.29	<LQ	0.22	<LQ	<LQ	<LQ	<LQ
SHALLOW	18/12/2018	<LQ	<LQ	54.51	n.m.	0.19	<LQ	<LQ	<LQ	<LQ
SHALLOW	22/02/2019	<LQ	<LQ	94.94	n.m.	0.23	<LQ	<LQ	<LQ	<LQ
SHALLOW	25/04/2019	<LQ	<LQ	43.28	n.m.	0.19	<LQ	<LQ	<LQ	<LQ
SHALLOW	19/06/2019	<LQ	<LQ	61.31	n.m.	0.19	<LQ	<LQ	<LQ	<LQ
DEEP	12/09/2018	n.m.	n.m.	n.m.	n.m.	n.m.	n.m.	n.m.	n.m.	n.m.
DEEP	13/11/2018	<LQ	<LQ	0.027	<LQ	<LQ	<LQ	<LQ	<LQ	<LQ
DEEP	18/12/2018	<LQ	<LQ	0.029	n.m.	<LQ	<LQ	<LQ	<LQ	<LQ
DEEP	22/02/2019	<LQ	<LQ	<LQ	n.m.	<LQ	<LQ	<LQ	<LQ	<LQ
DEEP	25/04/2019	<LQ	<LQ	<LQ	n.m.	<LQ	<LQ	<LQ	<LQ	<LQ
DEEP	19/06/2019	<LQ	<LQ	<LQ	n.m.	<LQ	<LQ	<LQ	0.02	<LQ

WELL	SAMPLING	Si (mg/L)	Sr (mg/L)	Ti (mg/L)	V (mg/L)	Zn (mg/L)	Zr (mg/L)
SHALLOW	12/09/2018	n.m.	n.m.	n.m.	n.m.	n.m.	n.m.
SHALLOW	13/11/2018	1.20	<LQ	<LQ	<LQ	<LQ	<LQ
SHALLOW	18/12/2018	n.m.	<LQ	<LQ	<LQ	<LQ	<LQ
SHALLOW	22/02/2019	n.m.	<LQ	<LQ	<LQ	<LQ	<LQ
SHALLOW	25/04/2019	1.42	<LQ	<LQ	<LQ	<LQ	<LQ
SHALLOW	19/06/2019	0.20	<LQ	<LQ	<LQ	<LQ	<LQ
DEEP	12/09/2018	n.m.	n.m.	n.m.	n.m.	n.m.	n.m.
DEEP	13/11/2018	5.48	0.01	<LQ	<LQ	<LQ	<LQ
DEEP	18/12/2018	n.m.	0.01	<LQ	<LQ	<LQ	<LQ
DEEP	22/02/2019	n.m.	0.01	<LQ	<LQ	<LQ	<LQ
DEEP	25/04/2019	5.29	0.01	<LQ	<LQ	<LQ	<LQ
DEEP	19/06/2019	5.72	0.01	<LQ	<LQ	<LQ	<LQ

AMOSTRAS DE ÁGUA SUPERFICIAL (CÓRREGO DO VALO)/STREAM WATER SAMPLES (VALO STREAM):

SITE	SAMPLING	pH	Cond. (µS/cm)	T °C	O.D. (mg/L)	Fe2+	Fe3+	Fe total	NH4+ (mg/L)
VALO	12/09/2018	5.5	50.5	n.m.	n.m.	n.m.	n.m.	n.m.	0.54
VALO	17/12/2018	5.8	63.3	21.5	4.90	0.08	0.13	0.21	0.87
VALO	22/02/2019	6.58	50.8	n.m.	3.77	0.05	0.60	0.65	0.67
VALO	30/04/2019	6.22	99.0	n.m.	1.32	0.25	0.52	0.77	1.11
VALO	19/06/2019	6.45	121.6	19	3.40	0.00	0.59	0.59	0.56

SITE	SAMPLING	Alk. (mg/L HCO3-)	δ^{13}C-DIC	δ^{13}C-DOC	DOC (mg/L)	F (mg/L)	Cl (mg/L)	NO3 (mg/L)	PO4 (mg/L)	SO4 (mg/L)
VALO	12/09/2018	20.25	-9.87	n.m.	2.68	n.m.	n.m.	n.m.	n.m.	n.m.
VALO	17/12/2018	5.08	-10.14	n.m.	n.m.	<LQ	26.06	contamination	<LQ	0.39
VALO	22/02/2019	48.86	-10.77	n.m.	1.85	<LQ	10.36	1.53	<LQ	0.44
VALO	30/04/2019	4.89	-7.05	-25.76	2.29	<LQ	21.21	1.78	<LQ	0.57
VALO	19/06/2019	12.22	-10.36	-28.31	1.70	<LQ	8.6	1.23	<LQ	0.35

SITE	SAMPLING	Ca (mg/L)	Mg (mg/L)	Na (mg/L)	K (mg/L)	Al (mg/L)	As (mg/L)	Ba (mg/L)	Cd (mg/L)	Co (mg/L)
VALO	12/09/2018	n.m.	n.m.	n.m.	n.m.	n.m.	n.m.	n.m.	n.m.	n.m.
VALO	17/12/2018	0.46	0.09	9.00	1.11	<LQ	<LQ	n.m.	<LQ	<LQ
VALO	22/02/2019	0.39	0.07	6.96	1.01	<LQ	<LQ	n.m.	<LQ	<LQ
VALO	30/04/2019	0.80	0.12	13.13	2.01	<LQ	<LQ	<LQ	<LQ	<LQ
VALO	19/06/2019	0.37	0.08	6.43	0.80	<LQ	<LQ	<LQ	<LQ	<LQ

SITE	SAMPLING	Cr (mg/L)	Cu (mg/L)	Fe (mg/L)	Li (mg/L)	Mn (mg/L)	Mo (mg/L)	Ni (mg/L)	P (mg/L)	Pb (mg/L)
VALO	12/09/2018	n.m.	n.m.	n.m.	n.m.	n.m.	n.m.	n.m.	n.m.	n.m.
VALO	17/12/2018	<LQ	<LQ	0.17	n.m.	<LQ	<LQ	<LQ	<LQ	<LQ
VALO	22/02/2019	<LQ	<LQ	0.14	n.m.	<LQ	<LQ	<LQ	0.02	<LQ
VALO	30/04/2019	<LQ	<LQ	0.23	n.m.	<LQ	<LQ	<LQ	<LQ	<LQ
VALO	19/06/2019	<LQ	<LQ	0.13	n.m.	<LQ	<LQ	<LQ	0.03	<LQ

SITE	SAMPLING	Si (mg/L)	Sr (mg/L)	Ti (mg/L)	V (mg/L)	Zn (mg/L)	Zr (mg/L)
VALO	12/09/2018	n.m.	n.m.	n.m.	n.m.	n.m.	n.m.
VALO	17/12/2018	n.m.	<LQ	<LQ	<LQ	<LQ	<LQ
VALO	22/02/2019	n.m.	<LQ	<LQ	<LQ	<LQ	<LQ
VALO	30/04/2019	2.01	<LQ	<LQ	<LQ	<LQ	<LQ
VALO	19/06/2019	1.98	<LQ	<LQ	<LQ	<LQ	<LQ